

**ISOLATION AND PURIFICATION OF GLUTATHIONE
S-TRANSFERASES FROM *Donax* sp.**

NORFARHAN MOHD ASSA'AD

**FACULTY OF SCIENCE
UNIVERSITY OF MALAYA
KUALA LUMPUR**

2011

UNIVERSITI MALAYA

ORIGINAL LITERARY WORK DECLARATION

Name of Candidate: NORFARHAN BINTI MOHD ASSA'AD (I.C/Passport No: 850730-10-5586)

Registration/Matric No: SGF 090006

Name of Degree: MASTER OF BIOTECHNOLOGY

Title of Project Paper/Research Report/Dissertation/Thesis ("this Work"):
ISOLATION AND PURIFICATION OF GLUTATHIONE S-TRANSFERASES FROM *Donax* sp.

Field of Study: BIOCHEMISTRY

I do solemnly and sincerely declare that:

- (1) I am the sole author/writer of this Work;
- (2) This Work is original;
- (3) Any use of any work in which copyright exists was done by way of fair dealing and for permitted purposes and any excerpt or extract from, or reference to or reproduction of any copyright work has been disclosed expressly and sufficiently and the title of the Work and its authorship have been acknowledged in this Work;
- (4) I do not have any actual knowledge nor do I ought reasonably to know that the making of this work constitutes an infringement of any copyright work;
- (5) I hereby assign all and every rights in the copyright to this Work to the University of Malaya ("UM"), who henceforth shall be owner of the copyright in this Work and that any reproduction or use in any form or by any means whatsoever is prohibited without the written consent of UM having been first had and obtained;
- (6) I am fully aware that if in the course of making this Work I have infringed any copyright whether intentionally or otherwise, I may be subject to legal action or any other action as may be determined by UM.

Candidate's Signature

Date

Subscribed and solemnly declared before,

Witness's Signature

Date

Name:

Designation:

ABSTRACT

Glutathione *S*-transferases (GSTs) are among the enzymes involved in the phase II detoxification metabolism of wide range exogenous and endogenous compounds in living cells. Bivalves GSTs often proposed as biomarker for marine pollution detection for several reasons; filter feeder, sessile, wide range distribution, and not affected by some biotic factors. In this study, GSTs from remis *Donax* sp. was purified by using two affinity column; GSTrapTMHP and GSH-agarose (C₃). The total recovery of CDNB-active GSTs was 12% and 3% for GSTrapTMHP and GSH-agarose (C₃), respectively. SDS-PAGE of GSTrapTMHP purified extract revealed two subunits with apparent molecular masses (MW) of 29 and 26 kDa while GSH-agarose (C₃) showed three subunits corresponding to 29, 28, and 26 kDa. Two-dimensional electrophoresis (2-DE) of GSTs purified from GSH-agarose (C₃) discovered nine similar spots to GSTs purified using GSTrapTMHP but with additional six distinct spots. Analysis by isoelectric focusing (IEF) illustrated most GSTs purified from both column resolved at *pI* in between 4.5 to 6.9. Apart from this cluster, there were also GSTs appearing each at *pI* 4.2 and 8.3. Purified GSTs from both columns exhibited activity towards 1-chloro-2,4-dinitrobenzene (CDNB), 1,2-dichloro-4-nitrobenzene (DCNB), sulfobromophthalein (BSP) and ethacrynic acid (EA). GSH-agarose (C₃) showed less specific activity in all substrates compared to GSTrapTMHP, except for EA which count about 10- fold. However, GSTs eluted from both columns did not show any activity with *p*-nitrobenzylchloride (NBC), *trans*-4-phenyl-3-butene-2-one (PBO), and nitrocinnamaldehyde (NCA). However, mass spectrometry analysis did not show any match with the available database. Therefore based on the current data, GSTs obtained in this study were summarized belong to pi- and mu-class.

ABSTRAK

Glutathione *S*-transferases (GSTs) merupakan salah satu enzim yang terlibat di dalam tapak jalan fasa II metabolisme penyahtoksikan pelbagai sebatian eksogen dan endogen di dalam sel. Kumpulan bivalvia sering dicadangkan sebagai penanda biologi untuk mengesan pencemaran marin kerana faktor-faktor seperti berikut; pemakanan menapis, sesil, taburan yang luas, dan tidak dipengaruhi oleh beberapa factor biotic. Dalam kajian ini, penulenan GST daripada remis, *Donax* sp. telah dijalankan dengan dua jenis kolum afiniti; GSTrapTMHP and GSH-agarose (C₃). Sebanyak 12% dan 3% GST yang aktif terhadap CDNB berjaya diperolehi melalui penggunaan GSTrapTMHP and GSH-agarose (C₃) ini. Analisis SDS-PAGE bagi ekstrak yang ditulenan daripada GSTrapTMHP menghasilkan dua subunit bersaiz 29 dan 26 kDa manakala GSH-agarose (C₃) menunjukkan tiga subunit dengan saiz 29, 28, dan 26 kDa. Elektroforesis dua dimensi bagi GST yang ditulenan daripada GSH-agarose (C₃) menunjukkan sembilan tompok serupa dengan GST yang dipencilkan daripada GSTrapTMHP, tetapi dengan tambahan enam lagi tompok lain. Analisis pemfokusan isoelektrik (IEF) memberi gambaran bahawa kebanyakan GST yang ditulenan daripada kedua-dua kolum menyerak di antara *pI* 4.5 - 6.9. Selain daripada kumpulan utama ini, terdapat juga GST yang muncul setiap satunya terletak di *pI* 4.2 dan 8.3. GST yang ditulenan daripada kedua-dua kolum memberi aktiviti terhadap 1-kloro-2,4-dinitrobenzena (CDNB), 1,2-dikloro-4-nitrobenzena (DCNB), sulfobromophtaleina (BSP), dan asid etakrinik (EA). GST daripada GSH-agarose (C₃) menunjukkan aktiviti yang lebih rendah di dalam semua substrat, kecuali EA yang memberikan aktiviti 10- kali ganda lebih banyak berbanding GST daripada GSTrapTMHP. Walau bagaimanapun, GST yang ditulenan daripada kedua-dua kolum tidak menunjukkan sebarang aktiviti dengan *p*-nitrobenzilklorida (NBC), trans-4-fenil-3-butena-2-one (PBO), dan nitrocinnamaldehyd (NCA). Walau

bagaimanapun, analisis spektrometri jisim tidak menunjukkan sebarang padanan dengan pengkalan data yang sedia ada. Oleh itu, berdasarkan kepada data semasa, GSTs yang diperoleh di dalam kajian ini dikelaskan sebagai pi- dan mu-GST.

ACKNOWLEDGEMENT

In the name of Allah, the Most Gracious and the Most Merciful. Alhamdulillah, I thank Allah for endowing me strength and ability to complete this work. I would like to express my deepest gratitude to my supervisor, Dr. Zazali Alias for his extensive guidance, continuous support, precious time, and inspiration. To all fellow friends who are directly and indirectly involved in this project; I really appreciate all your support. Great deals appreciated to University of Malaya for the facilities and all opportunities given to me, University Kebangsaan Malaysia for their support, and Ministry of Higher Education Malaysia (MOHE) to have financially supported me during my study.

My special thanks dedicated to both my parents and family members for their encouragement and infinity love. Last but not least, grateful acknowledgement to you-know-who for your endless support during this entire journey.

TABLE OF CONTENT

CONTENT	PAGE
PREFACE	
ABSTRACT	ii
ABSTRAK	iii
ACKNOWLEDGEMENT	v
TABLE OF CONTENT	vi
LIST OF FIGURES	ix
LIST OF TABLES	x
LIST OF SYMBOLS AND ABBREVIATIONS	xi
LIST OF APPENDICES	xii
1.0 INTRODUCTION	1
2.0 LITERATURE REVIEW	
2.1 GSTs	5
2.2 CLASSES OF GSTs	7
2.3 STRUCTURE OF GSTs	8
2.4 FUNCTION OF GSTs	13
2.5 GSTs DISTRIBUTION AND EXPRESSION	15
2.6 BIVALVES	17
2.7 GSTs IN BIVALVES	18
2.8 PURIFICATION OF GSTs	21
2.8.1 Purification of bivalves GSTs	24
2.9 PROTEOMIC APPROACHES	24
2.9.1 Two-dimensional electrophoresis (2-DE)	25
2.9.2 Peptide mass fingerprint	27
3.0 MATERIALS	
3.1 SAMPLE	30
3.2 REAGENTS AND APPARATUS	30
3.3 INSTRUMENTS	34
4.0 METHODOLOGY	
4.1 SAMPLE PREPARATION	35
4.2 AFFINITY CHROMATOGRAPHY	35
4.3 PROTEIN CONCENTRATION	36
4.4 QUANTITATIVE PROTEIN ESTIMATION (BRADFORD)	36

4.5 ENZYME ASSAYS FOR SUBSTRATE SPECIFICITY AND ACTIVITY CALCULATION	37
4.6 ELECTROPHORETIC ANALYSIS	
4.6.1 Laemmli Discontinuous Sodium Dodecyl Sulfate-Polyacrylamide Gel Electrophoresis (SDS-PAGE)	37
4.6.2 Subunit Molecular Weight Determination	37
4.6.3 Isoelectric Focusing (IEF)	38
4.7 TWO-DIMENSIONAL GEL ELECTROPHORESIS (2-DE)	
4.7.1 Sample application by in-gel rehydration	38
4.7.2 Preparation for the first dimension – isoelectric focusing (IEF)	39
4.7.3 Preparation of the second dimension (SDS-PAGE)	40
4.8 GEL STAINING	
4.8.1 Silver Staining	41
4.8.2 Coomassie Colloidal blue-staining (MALDI-TOFF compatible)	42
4.9 MALDI-TOFF ANALYSIS	42
5.0 RESULT	
5.1 PURIFICATION OF GST USING DIFFERENT GSH-AGAROSE BASED MATRICES	44
5.1.1 Purification of GST using GSH-agarose (C ₁₂)	44
5.1.2 Purification of GST using GSH-agarose (C ₃)	45
5.2 SDS-PAGE ANALYSIS	49
5.2.1 SDS-PAGE for protein purified from GSH-agarose (C ₁₂)	49
5.2.2 SDS-PAGE for protein purified from GSH-agarose (C ₃)	50
5.3 TWO-DIMENSIONAL ELECTROPHORESIS (2-DE)	51
5.3.1 Two-dimensional electrophoresis (2-DE) for proteins purified from GSH-agarose (C ₁₂)	52
5.3.2 Two-dimensional electrophoresis (2-DE) for proteins purified from GSH-agarose (C ₃)	52
5.4 ISOELECTRIC FOCUSING (IEF)	54
5.4.1 Isoelectric focusing on GSTs eluted from GSH-agarose (C ₁₂)	54
5.4.2 Isoelectric focusing on GSTs eluted from GSH-agarose (C ₅)	54
5.5 SUBSTRATE SPECIFICITY OF PURIFIED GSTs	55
5.5.1 Substrate specificity of GSTs eluted from GSH-agarose (C ₁₂)	56
5.5.2 Substrate specificity of GST eluted from GSH-	56

agarose (C ₃)	
5.6 IDENTIFICATION OF PURIFIED GSTs USING MALDI-TOFF	57
6.0 DISCUSSION	
6.1 PURIFICATION OF GSTs USING GSH-AGAROSE BASED MATRICES	58
6.2 GEL VISUALIZATION	62
6.3 SUBSTRATE SPECIFICITY	66
6.4 IDENTIFICATION OF GSTs OBTAINED FROM GSTrap™ HP MATRIX	69
7.0 CONCLUSION	71
REFERENCES	73
APPENDICES	84

LIST OF FIGURES

Figure 1.1	Images of <i>Donax</i> sp.	4
Figure 2.1	Glutathione conjugation to xenobiotics through GST action producing glutathione-S-conjugate.	6
Figure 2.2	Diagram of TRX proteins secondary structure.	12
Figure 2.3	Structures of different types of affinity matrix used for GST purification.	23
Figure 2.4	Outline of MALDI-TOF analyzer.	29
Figure 5.1	Chromatogram of GST purification using GSTrap TM HP.	46
Figure 5.2	Chromatogram of GST purification using GSH-agarose (C ₃).	47
Figure 5.3	SDS-PAGE (12%) of active proteins fraction eluted from GSTrap TM HP matrix.	50
Figure 5.4	SDS-PAGE (12%) of GSTs purified from GSH-agarose (C ₃) matrix.	51
Figure 5.5	Two dimensional gels of GST purified from affinity chromatography.	53
Figure 5.6	Separation of <i>Donax</i> sp. purified GSTs on silver stained IEF gel.	55
Figure 6.1	Effect of different linker arm on GSH-agarose (C ₁₂ and C ₃) on their behavior to capture GST	60

LIST OF TABLES

Table 5.1	Purification of GSTs from remis by two different GSH-based affinity matrix.	48
Table 5.2	Substrate specificity of remis GSTs purified using GSH-agarose (C ₁₂) and GSH-agarose (C ₃) columns.	57

LIST OF SYMBOLS AND ABBREVIATIONS

GST	Glutathione S-transferase
PAH	Polycyclic aromatic hydrocarbons
GSH	Glutathione
ROS	Reactive oxygen species
cGST	Cytosolic GST
MAPEG	Membrane associated protein
TRX	Thioredoxin
RP-HPLC	Reverse-phase HPLC
SDS-PAGE	Sodium dodecyl sulfate polyacrylamide gel electrophoresis
<i>pI</i>	Isoelectric point
2-DE	Two dimensional electrophoresis
IPG	Immobilized pH gradients
IEF	Isoelectric focusing
PMF	Peptide mass fingerprinting
ESI	Electrospray ionization
MALDI	Matrix-assisted laser desorption ionization
TOF	Time-of-flight

LIST OF APPENDICES

APPENDIX A	Buffer solution preparation	84
APPENDIX B	Laemmli Discontinuous SDS Polyacrylamide Gel Electrophoresis	85
APPENDIX C	Electrophoresis in Tris-Glicine Buffer System	86
APPENDIX D	Coomasie Blue Reagent for Protein Determination	87
APPENDIX E	Substrate preparation and Enzyme Assay conditions	88
APPENDIX F	Reagent for Proteomic Analysis	90
APPENDIX G	Standard Curve of BSA	91
APPENDIX H	Standard Curve of Molecular Weight Protein Marker	92
APPENDIX I	Peptide masses for GSTs purified from GSTrap TM HP	93

CHAPTER 1

INTRODUCTION

It is beyond doubt all creatures constantly exposed to toxic compounds from either external environment or naturally produced in their cells. With current increase in worldwide production of waste, it is not a surprise many compounds are found to be a major threat to human health and environment. Therefore, species must possess highly effective system to respond to challenges from continuous contact with unhealthy environment in order to ensure their survival. The systems are crucial to keep the toxic residue and the activity towards detoxification well balanced. Disruption to the system would affect biological cells activities which in worst case scenario would lead to cell death (Sheehan & McDonagh, 2008).

One of cell detoxification remarkable adaptations is through collective enzymes activity known as glutathione *S*-transferases (GSTs) (Frova, 2006; Masella et al., 2005; Townsend & Tew, 2003). This superfamily of multifunctional proteins can be detected in broad range kingdom, from a single cell organism i.e. bacteria to higher living organisms including human, plants, and animals. Salinas and Wong (1999) reported that GSTs are identified in most aerobic eukaryotes and some prokaryotes which account about 1% of total cellular protein. Many studies reported GSTs fundamental role in detoxification of wide range exogenous and endogenous compounds, including numerous environmental carcinogens such as benzo [a]-pyrene and other polycyclic hydrocarbons (Deng et al., 2009; Frova, 2006; Habig et al., 1974; Wang et al., 2008; Ye et al., 2006; Zablutowicz et al., 1999). This significant task of GSTs might be the main reason why GSTs are found across various organisms.

As GSTs respond specifically towards toxic substances, GSTs offer an enormous potential to be used as biomarker for environmental pollution detection. Park et al. (2009) portray GSTs as the most interesting biomarkers of exposure to environmental pollutant. Similar to most proteins, expressions of GSTs are induced under a defined condition. The respond of GSTs are correlated with existing number of substrates thus substrate accumulation will enhance GSTs expression to the optimum level. In a study conducted by Gowland et al. (2002), they reported that GSTs activity from reference site mussel was considerably lower by 30-60 times compared to mussel collected from the field containing high concentration of parent polycyclic aromatic hydrocarbons (PAHs). Buhler and Williams (1988, as cited in Kaaya et al., 1999) also mentioned that GSTs expressions are influenced by exposure to various foreign compounds. These reports showed that GSTs have a very good prospective to be used as an alarm when selected organism is exposed to over polluted environment.

One of the major pollutions gaining more and more attention is marine contamination. Marine pollution becomes a massive threat ever because marine serve as habitat for innumerable species and human are highly dependent on marine ecosystem. For that reason, it is vital to identify level of marine pollution therefore; biomarker can serve as an early warning tool in environmental quality assessment (Cajaraville et al., 2000). Consequently, to obtain optimum result from biomarker application, appropriate organism should be chosen carefully. At present, bivalves are used widely as sentinel species in environmental toxicology due to its major importance in aquatic ecology as well as aquaculture and are proven to have notable plasticity towards molecular oxygen (Sheehan & McDonagh, 2008). Bivalves appear to show considerable flexibility in various conditions resulting a wide-range distribution in aquatic environment. Sheehan and Power (1999) characterized bivalves as filter-feeding organisms which fed on

anything pass through, thus expose them to large amount of pollutants. Bivalves are also capable to endure the baseline level of pollution and can be found abundantly in estuaries area (Sheehan et al., 1995). Furthermore, bivalves are sessile and this behavior becomes a great advantage for biomonitoring purpose because they are likely to reflect the quality status of a particular study area. Therefore, accumulated contaminants detected within bivalves could represent the actual contaminants in the specific area (da Silva et al., 2005). More importantly, the expressions of bivalve GSTs are not affected by temperature thus make the enzyme suitable to be used in biomonitoring program (Huang et al., 2008). As bivalves survive in continuous toxic exposure, it can be assumed that bivalves have a very effective detoxification system, where GSTs are most likely take part in this process. Therefore, GSTs activity in bivalves could be a good starting point for marine quality assessment bioindicator. By combining a sentinel species with a specific biomarker, it can provide information on the overall impact of xenobiotics on the health of ecosystems (Won et al., 2005). In fact, a ‘mussel watch’ programs are being carried out in the United States to monitor the levels of pollutants in coastal environment (Cajaraville et al., 2000).

Implementation of local bivalves GSTs as biomarker is expected to be very attractive but more detailed research must be carried out to get better comprehension, especially on interaction between pollutants and GSTs expression. Many species of bivalves can be found around Malaysian waters, including one of them, an edible *Donax* sp. or known as remis by local people (Figure 1.1). This study will be emphasized on GSTs expressed in local bivalve species, *Donax* sp. as an attempt to understand them for future application.

Therefore, objectives of this study are:

1. To isolate and purify glutathione *S*-transferases from *Donax* sp.
2. Determination of substrate specificity for purified glutathione *S*-transferases in a series of assay study.
3. To identify glutathione *S*-transferases purified from *Donax* sp.



Figure 1.1 Images of *Donax* sp.

CHAPTER 2

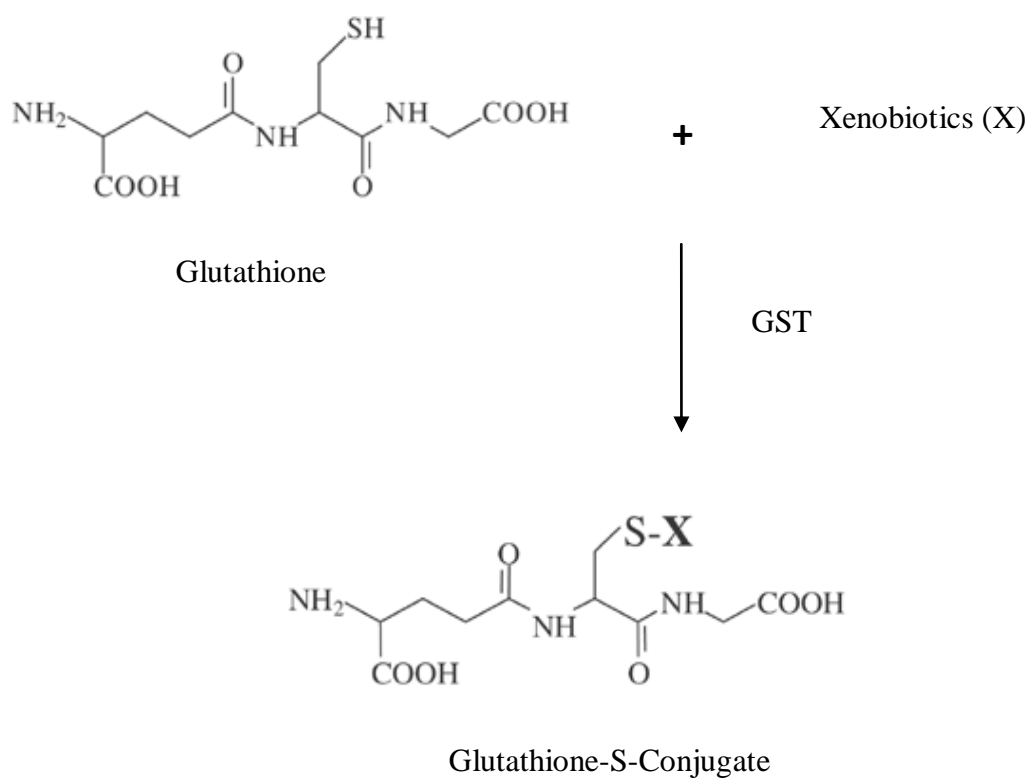
LITERATURE REVIEW

2.1 GSTs

Glutathione *S*-transferases (GSTs) (EC 2.5.1.18) are a superfamily of multifunctional proteins which play an important role in detoxification of a wide range of exogenous and endogenous compounds. GSTs received much attention and many studies have been conducted since its first discovery in 1961. They are known to be a part of Phase II enzymic detoxification metabolism which converts toxins to a more water soluble molecule hence become biologically inactive by the addition of hydrophilic moieties (Knapen et al., 1999; Sheehan et al., 2001). The deactivation process is achieved when GSTs catalyze the transfer of a tripeptide glutathione (GSH : L- γ -Glu-L-Cys-Gly) with electrophilic centre of a compound, thereby neutralizing their electrophilic sites with the thiol group (-SH) from GSH to form a polar S-glutathionylated reaction product (R-SG) (Dixon et al., 2002; Habig et al., 1974). This process involves either nucleophilic substitution or addition, depending on the hydrophobic substrate (Amstrong, 1991). The conjugation between GSH and xenobiotics are illustrated in Figure 2.1.

GSH plays a pivotal role to protect cells against oxidative and electrophilic stress through their action as a cofactor for several enzymes that catalyze the inactivation and removal of toxic compounds, including GSTs (Antognelli et al., 2006; Jia et al., 2008). The conjugation of GSH and GSTs directly deactivates reactive molecules thus eliminate further damaging effects in cells. An oxidative stress is referring to a situation where homeostasis process is altered and the balancing

mechanism tilts in favor of reactive oxygen species (ROS) accumulation (Halliwell, 1999 as cited in Masella et al., 2005; Sheehan & McDonagh, 2008). In other word, it happens when the rate of ROS production is higher in comparison to the rate of neutralization process. Electrophilic stress refers to the reaction of a compound towards nucleophilic centres present in biomolecules resulted in the formation of new chemical bonds (Knapen et al., 1999).



Adopted from Townsend and Tew, (2003)

Figure 2.1 Glutathione conjugations to xenobiotics through GST action producing glutathione-S-conjugate

2.2 CLASSES OF GSTs

An early attempt to classify different forms of GST was made by Boyland and Chasseaud (1969, as cited in Mannervik and Danielson, 1988), introduced the terms aryltransferase, epoxide transferase, alkyltransferase, aralkyltransferase, and alkenetransferase. During that period, existing evidence suggested that GSTs could be discriminated based on their specificities toward electrophilic substrates. However, subsequent studies proposed that this classification method was no longer relevant. Separation and extensive purification of several forms of GST clearly demonstrated that they exhibited overlapping substrate specificities and their reactions were not restricted to a single functional group of the second substrate (Mannervik & Danielson, 1988; Sheehan et al., 2001). As an example, Pabst et al. (1973) in their paper revealed that the protein isolated as 'epoxide transferase' was also active with alkyl and aralkyl halogenides. Some more, even if they are included in the same family, their reactions towards various substrates are quite diverse; consistent with their physiological role (Wigger et al., 1997).

Currently, GSTs are divided into classes based on their amino acid sequence, immunological, kinetic, and structural properties (Alias & Clark, 2007). In general, GSTs with at least 40% identity (Sheehan et al., 2001 reported 60% identity) are belongs to the same family while less than 30% will be assigned into different family (Knapen et al., 1999; Yang et al., 2004). Generally, they are recognized as three main subfamilies which are; 1) the soluble or cytosolic GST (cGST), also known as canonical that can further be divided into subclasses depending on several criteria, 2) the microsomal GSTs or termed as MAPEG (membrane associated protein involved in eicosanoid and glutathione metabolism), and 3) the plasmid-encoded bacterial

for fomycin resistance GST (Frova, 2006). Within a particular subfamily, they may have diverged classes that share as much or greater than 90% identity (Hayes and Pulford, 1995 as cited in Sheehan et al., 2001). Apart of these three classes, Hayes et al. (2005) added another class of GST; mitochondrial GST which comprise soluble enzymes that make the whole group of four subfamilies. Mitochondrial GST, sometime termed as Kappa GST was previously misguided as Theta-class GST due to the basis of limited N-terminal sequence analysis before their cDNA and protein sequence were found to have major differences with other known mammalian GSTs (Frova, 2006). In addition to that, many other novel GSTs have been found currently with exclusive characteristics that do not suit in any classes described earlier (Frova et al., 2006).

Since GSTs are found in almost all living organism, there is a probability that the existence number of GSTs classes is actually larger than so far thought. As their presence is ranging from an aerobic single cell organism to higher organisms, it is thought they might have evolved over period of time thus producing a complex super family tree. Hansson et al. (1999) came out with of a hypothesis i.e. GST classes arose during DNA replication followed by divergence, perhaps involving a mechanism similar to DNA shuffling, resulting in novel catalytic activities. Up till this point, only a small number of GSTs have yet been described and it is possible that other classes actually exist which require more effort to be discovered. This literature, however, will be focused more on the soluble class of GSTs.

2.3 STRUCTURE OF GSTs

Each of GST family has their own unique structural design which thought to represent exclusive abilities that they carry. To be classified in the same subfamily, they must

share common features no matter how far their family trees are. For example; plant, animal, and bacterial cGSTs crystal structures show high level of structural conservation with common 3-D fold (Frova, 2006). They are found in dimer forms; either homodimers (identical subunits) or heterodimers (different subunits) (Frova, 2006). For a dimerization to take place, both subunits must be from the same gene class because it is accepted that different classes of monomers are incompatible (Dirr et al., 1994; Frova et al., 2006). Each of subunits commonly counts for 23-30 kDa with an average length of 200-250 amino acids (Frova et al., 2006).

The folding pattern of cGSTs is identical; each subunit consists of two spatially distinct domains that are N-terminal domain (domain I – comprise of β strands and α helices) and C-helical domain (domain II – all helices) (Frova et al., 2006; Sheehan et al., 2001). Each subunit contains about 48-59% α helix and 8-10% β strands (Dirr et al., 1994). Arrangement of Domain I is analogous to thioredoxin (TRX) fold in glutaredoxin ($\beta\alpha\beta\alpha\text{domain}\beta\beta\alpha$), which consist of N-Ter $\beta_1\alpha_1\beta_2$ and C-ter $\beta_3\beta_4\alpha_3$, linked by a long loop of α_2 (Frova, 2006). Structural design of TRX is illustrated in Figure 2.2 (a). Those N- and C-terminal regions form a β -sheet of three parallel and an antiparallel of β chain, squeezed in between α_2 and α_1 as well as α_3 on the other side. A loop containing highly conserved cis-Proline act as a connector between α_2 and β_3 strands, where this cis-Pro is important to maintain the protein in a catalytically competent structure (Frova, 2006 & Sheehan et al., 2001). Domain I is attached to Domain II (on downstream region) by a short linker sequence consist of ~ 10 amino acids (Frova, 2006). Domain II is predominantly an all- α -type core structure composed of five amphipathic α -helices (Dirr et al., 1994). Figure 2.2 (b) shows the organization of Domain II and its connection to adjacent Domain I. However, total numbers of α -helix strands may vary; depending on which GST class they are in (Sheehan, et al., 2001).

Intersubunit interaction between Domain I and Domain II that essential for dimerization and stability of quaternary structure can be either hydrophilic or hydrophobic interaction (Axarli et al., 2009; Board et al., 2000; Frova, 2006).

In each GST subunit, there are two distinct functional regions; 1) a hydrophilic G-site for glutathione association and 2) H-site that is important for electrophilic substrates binding (Chronopolou & Labrou, 2009; Dirr et al., 1994; Frova, 2006). Although they are catalytically independent, it is crucial to maintain the stability of dimeric form. Similar to other enzymes, any disruption in quaternary structure will affect substrate accessibility thus demolish the real function of GSTs. Dirr et al. (1994) reported that GSTs active sites will only be functioning when structural elements from both subunits are present, where the major structural framework is contribute by the conserved core of Domain I.

Binding of glutathione or its analogues at G-site is achieved through a specific polar interaction between the tripeptide and a number of protein moieties in Domain I of one subunit and one or two amino acid residues (depending on the GST classes) in Domain II of the other subunit. A molecule called G-site ligand is responsible in assisting glutathione binding to G-site which some of the residues are conserved within a class while some are either conserved or conservatively replaced between classes (Dirr et al., 1994). Involvement of these two subunits in G-site activation clarifies the necessity of GSTs dimeric form.

Clusters of non-polar amino acid side chains are found in the H-site structure which provides the hydrophobic surface that is accessible to bulk solvent in the absence of xenobiotic substrate or product (Dirr et al., 1994). The constitution of this site

involve elements from both Domain I and II of the same subunit, including the loop connecting $\beta 1$ to $\alpha 1$, the C-terminal terminal region of $\alpha 4$, and the C-terminal of segment of the polypeptide chain (Dirr et al., 1994). Since GSTs are highly specific toward substrate electrophiles and this interaction occur in the H-site, they must have some modification in the site structure that causes variation in substrate susceptibility. Dirr et al. (1994) reported the existence of different H-site topologies is due to sequence variability between gene classes explain the reasonably distinct xenobiotic-substrate specificities among various gene classes.

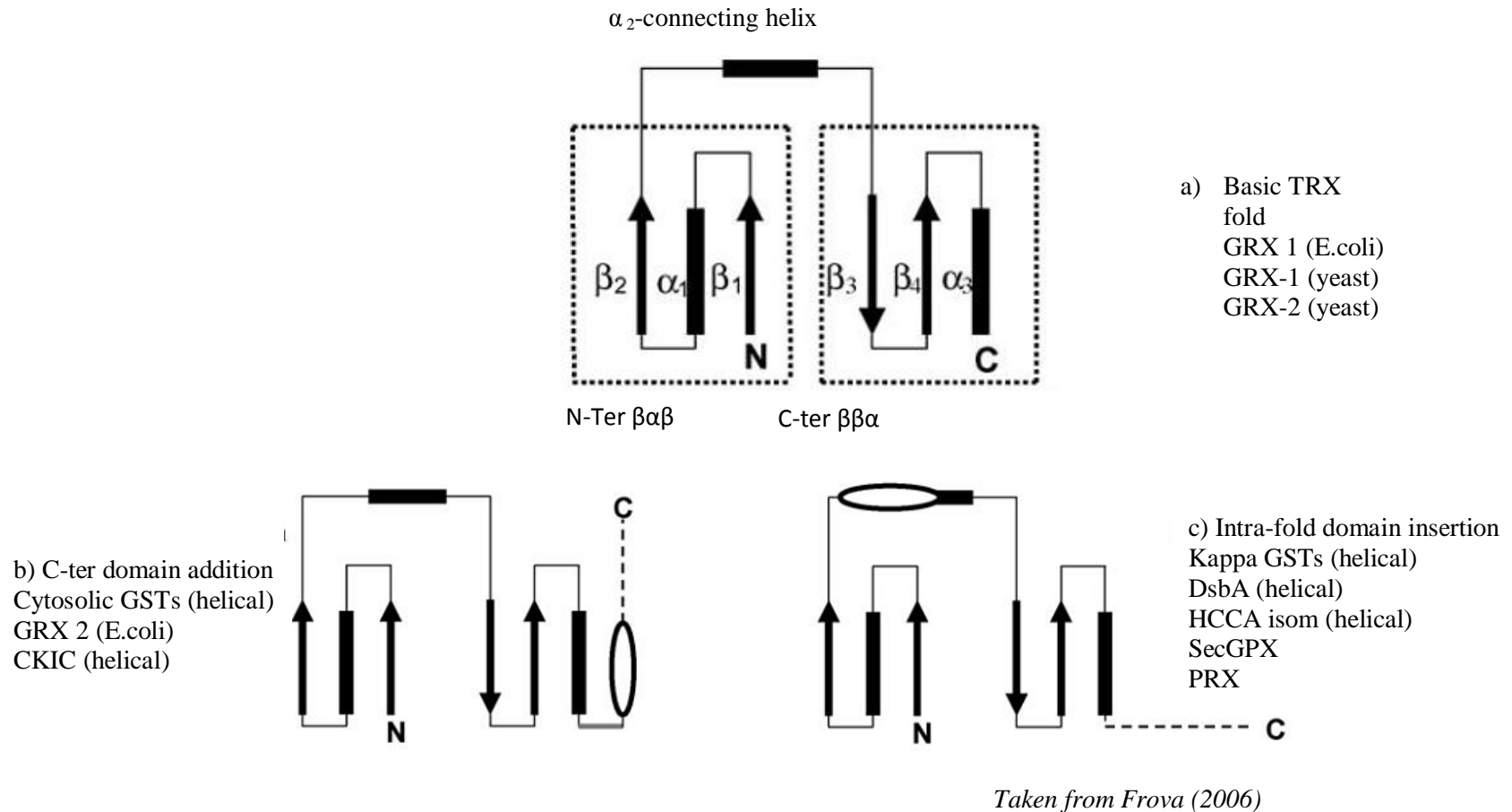


Figure 2.2 Diagram of TRX proteins secondary structure. Arrows indicate β strands, rectangles indicate α helices. Dotted squares in (a) indicate the N-terminal and the C-terminal motifs of the thioredoxin fold, connected by the α_2 helix. In (b and c), ovals mark the position of the second domain, while dashed lines indicate extra domains in some of the proteins listed below the diagrams. The grey thick line in (b) indicates the short linker between domains I and II of GSTs. The nature of the second domain is indicated in parenthesis near the proteins.

2.4 FUNCTION OF GSTs

At a glance, GSTs participate in the survival route of an organism when the organism is exposed to both exogenous and endogenously derived toxic compounds. Lee et al. (2007) reported that GSTs expression in most organisms is modulated in response to prooxidant xenobiotics, which was also reported by Masella et al. (2005). In that condition, cells will sense the hazard and confer corrective signals by stimulate GSTs production that later will convert toxic compound into a harmless substance.

As mentioned earlier, detoxification process is completed by the addition of thiol group ($-SH$) from glutathione thus neutralize the electrophilic sites of the toxic compound and rendering the products more water-soluble. It is then further metabolized by cleavage of the glutamate and glycine residues, followed by acetylation of the resultant free amino group of the glutamate and glycine residues to produce the final product; mercapturic acid (Habig et al., 1974). The mercapturic acids, i.e. S-alkylated derivatives of N-acetylcysteine, are then excreted by another enzyme (Habig et al., 1974). This mechanism shows the important function of GSTs in converting reactive molecules into a molecule that can be tolerated by the cells which indicates the ability of GSTs as a bioconversion agent in a living organism. Therefore, this mechanism enables cells to endure the stress and keep living in hazardous environment to maximal limit.

A part of their function in neutralizing exogenous toxic compound, GSTs also known to play a pivotal role as an endogenous antioxidant defense (Masella et al., 2005; Leiers et al., 2003). One popular example is through their action towards ROS which occur in abundant amount as many oxidative reactions take place within cells. Even

though ROS acts in different positive roles *in vivo*, it may also create damage at high oxidative level as ROS could attack the biological macromolecules; induce oxidation, cause in membrane and DNA damage, also enzyme inactivation (Halliwell, 1999 as cited in Masella et al., 2005). As a response to cope with the stressful condition, an organism would develop a sophisticated mechanism to maintain the level of ROS they could resist with, that is by GST involvement. A study conducted by Leiers et al. (2003) demonstrated an increase resistance level towards intracellular induced oxidative stress was achieved in transgenic BL1 *Caenorhabditis elegans*, with overexpression of *Ce-GST-p24*. When *Ce-GST-p24* gene was knocked out by RNAi manner, they found a decrease level of tolerance in RNAi-treated BL1 as compared to the untreated ones. However, RNAi-treated BL1 showed a better reaction in comparison to the wild type *C.elegans*. This study showed the direct correlation between those two variables thus indicates the function of GSTs in protecting cells from ROS negative effects. In this study, GSTs shows their capacity to normalize and balance the overproduction of ROS to keep the cell viability.

The original view of GSTs as solely detoxification enzymes has gradually changed with various findings in other functions it carries within the body system. It is now become assimilated that the roles of GSTs has extended from detoxification and antioxidant to non-stress metabolism, such as leukotrienes and prostglandins biosynthesis (Jakobsson et al., 1999; Knapen et al., 1999; Lee et al., 2007) and the catabolism of aromatic aminoacids (Thom et al., 2001). GSTs can serve as peroxidases, isomerases, and thiol transferases (Board et al., 2000), or have non-catalytic functions among which binding of non-substrate ligands and modulation of signaling processes (Axarli et al., 2004; Blanchette et al., 2007). These discoveries provide a strong foundation on their competency to work in several pathways thus show the importance

of this enzyme in the whole body systems, not only limited to their main function as detoxifying agent.

2.5 GSTs DISTRIBUTION AND EXPRESSION

GSTs are ancient protein with multiple roles found in all eukaryotic organisms and some prokaryotes, suggesting a wide-range distribution of GSTs in various kingdoms. For instance, cGST can be found ubiquitously in all aerobic organisms and often counting tens of members in each species; 15-20 different cGST genes have been identified in human and other mammalian species (Hayes et al., 2005), 40-60 in plants, 10-15 in bacteria, and over 10 in insects (Frova et al., 2006). The high occurrence of cGSTs found in wider taxonomic distribution suggest the importance of this enzyme hence indicates dependency of living organisms towards them in maintaining basic cell functions.

Depending on several criterias, cGSTs is further divided into numerous classes which some of them can be found throughout taxa and even kingdoms, while others are organism-specific (Frova et al., 2006). Till these very seconds, seven classes of cGSTs are recognized in mammals; Alpha, Mu, Pi, Sigma, Theta, Zeta, and Omega where the first three mentioned are unique to mammals only (Board et al., 2000; Robinson et al., 2004; Frova et al., 2006). On the other hands, plants consist of four specific GSTs; Lambda, Phi, Tau and DHAR (dehydroascorbate reductases), together with another two common GSTs; Theta and Zeta (Frova et al., 2006). In bacteria, the overall knowledge is still ambiguous but it is reported that they might possess a specific class named Beta, in addition to other enzymes mostly related to the common Theta GSTs (Frova et al., 2006). Classes of Sigma, Theta, Zeta and Omega are the common GSTs can be found

within the insects with addition of Delta and Epsilon classes that are unique to insect (Frova et al., 2006; Wang et al., 2008; Deng et al., 2009). It can be concluded that each species is more likely to comprise of two types of cGST which are; 1) unique to their taxa that function exclusively according to their physiological activities and 2) universal cGSTs that are shared among distinct taxa which probably functions in basal cell activities.

The distribution is not only take place between species but the isoenzymes are also distribute diversely within the organism i.e. tissue specific (Desmots et al., 2001; Knapen et al., 1999). Meister (1988, as cited in Knapen et al., 1999) reported that the highest GSTs activity appears to be in kidney and liver, probably related to the main function of these two organs in removing toxins produced from the body. Similar to the idea of their presence in different life forms, they might present in several organs or some might only expressed in a particular body part. For instance, Alpha class of GSTs that comprise at least four genes encoding hGSTA1, A2, A3, and A4 including several pseudogenes were found to be expressed in most human organs (Desmots et al., 2001). In other example, only a single GST was found to be appeared in the pollen while five distinct isozymes were found in the scutellum (Dixon et al., 2002). Their positioning is most likely due to the occurrence of their specific substrate at that specific site. Knapen et al. (1999) propose that variation of specific substrates between organs become the reason for specific expression of GST isozymes. However, this differential tissue profile is also correlated to other factors such as sex, age, and to physiopathological and genetic factor (Desmots at al., 2001).

2.6 BIVALVES

Similar to chitons (chain shells), gastropods (abalones) and cephalopods (squid and octopus), bivalves are included in the Phylum Mollusca and are one of six members of Class Bivalvia (Helm et al., 2004; Prado et al., 2010). They are said to first appear in the late Cambrian explosion which took ~530 million years ago and eventually dominate over brachiopods in the Paleozoic era (Gould & Calloway, 1980 as cited in Sheehan & McDonagh, 2008).

They are described by a shell which is divided from front to back producing two hinged valves that completely or partially cover the soft body parts (Prado et al., 2010; Sheehan & McDonagh, 2008). Their gills are very structured and not only function as a respiratory organ, but also serve as a filter-feeding apparatus (Helm et al., 2004; Prado et al., 2010; Sheehan & McDonagh, 2008; Sheehan & Power, 1999). When they are in substrate, water will be drawn through the inhalant opening, through the gills before returning back to the surrounding water through the exhalant opening (Helm et al., 2004).

Bivalve molluscs possess high commercial values as they are integrated in the human food chain thus forming a significant part of the world's fisheries production. In 2000, landings of bivalves from captured fisheries and aquaculture operations summed up 14 204 152 tonnes (Helm et al. 2004). During 1991 to 2000, bivalves show a continuing increase in production, and landings more than doubled from 6.3 million tonnes to 14 million during that decade (Helm et al., 2004). These figures explain that there is a high demand for bivalves in fishery industries hence showing that they are important for human consumption. They are harvested for food consumption or for other reasons such as pearl

oysters (Tanguy et al., 2008). In addition to that, many culture operations are developed to keep up with the increase of market demand towards bivalves. Helm et al. (2004) reported the growth of market operations which indicated from double amount of landings from culture operations compared to the wild landing during 1991 to 2000.

2.7 GSTs IN BIVALVES

Bivalves are capable to bioaccumulate environmental pollutants since they filter large amounts of water in order to meet their nutritional and respiratory need, therefore this activity could reflect the degree of pollution in their surrounding environment (Vidal et al., 2002; Yang et al., 2003). Their ability is extended to concentrate xenobiotics to many thousands times of the background which can facilitate a better chemical analysis (Sheehan & Power, 1999). Due to that reason, bivalves have been proposed to be used in biomonitoring programme. However, the capability possessed by bivalves to withstand stress condition alone could not provide adequate information about the level of contamination hence a complementary approach is needed.

Even though there are many other components related to the detoxification metabolism are available, GSTs always become the preferred module as a biomarker in environmental assessment (Vidal et al., 2002). Bivalves GSTs are gaining more popularity to be chosen as biomarker in marine pollution for several reasons. One of the remarkable findings in mussel shows that response of mussel GSTs towards environmental pollutants are unaffected by several biotic factors such as temperature, season, or age (Sheehan & Power, 1999; Vidal & Narbonne, 2000). The expression of mussel GSTs is different in fish which the activity of fish GSTs are found to be

dependent on environment temperature (Huang et al., 2008). It is assumed that GSTs from other molluscs species generally would retain this character thus, the use of bivalve GSTs become a great advantage to get a more consistent data in marine quality evaluation.

Until this very moment, purification and characterization of GST from vertebrate species is well developed but is less documented for invertebrates' species (Yang et al., 2003). Lack of information on GSTs from marine organisms was also reported thus result in ambiguous criteria in GSTs classification since current classification is based on the characterization of mammalian GSTs (Blanchette et al. 2007). However, recent evidence showed studies of marine organisms GSTs as well as GSTs induction in molluscs are increasing (Bebianno et al., 2007; Fitzpatrick et al., 1995; Looise et al., 1996; Vidal & Narbonne, 2000). So far, research evidence showed that there are different pattern in expression and distribution of GSTs observed within mussels, depending on their species. For example, Vidal and Narbonne (2000) reported that bulk of GST activity towards 1-chloro-2,4-dinitrobenzene (CDNB) were found to be localized in visceral mass of *Corbicula fluminea* and to a lesser extent in gill while Fitzpatrick and Sheehan (1993) reported the other way around in blue mussel, *Mytilus edulis*. This discrepancy may be caused by several factors while dissimilarities in physiological state may also contribute to the unique expression of GSTs among bivalve species.

To date, there is not many information available about overall classes of GSTs collected from bivalve molluscs. However, existing studies involving bivalves showed that most found GSTs were included in the pi-class (Fitzpatrick et al., 1995; Hoarau et al., 2002, Vidal et al., 2002) and only small amount are belongs to alpha-, mu-, and

sigma- class (Hoarau et al., 2002; Yang et al., 2002; Vidal et al., 2002). In a paper reported by Yang et al., (2004), they found that N-terminal domain of *MeGST* from *Mytilus edulis* possesses a thioredoxin fold, and the six helices of the C-terminal domain make a helical bundle which indicates this *MeGST* belongs to pi-class GST. Apart of that, blast analysis of *MeGST* protein sequence enclosed 40% identity with the pi class GSTs isolated from different organism, but less than 30% identity with other classes. This bioinformatics analysis provides a strong support to the first discovery about *MeGST* structure thus reaffirm the relation of *MeGST* and pi- class GST.

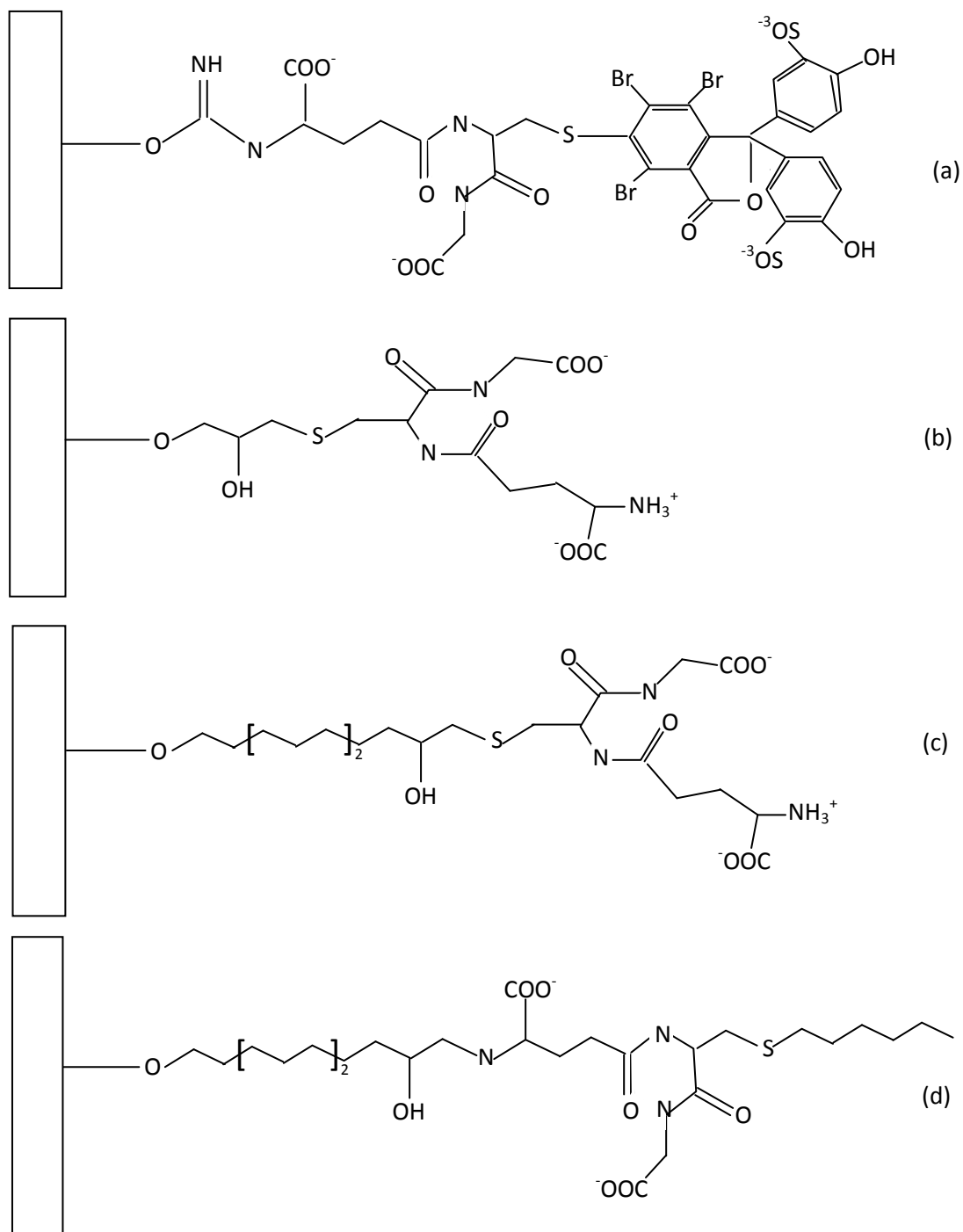
In other study conducted by Vidal et al., (2002), immunoblot analysis revealed all GST subunits obtained from visceral mass of *Corbicula fluminea* were related to pi-class GSTs while minor subunit were slightly related to mu-class. In a different study, Hoarau et al. (2002) investigated the immunological properties of each purified *Ruditapes decussates* GSTs using antisera anti-pi, anti-mu, and anti-alpha mammalian GST. Their study revealed that three isoforms showed similarity with pi-class, two isoforms reacted with antisera pi- and alpha-, one isoform reacted with antisera mu- and pi- and another one isoform recognized to show high identity (53%) with an alpha/mu/pi- GST from *Fasciola hepatica*. In a study conducted by Park et al. (2009), they managed to characterize the complete cDNA sequence of two GSTs from *Laternula elliptica* in the northern Antarctic peninsular that belongs to rho- and sigma-class of GST. This is such an interesting breakthrough since rho- class GST was previously found only in teleost fish (Liang et al., 2007). It further suggests that there is likely more extensive knowledge about bivalves GSTs have not been explored yet and remains a mystery. Therefore, more knowledge about the possible novel GSTs in bivalve will be a lot more than meaningful while possibility to discover new classes is available as long as long operations are conducted.

2.8 PURIFICATION OF GSTs

Jack bean urease became the first enzyme isolated ever in 1926 and since then, interest in protein purification began to grow rapidly. During the first half of twentieth century, the protein purification method were incredibly crude compared to current protocols, but there was increase since the first isolation where ~20 enzymes was successfully purified by 1940 (Voet & Voet, 2004). In general, proteins are purified using fractionation procedures by exploiting knowledge about physicochemical properties of selected proteins to separate them from undesired substances. The main idea of purification is not necessarily limited only to minimize the loss of desired protein, but to selectively eliminate the other components of the mixture thus leaving only the proteins of interest.

Many different strategies can be employed to purify GSTs and one of those ways is by applying affinity chromatography technique using various types of affinity matrices. This technique exploits the biochemical properties that are unique to the desired protein which brings huge advantage over the utilization of knowledge on physicochemical properties between proteins (Voet & Voet, 2004). The principle lies behind this technology is the ability of desired protein to bind tightly but noncovalently to specific molecules called ligand (Voet & Voet, 2004). In this method, a ligand that is covalently attached to an inert and porous matrix will bind specifically to the protein of interest. This specific interaction causes other protein to be washed through the column, thus allow elimination of undesired protein. Later, the ability to exploit sustainably the non-covalent interaction of proteins and ligand become a great advantage to recover protein of interest by changing the elution conditions such that the protein is discharged from the matrix.

Among many matrices widely used for GSTs purification are sulfobromophthalein-glutathione (BSP) conjugate immobilized to agarose matrix, GSH-agarose matrix (C₃ and C₁₂), and immobilized *S*-hexylglutathione (Figure 2.3). All the columns are different in such behavior they capture GSTs molecules. Therefore, it is assumed that application of different individual column or combination of columns in GSTs purification will produce variation results which allow the researchers to strategize their purification scheme. As an example, Alias and Clark (2007) used three different types of affinity matrix to isolate GSTs from *Drosophila melanogaster* and they had produced various results. In their study, the use of GSH-agarose (C₃) matrix results in purification of Sigma and Delta classes of GST, GSH-agarose (C₁₂) matrix results in purification of the same Sigma and Delta classes of GST with additional single putative Epsilon class (CG16936). The third matrix, BSP-GSH-Sepharose matrix were reported to isolate the widest spectrum of GSTs among all matrices used in their study.



Adapted from Alias (2006)

Figure 2.3 Structures of different types of affinity matrix used for GST purification. (a) Sulfobromophthalein-glutathione linked to agarose (Clark et al., 1977) (b) Glutathione with C₃ spacer linked to agarose by Clark et al. (1990) (c) Glutathione with C₁₂ spacer linked to agarose developed by Simons and van der Jagt (1977) and (d) S-hexylglutathione with C₁₂ spacer linked to agarose (Mannervik & Guthenberg, 1981)

2.8.1 Purification of bivalves GSTs

Most of the documented studies since have involved affinity chromatography to purify bivalves GSTs, particularly glutathione-sepharose affinity matrix and many scholar used more than one purification strategy. Yang et al. (2004) successfully recovered a recombinant protein of *MeGST* expressed in *Eschericia coli* by using GSH–Sepharose 4B affinity column. In a separate work conducted by Hoarau et al. (2002), they applied two affinity columns; GSH-agarose and S-hexyl GSH-agarose in the first step of purification, followed by purification using anion exchange chromatography. By using this approach, they collected seven fractions which present a GST activity with CDNB before analyzed the enzymes by using reverse-phase HPLC (RP-HPLC). Vidal et al. (2002) also used a similar approach; GSH-sepharose affinity chromatography and anion-exchange chromatography to purify cytosolic GSTs from freshwater clam, *Corbicula fluminea*. Yang et al. (2002) purified an isozyme of GST from liver intestine of *Asaphis dichotoma* using sepharose 4B affinity chromatography followed by RP-HPLC analysis. Therefore, despite the use of many available methods it can be assumed that affinity chromatography is still being a method of choice in purification strategy of bivalves GSTs.

2.9 PROTEOMIC APPROACH

Every biological sample expresses a set of proteins encoded in their genome and their expression either can be induced or suppressed by certain specific condition. Proteins are vital parts of living organism which constitute a huge portion of the mass of all organisms, and have significant role in the physiological metabolic pathways of biological systems. The term proteome was first coined in 1995 as an analogy term of

'genome' and was defined as the total protein complement to genome (Wasinger et al., 1995). Later, the term of proteomics were used in the study of proteome which is now defined as the aggregate of all proteins expressed by a cell or organism, but with emphasis on their quantitation, localization, modifications, interactions and activities, as well as their identification (Voet & Voet, 2004). Apart of this definition, Sheehan and McDonagh (2008) specifies the meaning by defining this term as total proteins expressed in a given sample under a defined set of conditions.

The idea of proteome is actually parallel to the central dogma of molecular biology principle that correlates DNA, RNA, and protein in the same frame. Unlike genome, proteome is highly dynamic; their expression is diverse depending on the cell type and their response to variables such as diet intake and exposure to environmental factors (Sheehan & McDonagh, 2008). Therefore, combination of techniques used in proteomic study can be a powerful tool to enhance our understanding in a biological system because proteomics can provide a rich source of information since proteins are involved in almost all metabolic activities. They could provide detail descriptions of the structure, function, and control of biological systems in health and disease by systematic study of the many and diverse properties proteins in a parallel manner (Patterson & Aebersold, 2003).

2.9.1 Two dimensional electrophoresis (2-DE)

Each protein molecule possesses charged groups of both polarities therefore has an isoelectric point, pI that is the pH at which proteins are static in an electric field. Hence, if a mixture of proteins runs through a solution in which the pH gradually increases

from anode to cathode, each protein will be separated according to their isoelectric point (Voet & Voet, 2004).

By combining isoelectric focusing (IEF) principle together with polyacrylamide gel electrophoresis, O'Farrell (1975) introduced a powerful technique named 2-dimensional electrophoresis (2-DE) that is able to separate protein according to their isoelectric point in the first dimension, followed by molecular weight separation using SDS-PAGE electrophoresis. This technology has evolved over time to improve the original version of 2-DE from a problem called 'cathodic drift'; a condition where the entire gradient tend to migrate towards the cathode area (Lognonné, 1994). Consequently immobilized pH gradients (IPGs) were developed with incorporation of ampholytes that works strips as a protein carrier along the plastic (Görg et al., 2004). After IEF step, the strips were laid on the SDS-PAGE gel and in this second dimension part; protein will further be resolved according to their molecular weight producing distinct and sharply defined spots when gel is stained.

This technology is mainly used as a protein expression profiling tool. They can separate complex protein mixtures from paired (or multiple) samples thus allow comparison of their relative abundance using image analysis tools (Patterson & Aebersold, 2003). The smallest gels used in 2-DE are able to isolate several hundred spots and up to thousands of spots may be resolved in the bigger size of gels (Sheehan & McDonagh, 2008). The great thing about this technique is proteins separated via 2-DE can be extracted from the gel matrix for subsequent analysis (Patterson & Aebersold, 2003). Due to that reason, regardless the presence of much more sophisticated technology in proteomic analysis, currently 2-DE become the only

technique that can be routinely applied for parallel quantitative expression profiling of large sets of complex protein mixture (Görg et al., 2004).

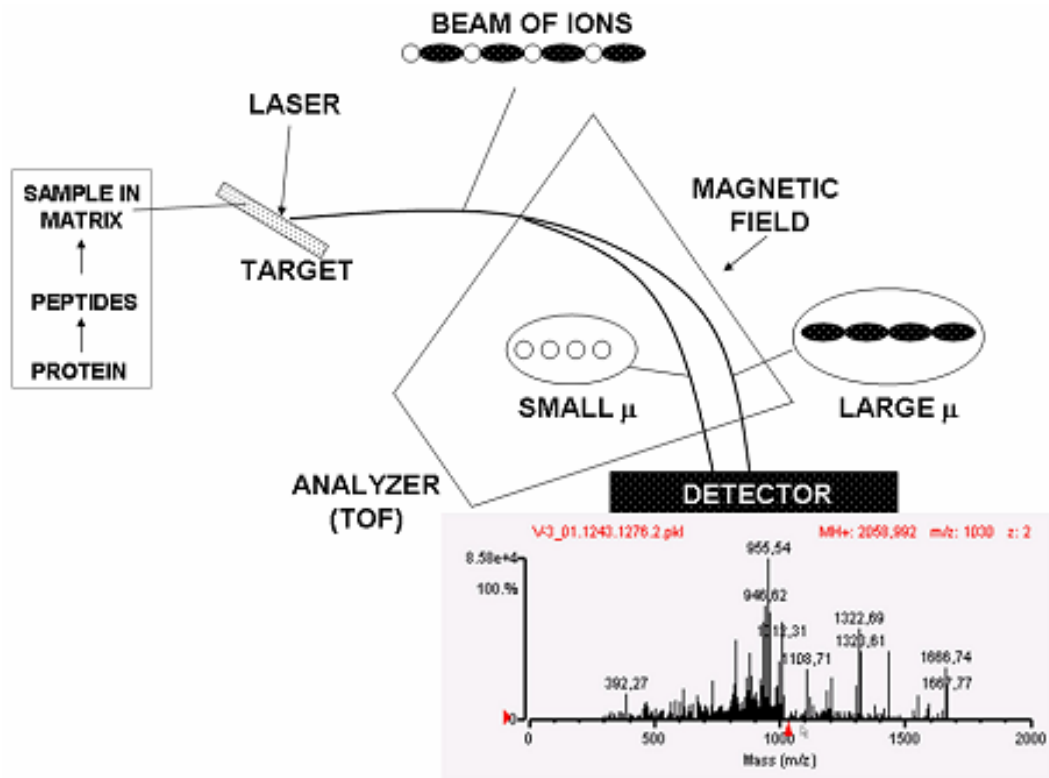
2.9.2 Peptide mass fingerprinting

Similar to DNA sequencing, peptide mass fingerprinting (PMF) was developed as an analytical means for protein identification by matching their fragment masses to the peptide masses in the established database. This technique becomes an effective way for identification of proteins provided the proteins has a relatively high purity since PMF often fails to identify a protein mixture (Thiede et al., 2005). Therefore, separations of complex protein samples are crucial before PMF could be applied. In PMF, proteins of interest are first cleaved using sequence-specific endoproteases, most notably trypsin to produce several fragments. Afterward, the digested products are investigated by determination of molecular masses, which resulted masses are compared with the protein peptide masses in database for protein identification.

Since many years ago, mass spectrometry has been the method of choice for analytical chemist's to analyze small molecules due to their ability to distinguish closely related species (Patterson & Aebersold, 2003). However, to measure mass-to-charge ratio (m/z) of molecule in a mass spectrometer, the analyte need to be ionized and transferred into the high vacuum system of the instrument, in which peptides and protein do not favor the condition that could destroy the molecule. During late 1980s, two methods that allowed ionization of peptides and proteins at high sensitivity without excessive fragmentation were developed; electrospray ionization (ESI) and matrix-assisted laser desorption ionization (MALDI) (Patterson & Aebersold, 2003). Both two

methods were first introduced by Fenn et al. (1990) and Tanaka et al (1988) respectively.

Among those two methods, MALDI is the most frequently used technique in conjunction with a ‘time-of-flight’ (TOF) detector to perform PMF (Sheehan & McDonagh, 2008). Combination of these two principles produce a platform namely MALDI-TOF. By using this platform, sample is mixed with a ‘matrix’ that have the ability to absorb some of the laser energy used to ionize the protein and then placed on a target for laser-induced ionization. Figure 2.4 shows the schematic diagram of MALDI-TOF system. This technology is known to give rapid detection, easy to perform, sensitive, able to produce accurate result, tolerant to a certain level of contaminants and can be automated (Thiede et al., 2005).



Courtesy of Sheehan and McDonagh (2008)

Figure 2.4 Outline of MALDI-TOF analyzer. Sample is mixed with matrix (e.g. sinapinic acid) on a target. A laser beam impacts on this imparting sufficient energy to peptides or proteins to propel them through the TOF analyser. From the estimation time required by each peptide to reach the detector, an accurate m/z value can be calculated and by aligning masses of tryptic peptides to masses predicted from sequence databases could identify proteins of origin by Peptide mass fingerprint.

CHAPTER 3

MATERIALS

3.1 SAMPLE

Remis (*Donax* sp.) used in this study was kindly provided by Dr. Zazali Alias, Senior Lecturer of Universiti Malaya and was collected from Pantai Remis, Jeram, Selangor. The nomenclature of the species was based on guidance taken from www.fishdepat.sabah.gov.my/download/redtideInfo.doc.

3.2 REAGENTS AND APPARATUS

Biorad Laboratories, Richmond, USA

30% Acrylamide/Bis Solution, 29:1 (3.3% C)

1.5 M Tris, HCl, pH 8.8

1.5 M Tris, HCl, pH 8.8

N,N,N',N'-methyleneethylenediamine (TEMED)

3-[(3-cholamidopropyl)dimethylammonio]-1-propanesulfonate (CHAPS)

Invitrogen™, California, USA

BENCHMARK™ Protein Ladder

Pre-cast Novex® IEF Gel

Novex® IEF Anode (Lower) Buffer (50X)

Novex® IEF Cathode (Upper) Buffer (10X)

Novex® Tris-Glycine SDS Running Buffer (10X)

ZOOM® Carrier Ampholyte (3-10)

Merck KGaA, Darmstadt, Germany

Iodoacetamide (IA)

Sodium hydroxide (NaOH)

Dithiothreitol (DTT)

Sartorius Stedim Biotech, Germany

Minisart® syringe filter (20 µm)

Vivaspin concentrator (10000 MWCO; 20 ml)

Sigma-Aldrich, St. Louis, USA

Ethylenediaminetetraacetic acid (EDTA)

Proteinase inhibitor cocktail

N-phenylthiourea (PTU)

Sodium dodecyl sulphate (SDS)

Coomassie brilliant blue (CBB)

4-nitrocinnamaldehyde (NCA)

Brilliant Blue G (Coomassie Blue G-250)

Thiourea

1-chloro-2,4-dinitrobenzene (CDNB)

1,2-dichloro-4-nitrobenzene (DCNB)

p-nitrobenzylchloride (NBC)

Sulfobromophtalein (BSP)

Ethacrynic acid (EA)

Trans-4-phenyl-3-butene-2-one (PBO)

Albumin bovine serum (BSA)

R & M Chemicals, Malaysia

Sodium dihydrogen phosphate

Ammonium persulfate (APS)

Trichloroacetic acid (TCA)

Urea

Sodium carbonate

System, Malaysia

Glycerol

Methanol

Acetic acid

Formaldehyde

Ethyl alcohol 95%

Sodium thiosulfate

Silver nitrate

Ortho-phosphoric acid-85%

Ammonium sulfate

Promega, Madison, USA

Tris base

Agarose

BDH Laboratory Supplies Poole, England

Bromophenol blue

Fisher Scientific (M) Sdn. Bhd.

Absolute ethyl alcohol

GE Healthcare, Uppsala, Sweden

ImmobilineTM DryStrip, pH 3-10, 7 cm

PlusOne DryStrip Cover Fluid

GSTrapTM HP Columns (5 ml)

SERVA Electrophoresis GmbH, Heidelberg, Germany

SERVALYTTM PRECOTESTM (pH 3-10)

3.3 INSTRUMENTS

WiseTis® homogenizer (Witeg, Germany)

Mini-PROTEAN® Tetra Cell electrophoresis (Biorad Laboratories, Richmond, USA)

PowerPac™ Basic power supply (Biorad Laboratories, Richmond, USA)

XCell *SureLock*™ Mini-Cell (Invitrogen™, California, USA)

PowerEase® 500 power supply (Invitrogen™, California, USA)

ÄKTAprime™ Plus (GE Healthcare, Uppsala, Sweden)

Image Scanner III (GE Healthcare, Uppsala, Sweden)

Multiphor™ II Electrophoresis System (GE Healthcare, Uppsala, Sweden)

Weighing balance (Mettler-Toledo International Inc., Columbus, USA)

Centrifuge 5810 R (Eppendorf, Hamburg, Germany)

CHAPTER 4

METHODOLOGY

4.1 SAMPLE PREPARATION

Sodium phosphate buffer was used to prepare sample for chromatography analysis. The total of 5 g of *Donax* sp. (remis) whole flesh was homogenized in 40 ml buffer by using a WiseTis® homogenizer. Homogenizing buffer in this study was a 25 mM phosphate buffer (pH 7.4) containing 500 µl protease inhibitor cocktail (prepared as instructed in manual), 1.0 mM EDTA, 0.1 mM DTT, and a half spatula of PTU. The homogenate then centrifuged for 60 minutes at 10 000 rpm. Pellet was discarded and supernatant collected was filtered using syringe filter. This filtered supernatant was designated as 'crude enzyme'. All preparation was performed at all times 4°C. Details can be acquired in Appendix A.

4.2 AFFINITY CHROMATOGRAPHY

In this study, two different types of matrices were used; 1) GStap™ HP column (bed volume : 5 ml ; binding capacity of 10 mM/ml) and 2) GSH-agarose (C₃) column (bed volume : 1 ml; binding capacity of 10 mM/ml) supplied by Dr. Zazali Alias. Affinity chromatography was carried out using an automated sytem (ÄKTAprime Plus™) equipped with PrimeView 5.0 software. Both columns were equilibrated with 20 ml of 25 mM sodium phosphate buffer, pH 7.4 prior usages (Appendix A). The flow rate was set at 18 ml/hour during sample application and protein profile was monitored during the whole process. Proteins bound to the column were eluted using 10 mM glutathione in 25 mM sodium phosphate buffer, pH 7.4.

4.3 PROTEIN CONCENTRATION

Protein was concentrated by using Vivaspin concentrator (10000 MWCO; 20 ml). Sample was centrifuged at 10 000 rpm for 5-10 minutes. The temperature was set at 4°C.

4.4 QUANTITATIVE PROTEIN ESTIMATION (BRADFORD)

The Bradford assay procedure was carried out as outlined by Spector (1978) to estimate protein concentration. Bradford reagent was prepared as in Appendix D. The absorbance readings were taken by using a spectrophotometer and protein standard was prepared in duplicate. Aliquots of BSA stock (2 µg/µl) were pipette into test tubes (5, 10, 15, 20, 25, 30, 35, 40, 45, and 50 µl corresponded to 10, 20, 30, 40, 50, 60, 70, 80, 90, and 100 µg of BSA). Distilled water was added to each test tube making the final volume as 100 µl while reagent blank was prepared by addition of 100 µl distilled water. Unknown samples were prepared in dilutions of 2 to 10-fold. To every samples and standard, 5 ml of Coomassie blue reagent was added, pursued by vortexing. Samples were left for at least 5 minutes (but less than 1 hour) before the absorbance was read at 595 nm. A standard graph was prepared by plotting average absorbance reading against BSA content. Protein content of unknown samples was estimated through the standard. The standard curve is shown in Appendix G.

4.5 ENZYME ASSAYS FOR SUBSTRATE SPECIFICITY AND ACTIVITY CALCULATION

Enzyme activities were determined at 25°C in a spectrophotometer. Each assay was run in triplicate together with a control that was a complete assay mixture without sample. Total volume of each assay was 3 ml. Procedures of all assays are similar; buffer, enzyme, and GSH were added in that order into the cuvette followed by incubation in the cuvette compartment. After 10 minutes, substrate was added to initiate the reaction. Details for each assay conditions are included in Appendix E.

4.6 ELECTROPHORETIC ANALYSIS

4.6.1 Laemmli Discontinuous Sodium Dodecyl Sulfate-Polyacrylamide Gel Electrophoresis (SDS-PAGE)

SDS-PAGE analysis was performed according to the procedure set by Laemmli (1970) using a Mini-PROTEAN® Tetra Cell electrophoresis unit with a PowerPac™ Basic power supply. The apparatus was prepared according to the instruction set by the manufacturer. Gel was prepared in two layers which the pH of resolving gel is usually much higher with more polyacrylamide content contrast to stacking gel. Gel preparation was as set out in Appendix B. The electrophoresis was run at 120 V for about 2 hours.

4.6.2 Subunit Molecular Weight (MW) Determination

SDS-PAGE allows dissociation and separation of GST dimers. For the purpose of MW estimation, a protein standard (BENCHMARK™ Protein Ladder) was applied

alongside the samples. A linear graph of relative mobility against \log_{10} MW of protein standard was plotted and used to determine the subunit molecular weight. Bands of 20, 25, 30, 40, 50, 60, 70, and 80 kDa obtained from the protein standard were used to construct the calibration plot (Appendix H).

4.6.3 Isoelectric Focusing (IEF)

The IEF method was carried out by using XCell *SureLock*TM Mini-Cell apparatus connected to PowerEase® 500 power supply. Gel used was a pre-cast Novex® IEF Gel containing 5% polyacrylamide with pH 3-10. Two different buffers were prepared before the experiment was run; anode and cathode buffer where both were pre-chilled to 4⁰C prior use. Samples were prepared by addition to sample buffer in the ratio of 1:1. A protein marker for IEF (SERVALYTTM PRECOTESTM, pH 3-10) was applied alongside the samples. The electrophoresis unit was assembled according to the manual instruction. A constant voltage of 100V was first applied at room temperature for one hour and then increased to 200V for another hour. The last stage required a constant power of 500V for 30 minutes. Then, the gel was removed from the cassette and fix in 12% TCA containing 3.5% sulfosalicylic acid for 30 minutes before silver stained. Preparation of all buffers can be obtained in Appendix C.

4.7 TWO-DIMENSIONAL GEL ELECTROPHORESIS (2-DE)

4.7.1 Sample application by in-gel rehydration

As sample was already dissolved in water, they were directly applied to the rehydration solution containing 8 M urea, 2% (w/v) CHAPS, 0.15% (w/v) DTT, 30 mM thiourea,

and 2% ampholyte (pH 3.0 – 10.0). The 70 mm strips used (Amersham Immobiline™ DryStrips, pH 3.0 - 10.0, 7cm) required 125 µl of rehydration buffer. Therefore concentrated GST was added with rehydration buffer to a total volume of 125 µl in an eppendorf tube. The immobiline drystrip was put into the plastic pipette that served as a rehydration tray in the position gel-side down. One end of the pipette was sealed with parafilm. Then, rehydration solution containing samples was distributed evenly under the strip. During this step, precautions were taken to ensure no bubbles trap between solution and gel. The gel was allowed to rehydrate for 10 to 24 hours at room temperature, preferably overnight rehydration. Details preparation of rehydration buffer can be seen in Appendix F (i).

4.7.2 Preparation for the first dimension – isoelectric focusing (IEF)

Approximately 5-10 ml of DryStrip Cover Fluid was pipette on to the cooling plate placed in Multiphor II Electrophoresis unit. Then, an Immobiline DryStrip tray was positioned slowly on the cooling trap to avoid formation of large bubbles between the tray and cooling plate thus create good contact between those two parts. An immobiline strip aligner was placed on top of the tray with its groove side up. Then, two IEF electrode strips was cut to a length of 110 mm each and placed onto a clean flat surface. The electrode strips were evenly soaked with 0.5 ml dH₂O. Excess water was removed by blotting with paper towel gently.

Next, rehydrated strips was pulled out by using clean forceps, rinsed with dH₂O and put on a sheet of damp filter paper; gel side up. Then, strip was transferred onto the groove of immobiline strip aligner with gel side up in the position where acidic end placed near the anode and vice versa. If several IPG strips were aligned in the grooves,

it is important to ensure that the anodic gel edges were lined up. Then, moistened IEF Electrode Strips was placed on top of the aligned strips at both cathode and anode side. The IEF Electrode Strips was put at least partially on top of the gel surface. Afterward, the electrodes was positioned on top of IEF electrode Strips.

Approximately 5 ml of DryStrip Cover Fluid was poured onto the tray to completely cover the strips. In this experiment, Amersham immobilized pH gradient strips at 70 mm length were used and the IEF was run using EPS 3501 XL power supply (GE Healthcare). Three stages were programmed in gradient mode that are; (1) first stage : 200 V : 5 mA : 2 W : 0:01 hour, (2) second stage : 3500 V : 5 mA : 2 W : 1:30 hour, (3) third stage : 3500 V : 5 mA : 2 W : 1:30 hour. Once the first dimension completed, IPG strips were immediately prepared for second dimension.

4.7.3 Preparation of the second dimension (SDS-PAGE)

All strips from the first dimension need to be equilibrated twice, 10 minute for every step. Each 70 mm IPG strip require 2.5 ml equilibration buffer containing 50 mM Tris-HCl (pH 8.8), 6 M urea, 35% (v/v) glycerol, and 2% (w/v) SDS. For first equilibration, 0.25% (w/v) of DTT was dissolved in equilibration buffer prior use. This equilibration solution, namely equilibration solution I was poured into a centrifuge tube and strip was placed into individual tubes with gel side up. The tube was capped and put on a shaker for 10 minutes. In the mean time, the second equilibration solution (equilibration solution II) was prepared by the addition of 4.5 % (w/v) of iodoacetamide (IA) and traces of bromophenol blue. Similar to first step of equilibration, strip was soaked in equilibration solution II for 10 minutes. Preparation of equilibration buffer can be seen in Appendix F (ii).

Once both equilibrations accomplished, the second dimension was performed. The equilibrated strip was positioned in between the plates with the gel edge touching the surface of the SDS-PAGE gel. At this step, extra precautions were taken to avoid bubbles between the two gels. The molecular weight marker was applied at one end (acidic) of the strip. Then, agarose sealing solution containing 0.5 % (w/v) agarose in SDS electrophoresis buffer was pipette onto the strip to stabilize them during electrophoresis. Details for agarose sealing solution preparation can be acquired in Appendix F (iii). Electrophoresis was run at a constant 120 V, similar to SDS-PAGE protocol.

4.8 GEL STAINING

4.8.1 Silver Staining

Silver stain used for staining the IEF native gel was adopted from Vorum and Blum (2000). In this procedure, the gel was fixed in a solution containing 50% (v/v) methanol, 12% (v/v) acetic acid, and 0.05% formaldehyde for 2 hours or overnight. It was subsequently washed three times in 35% (v/v) ethanol, 20 minutes each followed by soaking in sensitizing solution containing 0.025% (w/v) sodium thiosulphate for 2-3 minutes. Later, the gel was washed in water tree times, 5 minutes each. It was then submerged in fresh silver nitrate solution containing 0.2% (w/v) silver nitrate and 0.072% (v/v) formaldehyde. The gel was rinsed with water for 5-10 seconds, 2 times before soaked into developing solution containing 6% (w/v) sodium carbonate, 0.05% (w/v) formaldehyde and 0.0005% (w/v) sodium thiosulphate. The gel was left in the solution until dark enough before the reaction was stopped using 50% (v/v) methanol and 12% (v/v) acetic acid. The gel was stored in 1% (v/v) acetic acid in 4°C.

4.8.2 Coomassie Colloidal blue-staining (MALDI-TOFF compatible)

Colloidal Coomassie Blue was used to stain SDS-PAGE and 2D gel owing to its sensitivity and compatibility with subsequent mass spectrometric analysis. The procedure was adopted from Neuhoff et al. (1988). To prepare a liter stock solution, 100 g of ammonium sulfate was dissolved in approximately 500 ml milli-Q water. In a separate beaker, 2% (w/v) of *ortho*-phosphoric acid (85%) was poured into 20 ml of aqueous 5% (w/v) Coomassie Brilliant Blue G-250 (CBB). Then, mixture of CBB and phosphoric acid was poured slowly into the beaker containing ammonium sulfate and the volume was made up to 1000 ml. This solution was shaken vigorously before use for even distribution of colloidal particles. The actual staining solution was prepared by mixing 20 ml of methanol with 80 ml of stock solution. The staining solution was prepared fresh and discarded after use. During staining, the container was sealed properly and shaken gently overnight. After staining, the gel was immersed in a 20% (v/v) methanol to wash off the undissolved colloidal particles.

4.9 MALDI-TOF ANALYSIS

Protein spots (approximately 1 mm³) were excised from the GSTrapTM HP matrix gel using a clean scalpel and were transferred into individual Eppendorf tubes. Samples were dried and sent to Proteomics International (Perth, Australia) for mass spectrometry analysis. A standard technique of Bringans et al. (2008) was applied to the protein samples during the process and peptides generated were analyzed by MALDI TOF-TOF mass spectrometer using a 5800 Proteomics Analyzer (AB Sciex). Bovine serum albumin was used as a standard. Peptides generated were analyzed by the company

using Mascot, a search engine that uses mass spectrometry data to identify proteins from primary sequence databases (www.matrixscience.com)

Generated mass spectra of the peptides were also analyzed using ProFound software, a tool for searching a protein sequence collections with peptide mass maps (<http://prowl.rockefeller.edu/prowl-cgi/profound.exe>). ProFound was developed based on Bayesian algorithm to rank the protein sequences in the database according to their probability of producing the peptide map. The Z score was calculated for each candidate sequence indicating the probability of that candidate belongs to a random match population which value of 1.65 or lower signifies that the candidate is likely to be random match with 95 % confidence. ProFound included several informations, such as the type of digestion, links to the appropriate database and taxa, and range of *pI* and molecular masses of the samples. One missed cleavage *per* peptide was allowed and an initial mass tolerance of 0.05 Dalton was set up in all searches. Partial carbamidomethylation of cysteine and partial modification of methionine (methionine oxidation) were assumed.

CHAPTER 5

RESULTS

5.1 PURIFICATION OF GST USING DIFFERENT GSH-AGAROSE BASED MATRICES

The purification of GSTs expressed in *Donax* sp. was carried out using an automated system of chromatography (ÄKTAprime Plus™). In this study, two different GSH-agarose based matrices were used; GSTrap™ HP Matrix and GSH-agarose (C₃) matrix. These two matrixs are differed by the length of spacer arm between GSH and agarose hence result in variation of GSTs attachment behavior. In this report, term void is used to define collected fractions containing proteins that do not bind to the matrices.

5.1.1 Purification of GSTs using GSTrap™ HP matrix

Crude homogenate obtained from 5 gram of *Donax* sp. was loaded through a commercial GSH-agarose (C₁₂) matrix (GSTrap™ HP) and run at 18 ml/hour. The bound GSTs were eluted with 10 mM glutathione at pH 7.4 after all sample through the matrix. Chromatogram scheme for GST purification from GSTrap™ HP matrix is shown in Figure 5.1.

Results obtained for the purification of the conjugating activity with the GSTrap™ HP matrix are shown in Table 5.1 (a). By using Bradford assay, material eluted with GSH at pH 7.4 was known to contain 0.344 ± 0.146 mg of protein. In the enzymatic assay using CDNB, activity was detected not only in eluate fraction but was also detected in the void fraction. Of the enzyme activity, 12% was retained on the

affinity matrix and gave purification factor of 90- fold. Specific activity of 23.378 $\mu\text{mol}/\text{min}/\text{mg}$ was measured in eluate fraction.

5.1.2 Purification of GSTs using GSH-agarose (C₃)

Similar to section 5.1.1, crude homogenate obtained from 5 gram of *Donax* sp. flesh was run through a GSH-agarose (C₃) matrix and run at 18 ml/hour followed by elution with 10 mM glutathione at pH 7.4. Chromatogram scheme for GST purification from GSH-agarose (C₃) is shown in Figure 5.2.

Results obtained from this purification scheme are shown in the Table 5.1 (b). Total protein attained from eluate was 0.126 ± 0.061 mg, which was only about one third of protein eluted from GSTrapTM HP matrix. In CDNB assay, activities were detected not only in eluate fraction, but also in void volume which was similar to result in Table 5.1 (a). In this scheme, the yield percentage of eluate was 3% with purification factor of 60- fold. The specific activity of eluate was 9.054 ± 0.420 $\mu\text{mol}/\text{min}/\text{mg}$, which was lower than GSTs obtained from GSTrapTMHP matrix.

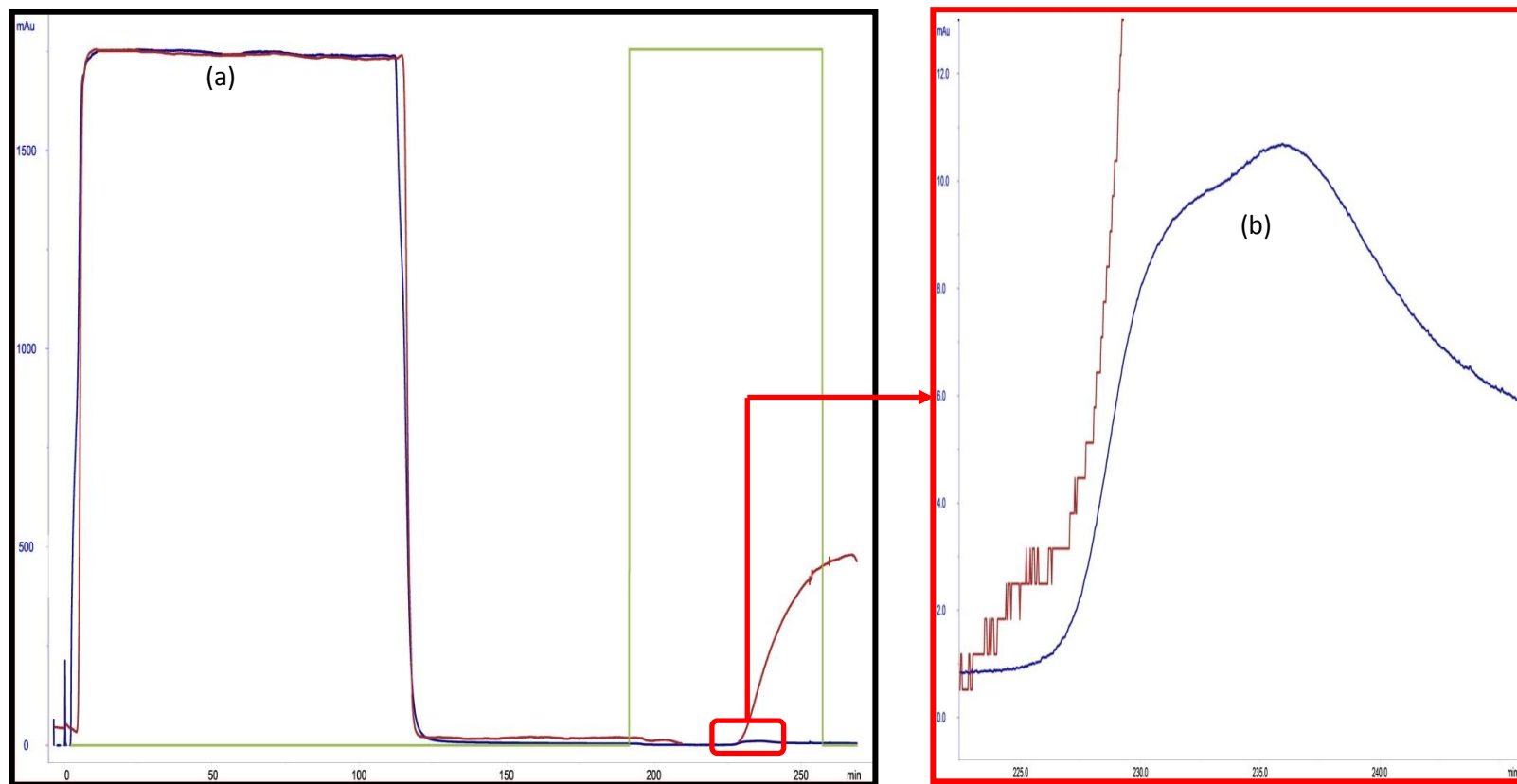


Figure 5.1 Chromatogram of GST purification using GSTrap™ HP. The crude extract obtained from 5 g of *Donax* sp. was charged on to the matrix (bed volume : 5 ml). The conditions of sample application and elution were programmed using ÄKTA PrimePlus. Area outline as (█) was fraction eluted with 10 mM GSH in 25 mM phosphate buffer, pH 7.4. (a) Unbound protein peak (void). (b) Enlarged image of affinity peak eluted with 10 mM GSH at pH 7.4.

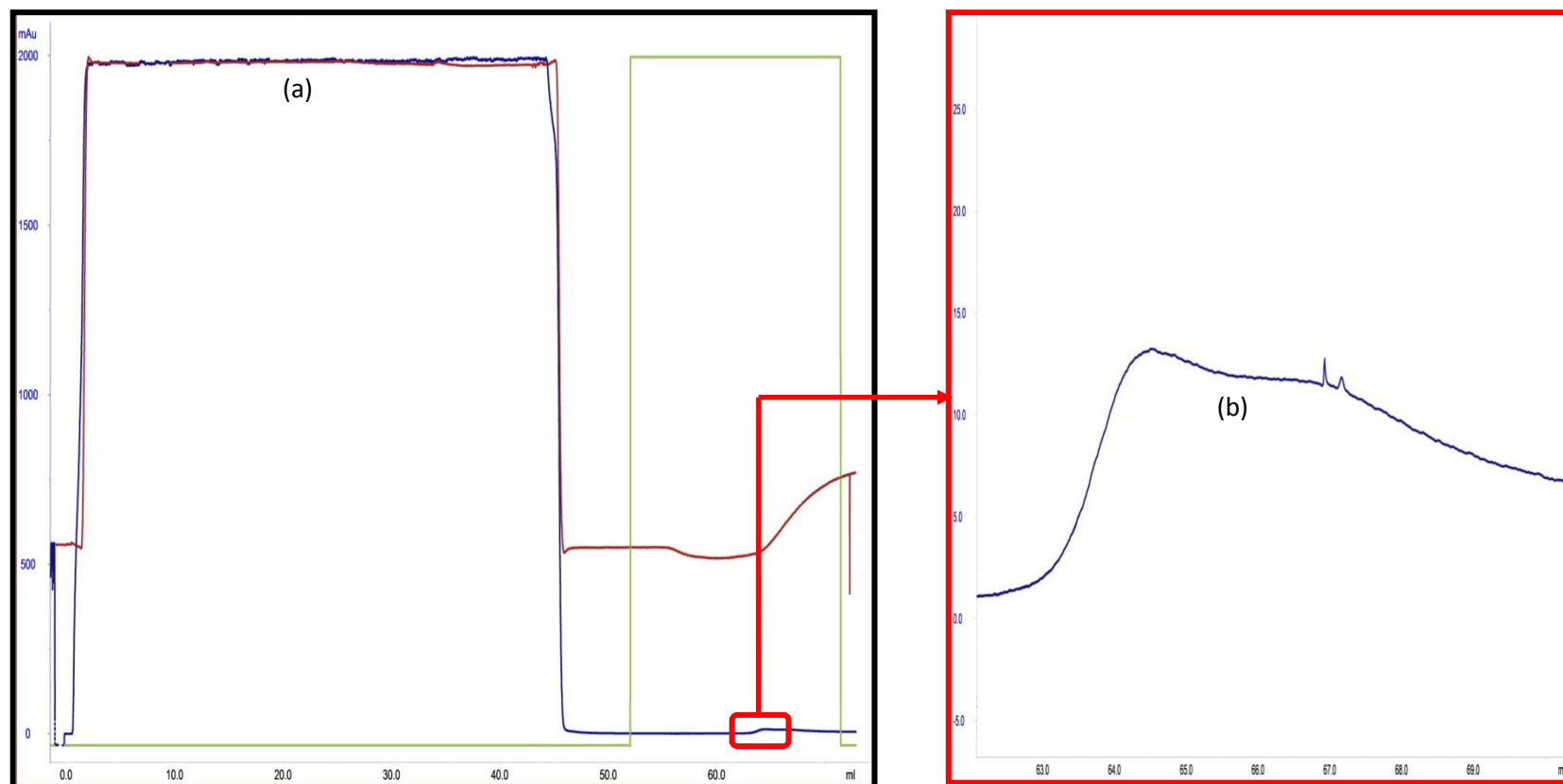


Figure 5.2 Chromatogram of GST purification using GSH-agarose (C₃). The crude extract obtained from 5 g of *Donax* sp. was charged on to the matrix. (bed volume : 1 ml). The conditions of sample application and elution were programmed using ÄKTA PrimePlus. Area outline as (█) was fraction eluted with 10 mM GSH in 25 mM phosphate buffer, pH 7.4. (a) Unbound protein peak (void). (b) Enlarged image of affinity peak eluted with 10 mM GSH at pH 7.4.

Table 5.1 Purification of GSTs from *Donax* sp. by two different GSH-based affinity matrix; GSTrapTM HP and GSH-agarose (C₃)

	Total protein (mg)	Total activity ($\mu\text{mol}/\text{min}$) (CDNB)	Specific activity ($\mu\text{mol}/\text{min}/\text{mg}$) (CDNB)	Purification fold (X) (CDNB)	Yield (%) (CDNB)
(a) GSTrap TM HP					
Crude homogenate	244.246 \pm 0.051	63.266 \pm 1.831	0.259 \pm 0.007	1	100
Void	240.758 \pm 26.104	53.788 \pm 3.902	0.224 \pm 0.019	0.846	83.43 \pm 0.062
Affinity Eluate	0.344 \pm 0.146	9.048 \pm 0.344	23.378 \pm 5.697	90.253	12.72 \pm 0.031
(b) GSH-sepharose (C ₃)					
Crude homogenate	226.762 \pm 27.544	33.582 \pm 2.094	0.148 \pm 0.009	1	100
Void	171.356 \pm 0.147	32.26 \pm 4.08	0.188 \pm 0.024	1.271	96.06 \pm 0.121
Affinity Eluate	0.126 \pm 0.061	1.144 \pm 0.053	9.054 \pm 0.420	61.13	3.41 \pm 0.002

*Values are means \pm SD taken from three independent replications

5.2 SDS-PAGE ANALYSIS

Purified GSTs in the eluate was concentrated prior protein analysis. In this study, SDS-PAGE was used to determine molecular weight of protein and as a preliminary means to illustrate the purity of protein gained during the whole process.

5.2.1 SDS-PAGE for protein purified from GSTrapTM HP matrix

Figure 5.3 shows gel visualization of proteins eluted from GSTrapTM HP matrix using 10 mM glutathione at pH 7.4. After the purification of *Donax* sp. GSTs by this GSH-based affinity matrix, SDS-PAGE revealed two distinct protein bands corresponding to the 26 and 29 kDa GST subunits. In addition to that, the smaller monomer subunit of GST shows considerable band intensity compared to the 29 kDa subunit.

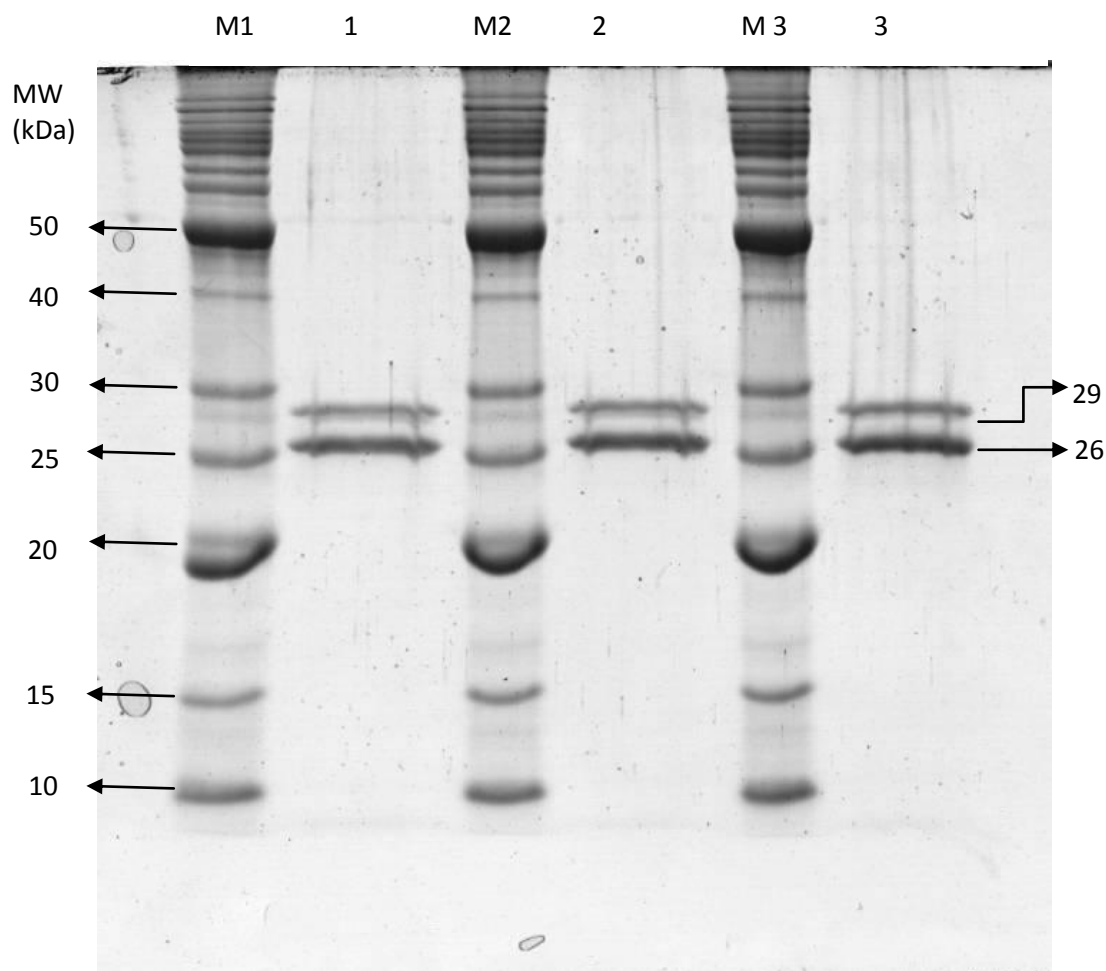


Figure 5.3 SDS-PAGE (12%) of active proteins fraction eluted from GSTrap™ HP matrix. A total of 8.6 µg protein was loaded into each Lane 1, 2, and 3. The gel is stained using Coomassie Blue G-250. (a) Lane M1-M3 : Protein marker (BENCHMARK™ Protein Ladder). (b) Lane 1-3 : Concentrated eluate.

5.2.2 SDS-PAGE for protein purified from GSH-agarose (C₃)

Figure 5.4 shows SDS-PAGE of GST purified using GSH-agarose (C₃) matrix. Unlike result in section 5.2.1, three bands were visualized on the gel equivalent to 26, 28, and 29 kDa GST subunits. Even so, the smaller monomer subunit of GST shows remarkable intensity compared to the same protein purified using GSTrap™ HP matrix (Figure 5.3).

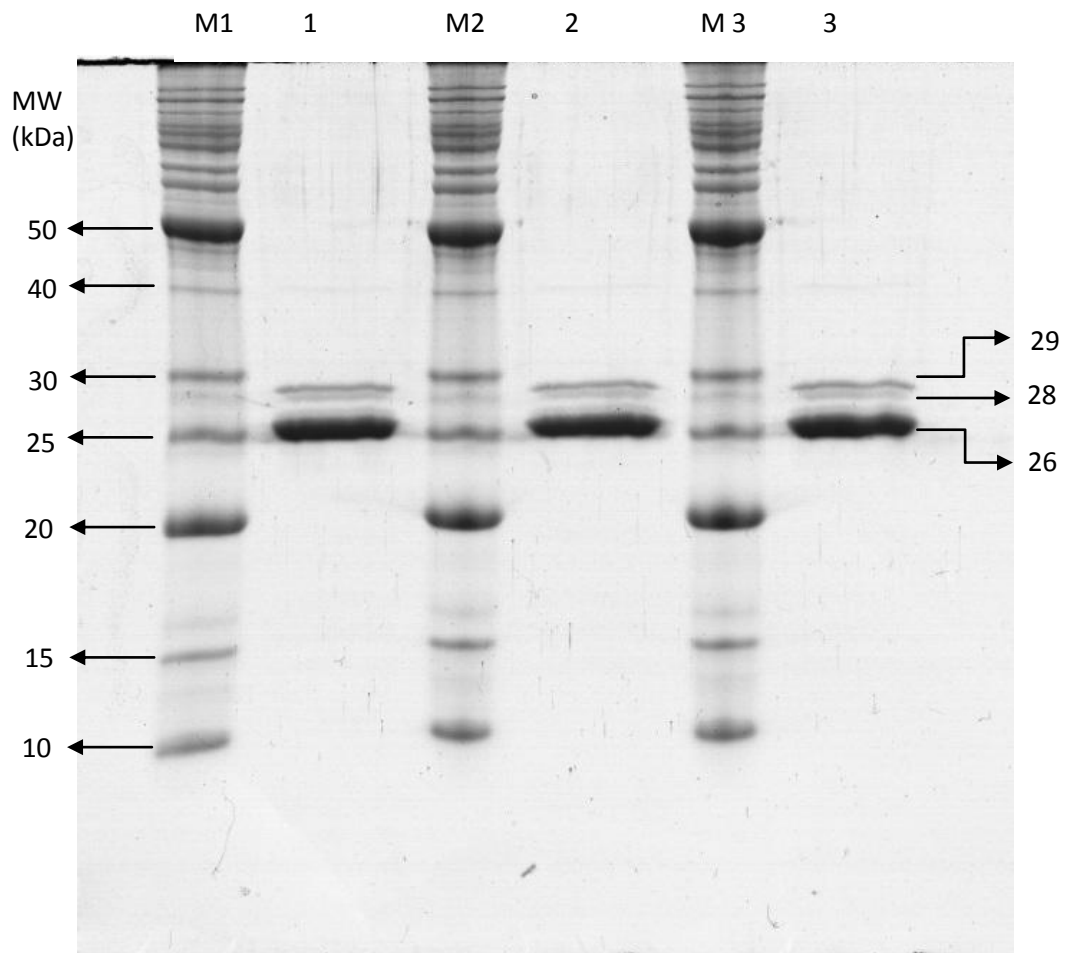


Figure 5.4 SDS-PAGE (12%) of GSTs purified from GSH-agarose (C_3) matrix. Approximately 8.4 μg protein was loaded into each Lane 1, 2, and 3. The gel is stained using Coomassie Blue G-250. (a) Lane M1-M3 : Protein marker (BENCHMARKTM Protein Ladder). (b) Lane 1-3 : Concentrated eluate.

5.3 TWO-DIMENSIONAL ELECTROPHORESIS (2-DE)

In this study, the two-dimensional electrophoresis (2-DE) technique was applied to separate GSTs from eluate fractions according to their isoelectric points (pI) and molecular weight (MW). The use of immobilize pH gradient enables separation of a complex protein mixture into single protein species represent by series of spot on the SDS-PAGE gel. Therefore, this method is able to separate different isoforms of GSTs that is useful for the collection of highly specific protein database.

5.3.1 Two-dimensional electrophoresis (2-DE) for proteins purified from GSTrapTM HP matrix

According to Figure 5.5 (a), nine different spots labeled as 1-9 were detected after 3 days of staining with Colloidal Coomassie Blue G-250. By using this method, protein spots were separated into three different MW during second dimension of gel instead of two MW in one-dimensional electrophoresis (Figure 5.3).

5.3.2 Two-dimensional electrophoresis (2-DE) for proteins purified from GSH-agarose (C₃) matrix

Referring to Figure 5.5 (b), the 2-DE gel of GSTs purified from GSH-agarose (C₃) showed the presence of 9 similar spots as obtained from GSTrapTM HP matrix, labeled as 1-9. However, the gel was observed to detain six additional spots marked as i, ii, iii, iv, v and vi compared to those in 5.5 (a) bringing the total number of spots 15.

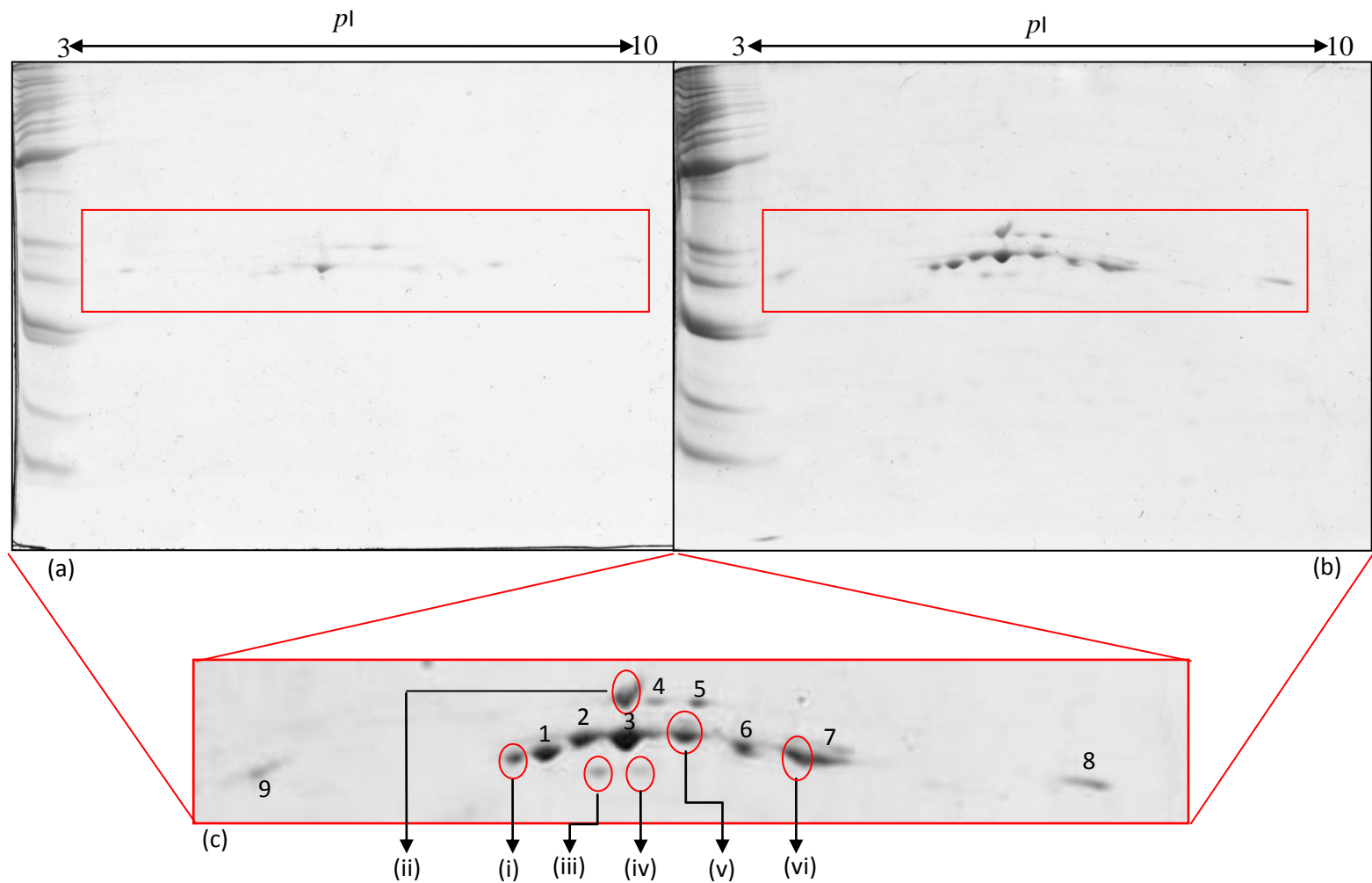


Figure 5.5 Two dimensional gels of GST purified from affinity chromatography. The gel (12%) was stained with Colloidal Coomassie Blue G-250. Approximately 8.6 μg and 16.8 μg protein purified from GSTrap[™] HP matrix and GSH-agarose (C₃) respectively was loaded into Immobiline[™] DryStrip during rehydration. (a) GSTrap[™] HP matrix (b) GSH-agarose (C₃). (c) Enlarged images from (a) and (b). GSH-agarose (C₃) captured extra spots labeled as i, ii, iii, iv, v, and vi.

5.4 ISOELECTRIC FOCUSING (IEF)

Isoelectric focusing (IEF) is a technique that separates proteins based on their isoelectric point (pI), i.e. the pH at which a particular protein carries no net electrical charge thus become static in an electric field. IEF gels can effectively create a pH gradient when an electric pulse is applied thus enable protein separation according to their unique pI . In this study, this method had been carried out to determine pI value of GST isoforms observed in 2-DE gel.

5.4.1 Isoelectric focusing on GSTs eluted from GSTrapTM HP matrix

GSTrapTM HP matrix was previously shown to bind different GST isoforms during 2-DE, mostly resolved at the middle part of the gel. To confirm their pI values, IEF was performed and the result showed that most GSTs were resolved at pI in between 4.5 to 6.9 (Figure 5.6). Apart of that cluster, there is one weakly focused band labeled as 8 at the basic part of the gel which was near to pI 8.3 and one separated at the acidic part of the gel, labeled as 9 which was at pI 4.2.

5.4.2 Isoelectric focusing on GSTs eluted from GSH-agarose (C₃)

GSTs collected from GSH-agarose (C₃) showed similar pattern of resolution with GSTrapTM HP in IEF gel. Most GSTs are migrated at pI between 4.5 and 6.9 with additional bands seen in the group designated as i, ii, iii, iv, v, and vi (Figure 5.6). These extra bands are seen to be in line with result observed in Figure 5.5 (c). There were also two similar bands as observed in GSTrapTM HP located near to pI 8.3 and at 4.2, designated as 8 and 9 respectively.

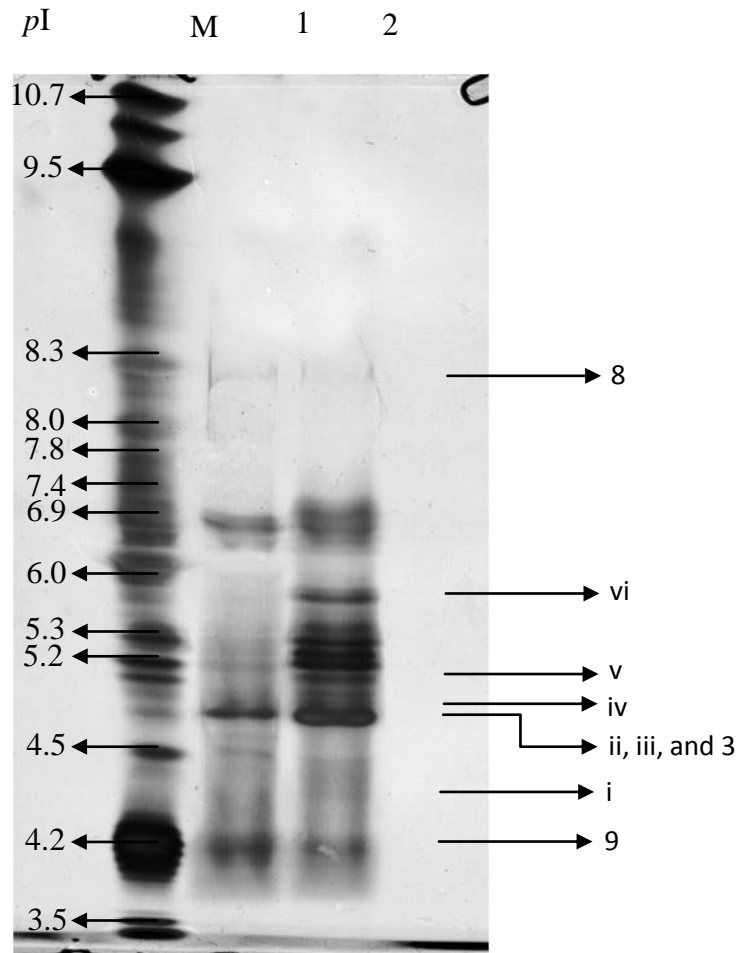


Figure 5.6 Separation of *Donax* sp. purified GSTs on silver stained IEF gel. Approximately 8.6µg of protein purified from GSTrap™ HP matrix and 16.8 µg of extract from GSH-agarose (C₃) were loaded into Pre-cast Novex® IEF Gel. (a) Lane M : IEF marker (SERVALYT™ PRECOTES™, pH 3-10). (b) Lane 1 : GSTs purified from GSTrap™ HP matrix. (c) Lane 2 : GSTs purified from GSH-agarose (C₃). (c) i, ii, iii, iv, v and vi : extra GSTs observed in GSH-agarose (C₃) as in Figure 5.5.

5.5 SUBSTRATE SPECIFICITY OF PURIFIED GSTs

Information about GST affinities towards specific substrate is very useful for initial recognition in classifying GSTs. It is also important to determine the range of substrate specificity to assess their physiological roles in biological systems. In this study, a set of substrates were used to identify the catalytic reaction of GSTs purified from GSTrap™ HP matrix and GSH-agarose (C₃) matrices.

5.5.1 Substrate specificity of GSTs eluted from GSTrapTM HP matrix

Result in Table 5.2 showed that GSTs eluted from GSTrapTM HP matrix was observed to have highest activity towards 1-chloro-2,4-dinitrobenzene (CDNB) with the value 23.378 ± 5.697 $\mu\text{mol}/\text{min}/\text{mg}$ followed by ethacrynic acid (EA) (1.281 ± 0.063 $\mu\text{mol}/\text{min}/\text{mg}$). Low activities were detected when GSTs were assayed with sulfobromophthalein (BSP) (0.726 ± 0.275 $\mu\text{mol}/\text{min}/\text{mg}$) and 1,2-dichloro-4-nitrobenzene (DCNB) (0.033 ± 0.002 $\mu\text{mol}/\text{min}/\text{mg}$). There was no activity observed during GSTs assay with *p*-nitrobenzylchloride (PBO), trans-4-phenyl-3-butene-2-one (PBO), and nitrocinnamaldehyde (NCA).

5.5.2 Substrate specificity of GST eluted from GSH-agarose (C₃)

As seen in Table 5.2, GSTs collected from GSH-agarose (C₃) matrix showed higher activity towards EA (11.353 ± 0.620 $\mu\text{mol}/\text{min}/\text{mg}$) which gave almost 10 times higher than that observed in GSTrapTM HP matrix. Similar to those obtained from GSTrapTM HP, GSTs eluted from GSH-agarose (C₃) was also active towards CDNB, however, with slightly lower activity (9.054 ± 0.420 $\mu\text{mol}/\text{min}/\text{mg}$). Their activity towards DCNB, and BSP were shown to be low that are 0.024 ± 0.002 $\mu\text{mol}/\text{min}/\text{mg}$ and 0.081 ± 0.011 $\mu\text{mol}/\text{min}/\text{mg}$, respectively. All these three values are lower compared to activity detected in GSTrapTM HP matrix. Similar pattern with GSTrapTM HP was observed when GSTs purified from this matrix were assayed with NBC, PBO, and NCA; no activity was detected.

Table 5.2 Substrate specificity of *Donax* sp. GSTs purified using GSTrapTM HP and GSH-agarose (C₃) matrices.

Substrates	Specific activity (μmol/min/mg)	
	GSTrap TM HP	GSH-agarose (C ₃)
1-chloro-2,4-dinitrobenzene (CDNB)	23.378 ± 5.697	9.054 ± 0.420
1,2-dichloro-4-nitrobenzene (DCNB)	0.033 ± 0.002	0.024 ± 0.002
Sulfobromophthalein (BSP)	0.726 ± 0.275	0.081 ± 0.011
Ethacrynic acid (EA)	1.281 ± 0.063	11.353 ± 0.620
<i>p</i> -nitrobenzylchloride (NBC)	ND	ND
Trans-4-phenyl-3-butene-2-one (PBO)	ND	ND
Nitrocinnamaldehyde (NCA)	ND	ND

*Values are means ± SD taken from three independent replications.

*ND, No detected activity.

5.6 IDENTIFICATION OF PURIFIED GSTs USING MALDI-TOFF

Spots obtained from GSTrapTM HP labeled as 2 to 8 in Figure 5.5 were subjected to tryptic digestion and analyzed using MALDI-TOF. Peptides generated from each spot were used for protein identification using ProFound software. However, all peptides generated showed no significant identity or ‘hits’ with the current GSTs protein database. The list of tryptic peptide masses of aforementioned spots can be seen in Appendix I.

CHAPTER 6

DISCUSSION

6.1 PURIFICATION OF GSTs USING GSH-AGAROSE BASED MATRICES

GSH-agarose matrices are commonly used for GST purification in recent years. The application of these matrices is straight forward, exploiting the basic knowledge of GST-GSH interaction in *in vivo* detoxification process. Theoretically, homogenized sample will pass through the immobilized GSH and GSTs in the sample bind tightly to this GSH during the process. The bound GSTs can be recovered by changing the elution conditions which loosen the binding of GST-GSH. In this study, a 10 mM GSH solution that has higher affinity towards bound GSTs compared to the immobilized GSH was used to pull the enzymes from the matrix. The advantage of using GSH to elute GSTs is due to the fact that GSH acts as stabilizing agent rather than inhibitor thus makes them able to preserve the enzymes activity (Habig et al., 1974).

The application of 10 mM GSH in this study was sufficient to collect bound proteins from both matrices, indicated by total yield percentage of eluate and void that gave almost 100% recovery. However, Alias (2006) reported that 20 mM GSH was required to elute *Drosophila melanogaster* GSTs from GSH-agarose (C₁₂). Current study indicated that *Donax* sp. GSTs bind to GSTrapTMHP in a manner less tight than *D.melanogaster* GSTs. This dissimilarity is probably due to protein composition differences in the samples used. When GSH-agarose (C₁₂) was used, Alias (2006) had successfully isolated Delta and Sigma class of GSTs, plus one additional predicted epsilon GST enzyme. Since the previously mentioned GSTs are exclusive to insect, it is hypothesized that GSTs obtained in this experiment was totally different from those

isolated by Alias (2006). Therefore, different classes of GSTs *Donax* sp. may require different concentration of GSH.

The use of GSTrapTM HP and GSH-agarose (C₃) matrix in this study produced interesting results, in fact some points are worthy of note. From the observation, it is revealed that both matrices were not capable to bind all GSTs efficiently denoted by the presence of activity towards CDNB in the void effluent (Table 5.1). The residual activity in void fractions suggested the presence of remaining GSTs that failed to bind to affinity matrix. Since *Donax* sp. flesh was used, it is anticipated that global GSTs composed of wider classes while GSH-agarose matrices were selective towards specific group of GSTs (Clark et al., 1990). Clark et al. (1990) also reported the capability of GSH-agarose (C₃) to capture CDNB-active *Musca domestica* GSTs but not to other isozymes group. Therefore, there is possibility that GSH-agarose (C₁₂ and C₃) could not retain some of *Donax* sp. GSTs and those unbound GSTs remain in the void fraction. In fact, Alias (2006) noted that activities were still detected in the flow-through fraction when GSH-agarose (C₃) and (C₁₂) were used.

This study also revealed GSTrapTMHP capability to recover more *Donax* sp. enzymes compared to GSH-agarose (C₃), which count about 3 times higher (Table 5.1). This finding is comparable to Alias (2006) who succeeded to isolate fruit fly GSTs from GSH-agarose (C₁₂) as much as 2-fold than GSH-agarose (C₃). These results indicated GSTrapTM HP capability to capture GSTs in a larger aptitude than GSH-agarose (C₃). As mentioned in earlier chapter, both matrices use the same ligand i.e GSH to capture GST molecules thus their appearance are similar, in exception to the arrangement of their linker arm. Since both matrices were attached to the same ligand (GSH), they will behave similarly thus has similar ability to trap the same active site of GST molecules

but practically that did not happen. It is hypothesized that this dissimilar result is contributed by the different length of linker arm that hold GSH. Results obtained from this study and Alias (2006) clarify the ability of GSH-agarose (C_{12}) to capture more GSTs compared to GSH-agarose (C_3) therefore being an indication that GSH-agarose (C_{12}) may have better sample exposure during the purification process. It is logical that the nature of GSH-agarose (C_{12}) longer arm contributed to this significant exposure difference to GSH-agarose (C_3) as illustrated in Figure 6.1.

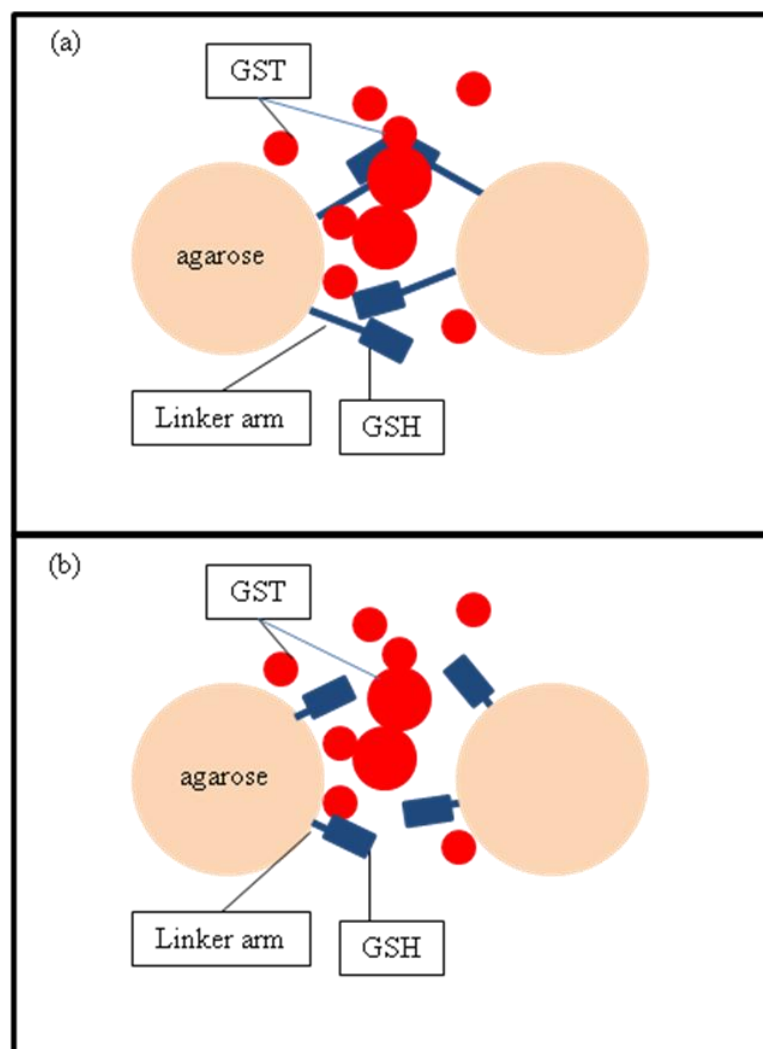


Figure 6.1 Effect of different linker arm on GSH-agarose (C_{12} and C_3) on their behavior to capture GST. (a) GSH-agarose (C_{12}) (b) GSH-agarose (C_3)

Enzyme activity was calculated to measure the quantity of active enzyme present per volume of solution in a specified condition or can be simplified as moles of substrates converted per unit time. The magnitude of enzyme activity that corresponds to total active enzyme recovered from the whole process can be used to determine the success of a purification strategy. In this study, total activity i.e. total number of enzyme units showed that purification of *Donax* sp. GST using GSTrapTMHP managed to get higher total activity, which was about 9-fold than what was obtained from GSH-agarose (C₃) (Table 5.1). This result is expected since total protein recovered from GSTrapTMHP was more than GSTs obtained from GSH-agarose (C₃), as mentioned in the earlier discussion. This is due to the fact that the rate of an enzymatic reaction is related to the concentration of enzyme-substrate complex (Voet & Voet, 2004). In principle, the formation of enzyme-substrate complex takes place within the active site of the enzymes which refers to the key and lock model. According to this law, if a sample contain larger amount of enzymes, the availability of active site will also be increased thus cause the increase in rate of reaction which represented by the enzymes activity.

As shown in Table 5.1, the use of GSTrapTMHP produced 12% yield of CDNB-active GSTs compared to 3% in GSH-agarose (C₃). This pattern is parallel to *Donax* sp. GSTs total activity which has reduced when GSH-agarose (C₃) was used to purify GSTs from the sample. This expectation is based on the principle which yield is reported as percent of total activity remaining from crude homogenate (William, 2005). The decrease of yield percentage in GSH-agarose (C₃) is related to the low amount of total protein available in the sample that was measured by total activity of the protein.

6.2 GEL VISUALIZATION

In present study, molecular weight of the purified GSTs from GSTrapTMHP were 29 and 26 kDa while GSH-agarose (C₃) revealed three subunits at 29, 28, and 26 kDa (Figure 5.3 and 5.4). The presence of two bands in GSTrapTMHP and three bands in GSH-agarose (C₃) signify high possibility of at least two and three different GST classes were successfully isolated from these purification procedures. Other bands were not detected outside 25 – 30 kDa range on both SDS-PAGE gels, means no contamination occur in GSTs purification using both matrices. It can be assumed that *Donax* sp. GSTs isolated from GSTrapTMHP and GSH-agarose (C₃) were highly pure.

GSTs obtained in this study fall within general GSTs range of 23-30 kDa. Previous study by Vidal et al. (2002) reported isolation of four subunits GSTs from Müller with apparent molecular weight between 27.2 to 30.2 kDa. Another work by Blanchette and Singh (1999) were able to purify two major and two minor subunit bands of northern quahog *Mercinaria mercinaria* ranging from 22 to 27 kDa. Supported by these data, it is highly recommended that all subunits discovered in this study were GSTs. Interestingly, result obtained in this study was inconsistent with Alias (2006) and Clark et al. (1990) where they reported less subunit was obtained when GSH-agarose (C₃) was used to purify GSTs from *D. melanogaster* and *M. domestica*. Furthermore, Figure 5.3 and 5.4 shows despite band thickness between subunits in GSTrapTMHP, the band intensity is not significant compared to GSTs obtained from GSH-agarose (C₃), meaning that the concentration of both subunits trapped by GSTrapTMHP were similar.

Assuming that substances in sample solution were evenly distributed, GSTrapTMHP have potential to capture both small and large molecules of GSTs because

it has higher exposure hence samples become more accessible. This might be the reason why GST subunits from GSTrapTMHP had similar intensity when viewed on SDS-PAGE showed that this matrix is capable to arrest small and large GSTs at similar capacity. Unlike GSTrapTMHP, GSH-agarose (C₃) contain shorter arm that make GSH become less accessible. Even so, image analysis showed that this matrix was able to trap more small molecules compared to the larger ones, indicated by the intensity of the bands in Figure 5.4. This result is consistent with result obtained by Alias (2006) which was able to isolate GSTs sized 23.5 kDa by using GSH-agarose (C₃) while GSH-agarose (C₁₂) trapped GSTs sized 23.5 kDa plus 24.1 kDa. Other than that, Clark et al. (1990) reported that they managed to purify GSTs of 24 kDa using GSH-agarose (C₃) which was the smallest GST subunits trapped by BSP-GSH matrix. This phenomenon is quite interesting regardless of their limited ability to capture GSTs in larger quantity. It is known that smaller molecules in a solution possesses better distribution compared to larger molecule simply due to their size factor, these small molecules can be distributed nearer to the agarose beads compared to the larger molecules. For this reason, GSH-agarose (C₃) may have advantage because of its shorter linker arm that enables binding of GSTs that cannot be reached by GSTrapTMHP.

However, analysis on SDS-PAGE is limited to the molecular mass only, means if there is more than one subunit have the same molecular mass; they will migrate at the same distance from the well and resolve at the same position on the gel. Therefore, single band is not necessarily denoting single protein but there is probability of multiple proteins present at the same size. For that reason, 2-DE was performed in order to have a better visualization of whole GSTs expressed in *Donax* sp.. The use of two different matrices in this study yielded different result with similar pattern; one spot was highly

acidic, one spot appeared to be basic, and the rest resolved at the middle part of the gel (Figure 5.5).

GSTs obtained from GSTrapTMHP were distributed along the gel and produced nine spots at three different MW instead of two during SDS-PAGE (Figure 5.3 and 5.5 (a)). Therefore, it is concluded that the thicker band sized 26 kDa in Figure 5.3 actually consists of two different bands rather than one. It is assumed that they may present as the majority GSTs and joined together to form one single thick band as seen in SDS-PAGE gel. In comparison, GSTs extracted from GSH-agarose (C₃) had diverse MW distribution while the same protein showed only three bands in SDS-PAGE (Figure 5.4 and 5.5 (b)). This result is identical to those obtained from GSTrapTMHP where some of these GSTs fuse together becoming a single concentrated band in SDS-PAGE gel.

Apart of that, GSH-agarose (C₃) produced an interesting result where additional six spots which apparently invisible in the GSTrapTMHP were detected on the gel. This observation shows that despite their ability to recover lower amount of protein, GSH-agarose (C₃) was able to capture more GST isoforms compared to GSTrapTMHP which most of those extra spots were at the smaller and intermediate sizes which further support the fact that GSH-agarose (C₃) performs better for smaller molecules. However, this result is different in terms of number of classes obtained by Alias (2006). Alias (2006) managed to isolate specific group of *D.melanogaster* GSTs; GSTD1 and GSTD3 (MW=23.89) by using GSH-agarose (C₃) without the presence of CG16936 (MW=25.44) that was observed in GSH-agarose (C₁₂) and *S*-hexyl-GSH-agarose matrices. However, from the size perspective similar trend was observed. Therefore, an early assumption can be made; *Donax* sp. possesses more small classes of GSTs compared to the bigger classes of GSTs. That is the possible reason so far since GSH-

agarose (C₃) is expected to have preference in capturing smaller molecules as discussed earlier. This dissimilarity is a very attractive subject to be investigated. Moreover, Clark et al. (1990) also stated that the differences between GSH-agarose (C₁₂) and GSH-agarose (C₃) is still not known whether due to the species differences or to properties of the matrix itself.

Although 2-DE can separate groups of protein according to their *pI*, this method however cannot show the actual *pI* value. Therefore, IEF was run to compare the *pI* value of samples GSTs with the commercial marker. From the Figure 5.6, it can be said that GSTs extracted from both matrices; GSTrapTMHP and GSH-agarose (C₃) showed similar pattern of resolution which was constant with the result from 2-DE. It can be seen that most isoforms resolved at the middle part of the gel (around 4.5 - 5.3) which match with the general *pI* value of soluble GSTs (Dixon et al. 2002, Kazemnejad et al., 2006). Other than that, more bands were appeared on the sample purified from GSH-agarose (C₃), particularly in the area within *pI* 4.5 - 6.0 which was in line with 2-DE result where more spots were detected as seen in Figure 5.5 (c). A part of that, it is highly recommended that spots labeled as ii, iii, and 3 in Figure 5.5 (c) shared the same *pI* value thus grouped together becoming a single intense and thick band located near to *pI* 4.5.

It is inappropriate to classify GSTs only based on their *pI* value because many other factors should also be taken into consideration before GSTs can be sorted into specific group. However, *pI* value can be used as a guide to classify GSTs based on generalization made by Mannervik & Danielson (1988); basic alpha (*pI* 8-11), the neutral mu (*pI* 5-7), and acidic pi (*pI* less than 5). From this range, it is predicted that

GSTs obtained from both matrices are from pi, mu, and alpha classes. This classification is still not supported with enough data.

6.3 SUBSTRATE SPECIFICITY

Determination of GSTs substrate specificity are well worth as it can be used to assess enzymes physiological role and is useful in characterization process. It is known that structural features of GSTs have significant catalytic similarity and differences among the GSTs classes (Blanchette et al., 2007). As mentioned earlier, despite the common use of substrate enzymatic activity in GSTs classification, this approach is also known to yield highly variable result and many class-defining substrates show cross reactivity between the major classes. Even so, other than to identify the range of substrate GSTs can react with, it is appropriate to mention that substrate specificity analysis is useful to provide a clue in GST classification and support other classification approaches.

Blanchette and co-workers (2007) in their paper reviewed that GST classes share some remarkable similarities in their G-site homology and mechanisms but shows a high degree of variability in their H-site homology. As mentioned in previous chapter, H-site on the GST subunit is essential for electrophilic substrates binding thus variation of H-site structure among GST classes will directly affect the acceptance of electrophiles substances. For instance, Singh et al. (2001) found that GST-2 had significant glutathione-conjugating activity towards 4-hydroxynonenal (4-HNE) despite low activity with typical GST substrates such as aryl-alkyl halides, epoxides, and nitro-aromatic compounds. Later, a structural study of GST-2 conducted by Agianian et al. (2003) revealed there were significant differences in H-site structure of GST-2 compared to the other sigma GSTs as well as alpha 4-4. A part of that, their study

displayed the surface of H-site GST-2 consist of a shallow largely flat surface that constitute a novel topography without a prominent hydrophobic-binding pocket due to the distinct orientation of helix α_6 . In addition to that, flat topography of the H-site was also contributed by the presence of Y208 residue which was found to “filling up” the space that is usually a hydrophobic cavity which binds the hydrophobic moiety of the electrophilic co-substrate. This unique topology of GST-2 is actually consistent with the geometry and polarity of 4-HNE, in fact it fixes the carbonyl oxygen and C-3 carbon in a suitable positions for catalysis. That is the reason why GST-2 showed remarkable activity towards 4-HNE compared to the other comparable GSTs.

In this study, a set of substrates; CDNB, DCNB, BSP, EA, NBC, PBO, and NCA were used to determine the specificity range of GSTs purified from GSTrapTM HP and GSH-agarose (C₃) matrices. GSTs reaction towards substrates was measured by enzyme specific activity which in definition, specific activity is enzyme units per microgram of enzyme protein (Colowick & Kaplan, 1976; Harisha, 2006). Result in Table 5.2 shows both purified extracts were reacted towards CDNB, DCNB, BSP, and EA. GSTs extracted from GSTrapTM HP showed higher activity towards all mentioned substrates except for EA. This occurrence is expected since the total protein of GSTs purified from GSTrapTM HP is higher than GSTs purified from GSH-agarose (C₃) which in turn affect the total activity of enzyme and directly cause the increase in specific activity. The specific activity is then having influence in the purification factor because purification factor is measured by the change in specific activity relative to the crude homogenate (Williams, 2005). That is the reason why purification fold of GSTrapTM HP was higher than GSH-agarose (C₃) (Table 5.1). In addition to that, higher purification factor obtained in GSTrapTM HP is due to the presence of more specific GSTs purified from this matrix compared to the GSH-agarose (C₃) which was represented by less

number of spots appeared on the 2-DE gel. A part of that, no activity was detected when samples were tested with NBC, PBO, and NCA for both matrices. The reason behind higher EA activity observed from GSH-agarose (C₃) will be discussed later.

Result in Table 5.2 shows high possibility of GSTs obtained from both matrices were pi- and mu-GSTs classes. This is because GSTs from both matrices exhibit activity towards BSP and DCNB which are specific to mu-class, as well as active with EA which is specific to pi-class GSTs (Blanchette et al., 2007; Huang et al., 2008; Mannervik & Danielson, 1988; Mannervik et al., 1985; Yang et al., 2003; Yang et al., 2004; Vidal et al., 2002). Therefore, the basic GST obtained during 2-DE is probably not an alpha-class GST but is actually a mu-class GST since no activity towards NBC and NCA were observed.

A part of that, it is observed that GSTs purified from GSH-agarose (C₃) showed higher activity towards EA compared to GSTs purified from GSTrapTM HP. From the 2-D and IEF gel observation, it is inferred that this extensive reactivity is due to the presence of additional spots designated as i, ii, iii, iv, v, and vi (Figure 5.5). These aforementioned spots are predicted belong to the pi-class of GSTs since GSTs purified from GSH-agarose (C₃) exhibit significant activity towards EA and resolved at acidic part of the gel during IEF (Figure 5.6). Many studies on bivalves had reported that activity towards EA is contributed by the presence of pi-class GSTs (Vidal et al., 2002, Yang et al., 2003). In addition to that, it is no surprise that pi-class of GSTs present as majority class in *Donax* sp. since finding of pi-class GSTs of molluscs had been reported by many researchers (Yang et al., 2003). Furthermore, it appears that pi-class GSTs are encountered in most aquatic invertebrate and vertebrate species (Yang et al., 2004; Pérez-López et al., 2000).

6.4 IDENTIFICATION OF GSTs OBTAINED FROM GSTrapTM HP MATRIX

The success of protein identification using mass spectrometer-based approach depends on several factors, including most importantly the quality of mass spectrometer data and also the accuracy of the database. Previous studies on bivalve GSTs identification has been successfully done by using this simple procedure of MALDI-TOF (Feng & Singh, 2009; Yang et al., 2004) thus giving hope that this approach will bring success in the current studies. An attempt to identify GSTs obtained in this study has been made by using MALDI-TOF to support data obtained from biochemical analysis.

However, no significant ‘hits’ on GSTs were observed when generated peptide masses were compared to the entries in Mascot and ProFound. Even though there are many GSTs have been fully characterized from other organism but noted that the full complement of GSTs has not been studied in marine organisms (Blanchette et al., 2007). This limitation makes classification of partially characterized GSTs becomes extremely difficult since successful application of peptide mass fingerprinting is highly dependent on the closest match of unknown protein to the available protein sequence in the database. Furthermore, cross-species identification is only possible for proteins with large amounts of sequence identity; homology is not sufficient (Henzel et al., 2003). Similar to current study, Rodriguez-Ortega et al. (2003) reported that despite the good MALDI-TOF spectra obtained from *Chamaelea gallina*, only 4 proteins out of 15 analyzed spots were identified. Poor representation of bivalve sequence databases is known to be the major cause of difficulty in identifying bivalve proteins (Blanchette et al., 2007). Later evidence of fully characterized marine GSTs and the response of the partially characterized GSTs to immunochemical reactivity showed that the marine

GSTs must constitute a dissimilar branch in the GST evolutionary process (Blanchette et al., 2007). Therefore, possibilities of distinct bivalves GSTs features in combination with incomplete database may be a contributing factor of failure in the protein identification.

CHAPTER 7

CONCLUSION

This study was conducted to isolate and purify GSTs from a local bivalve species, *Donax* sp. subsequently investigate the range of substrate acceptance of the purified GSTs. In addition to that, MALDI-TOF analysis was conducted as an attempt to classify proteins obtained from the purification method using GSTrapTM HP.

From data collected in this study, it can be concluded that *Donax* sp. GSTs have been successfully purified using two different GSH-agarose based matrices columns; 1) GSTrapTM HP which is the commercial column of GSH-agarose (C₁₂) and 2) GSH-agarose (C₃). This study discovered remis GSTs are active towards CDNB, DCNB, BSP, and EA, but inactive with NBC, NCA, and PBO. Nevertheless, no significant 'hit' were found when tryptic digested peptide masses were compared to the existence database using Mascot and ProFound software. Even though no significant score for peptide mapping, it is assumed that GSTs obtained in this study are belong to pi- and mu-class of GSTs which have been recorded in different bivalves' species before. This assumption is made based on the current result obtained from SDS-PAGE, 2-DE, IEF gel, and substrate specificity assays study. Most probably that the six additional spots appeared on the 2-DE gel from GSTs purified from GSH-agarose (C₃) are belonged to pi-class GSTs due to an extensive EA activity compared to GSTs purified from GSTrapTM HP. However, further analysis need to be carried out in order to strengthen and validate the current findings.

Several exciting results obtained during this study are worthy of note. It is interesting that *Donax* sp. GSTs behave differently towards GSTrapTM HP and GSH-

agarose (C₃) matrices which more classes were recovered on GSH-agarose (C₃), unlike in previous studies that obtained more specific classes by using GSH-agarose (C₃). Based on the overall result, it is safe to assume that this difference is due to different linker arm length of both columns and the nature of size related molecule (protein) distribution in solution. Further studies are recommended especially to get a better understanding in the physical interaction between GSTs and immobilized GSH in the matrix.

Hopefully that current finding will be beneficial for the future study to get more comprehension on *Donax* sp. GSTs. As MALDI-TOF analysis did not give satisfactory result, more effort on characterization need to be carried out thus the nature of GSTs in *Donax* sp. can be understood in further details. The alternative approach of N-terminal amino acid sequencing should be considered as it has the benefit of providing the definitive sequence the N-terminus as protein in general are well conserved at the N-termini part. Several aspects may need to be evaluated and considered before further research is conducted because often the results obtained in laboratory are rather conflicting with GSTs activity in the environmental studies which probably due to the fact that the expression of some bivalve GSTs are tissue-dependent. Therefore, a molecular approach may be more relevant to study the induction or inhibition of specific GST isozymes in environmental studies.

REFERENCES

- Alias, Z. (2006). The proteome of insect Glutathione *S*-Transferases in response to toxic challenge. Ph.D Thesis. Victoria University of Wellington.
- Alias, Z. & Clark, A.G. (2007). Studies on the Glutathione *S*-transferases proteome of adult *Drosophila melanogaster*. Responsiveness to chemical challenge. *Proteomics*, 7, 3618-3628.
- Agianian, B., Tucker, P.A., Schouten, A., Leonard, K., Bullard, B., & Gros, P. (2003). Structure of *Drosophila* sigma class glutathione *S*-transferase reveals a novel active site topography suited for lipid peroxidation products. *J. Mol. Biol*, 326, 151-165.
- Amstrong, R.N. (1991). Glutathione *S*-transferases : reaction mechanism, structure, and function. *Chem. Res. Toxicol.*, 4, 131-140.
- Antognelli, C., Francesca, B., Andrea, P., Roberta, F., Vincenzo, T., & Elvio, G. (2006). Activity changes of glyoxalase system enzymes and glutathione-*S*-transferase in the bivalve mollusc *Scapharca inaequalvis* exposed to the organophosphate chlorpyrifos. *Pestic. Biochem. Physiol.*, 86, 72–77.
- Axarli, I.A., Dhavala, P., Papageorgiou, A.C., & Labrou, NE. (2000). Crystallographic and functional characterization of the fluorodifen inducible glutathione transferase from *Glycine max* reveals an active site topography suited for diphenylether herbicides and a novel L-site. *J. Mol. Biol.*, 275, 24798-24806.
- Bebiano, M.J., Lopes, B., Guerra, L., Hoarau, P., & Ferreira, A.M. (2007). Glutathione *S*-transferases and cytochrome P450 activities in *Mytilus galloprovincialis* from the South coast of Portugal: Effect of abiotic factors. *Environ. Int.*, 33, 550-558.
- Blanchette, B., Feng, X., & Singh, B.R. (2007). Marine glutathione *S*-transferases. *Mar. Biotechnol.*, 9, 513-542.

- Blanchette, B. & Singh, B.R. (1999). Purification and characterization of the glutathione-S-transferases from the northern quahog *Mercinaria mercinaria*. *Mar. Biotechnol.*, 1, 74-80.
- Board, P.G., Coggan, M., Chelvanayagam, G., Easteal, S., Jermin, L.S., Schulte, G.K., Danley, D.E., Hoth, L.R., Griffor, M.C., Kamath, A.V., Rosner, M.H., Chrunk, B.A., Perregaux, D.E., Gabel, C.A., Geoghegan, K.F., & Pandit, J. (2000). Identification, characterization, and crystal structure of the Omega class Glutathione Transferases. *J. Biol. Chem.*, 275, 24798-24806.
- Boyland, E. & Chasseaud, F. (1969). The role of glutathione and glutathione S-transferases in mercapturic acid biosynthesis. *Adv. Enzymol. Relat. Areas Mol. Biol.*, 32, 173-219.
- Bringans, S., Eriksen, S., Kendrick, T., Gopalakrishnakone, P., Livk, A., Lock, R., & Lipscombe, R. (2008). Proteomics analyses of the venom of *Heterometrus longimanus* (Asian black scorpion). *Proteomics*, 8, 1081-1096.
- Cajaraville, M.P., Bebianno, M.J., Blascoc, J., Porte, C., Sarasquete, C., & Viarengo, A. (2000). The use of biomarkers to assess the impact of pollution in coastal environments of the Iberian Peninsula : a practical approach. *Sci.Total Environ.*, 249, 295-311.
- Chronopolou, E.G. & Labrou, N.E. (2009). Glutathione Transferases: Emerging multidisciplinary tools in red and green Biotechnology. *Recent Pat. Biotechnol.*, 3, 211-223.
- Clark, A.G., Letoa, M., & Ting, W.S. (1977). The purification by affinity chromatography of a glutathione S-transferase from larvae *Galleria mellonella*. *Life Sci.*, 20, 141-148.
- Clark, A.G., Marshall, S.N., & Qureshi, A.R. (1990). Synthesis and use of an isoform-specific affinity matrix in the purification of glutathione S-transferases from the house fly, *Musca domestica* (L.). *Protein Express. Purif.*, 1, 121-126.

- Colowick, S.P. & Kaplan, N.O. (1976). Methods in enzymology Volume XLV. Proteolytic Enzymes. Part B (Lorand, L.). San Diego : Academic Press, Inc.
- da Silva, A.Z., Zanette, J., Ferreira, J., F., Guzenski, J., Marques, M.R.F., & Bainy, A.C.D. (2005). Effects of salinity on biomarker responses in *Crassostrea rhizophorae* (Mollusca, Bivalvia) exposed to diesel oil. *Ecotox. Environ. Safe.*, 62, 376-382
- Deng, H., Huang, Y., & Zheng, S. (2009). Two epsilon glutathione S-transferase cDNAs from the common cutworm, *Spodoptera litura*: Characterization and developmental and induced expression by insecticides. *J. Insect Physiol.*, 55, 1174–1183.
- Desmots, F., Rissel, M., Loyer, P., Turlin, B., & Guillouzo, A. (2001). Immunohistological analysis of Glutathione Transferase A4 distribution in several human tissues using a specific polyclonal antibody. *J. Histochem. Cytochem.*, 49 (12), 1573-1579.
- Dirr, H., Reinemer, P., & Huber, R. (1994). X-Ray crystal structure of cytosolic Glutathione S-Transferases implication for protein architecture, substrate recognition and catalytic function. *Eur. J. Biochem.*, 220, 645-661.
- Dixon, D.P., Laphorn, A., & Edwards, R. (2002). Plant glutathione transferases. *Genome Biol.*, 3(3), 1-10.
- Frova, C. (2006). Glutathione transferases in the genomics era: New insights and perspective. *Biomol. Eng.*, 23, 149–169.
- Fenn, J.B., Mann, M., Meng, C.K., Wong, S.F., & Whitehouse, C.M. (1990). Electrospray ionization – principles and practice. *J. Mass spectrum. Rev.*, 9, 37-70.
- Feng, X. & Singh, B.R. (2009). Molecular identification of glutathione S-transferase gene and cDNAs of two isotypes from northern quahog (*Mercenaria mercenaria*). *Comp. Biochem. and Physiol. (C)*, 154 (1), 25-36.

- Fitzpatrick, P.J., Krag, T.O.G., Højrup, P., & Sheehan, D. (1995). Characterization of glutathione S-transferase and a related glutathione-binding protein from gill of the blue mussel, *Mytilus edulis*. *Biochem. J.*, 305, 145-150.
- Fitzpatrick, P.J. & Sheehan, D. (1993). Separation of multiple forms of glutathione S-transferase from the blue mussel, *Mytilus edulis*. *Xenobiotica.*, 23 (8), 851-861.
- Görg, A., Weiss, W., & Dunn, M.J. (2004). Review : current two-dimensional electrophoresis technology for proteomics. *Proteomics*, 4, 3665-3685.
- Gould, S.C. & Calloway, S.B. (1980). Clams and brachiopods ; ships that pass in the night. *Palaebiology*, 6, 383-396.
- Gowland, B.T.G., McIntosha, A.D., Daviesa, I.M., Moffat, C.F., & Webster, L. (2002). Implications from a field study regarding the relationship between polycyclic aromatic hydrocarbons and glutathione S-transferase activity in mussels. *Mar. Environ. Res.*, 54, 231–235.
- Habig, W.H., Pabst, M.J., & Jakoby, W.B. (1974). The first enzymatic step in mercapturic acid formation. *The J. Biol. Chem.*, 249 (22), 7130-7139.
- Halliwell, B. (1999). Antioxidant defense mechanisms : from the beginning to the end. *Free Radic. Res.*, 31, 261-272.
- Hansson, L.O., Bolton-Grob, R., Massoud, T., & Mannervik, B. (1999). Evolution of differential substrate specificities in Mu class glutathione transferases probed by DNA shuffling. *J. Mol. Biol.*, 287, 265-276.
- Harisha, S. (2006). An introduction to practical biotechnology. New Delhi : Laxmi Publications (P) Ltd.
- Hayes, J.D., Flanagan, J.U., & Jowsey, I.R. (2005). Glutathione transferases. *Annu. Rev. Pharmacol. Toxicol.*, 45, 51–88.

- Hayes, J.D. & Pulford, D.J. (1995). The glutathione *S*-transferase supergene family : regulation of GST and the contribution of the isoenzymes to cancer chemoprotection and drug resistance. *Crit. Rev. Biochem. Mol. Biol.*, 30 (6), 445-600.
- Helm, M.M., Bourne, N., & Lovatelli, A. (2004). Hatchery culture of bivalves. A practical manual. FAO Fisheries Technical Paper. No. 471, Rome, 177 pp.
- Henzel, W.J., Watanabe, C., & Stults, J.T. (2003). Protein Identification: The Origin of Peptide Mass Fingerprinting. *J. Am. Soc. Mass Spectrom.*, 14, 931–942.
- Hoarau, P., Garello, G., Gnassia-Barelli, M., Romeo, M., & Girard, P. (2002). Purification and partial characterization of seven glutathione *S*-transferase isoforms from the clam *Ruditapes decussates*. *Eur. J. Biochem.*, 269, 4359–4366.
- Huang, Q., Liang, L., Wei, T., Zhang, D., & Zeng, Q-Y. (2008). Purification and partial characterization of glutathione transferase from the teleost *Monopterus albus*. *Comp. Biochem. and Physiol. (C)*, 147, 96-100.
- Jakobsson, P.-J., Morgenstern, R., Mancini, J., Ford-Hutchinson, A., & Persson, B. (1999). Common structural features of MAPEG—a widespread superfamily of membrane associated proteins with highly divergent functions in eicosanoid and glutathione metabolism. *Protein Sci.*, 8, 689–692.
- Jia, Z., Zhu, H., Misra, H.P., & Li, Y. (2008). Potent induction of total cellular GSH and NQO1 as well as mitochondrial GSH by 3*H*-1,2-dithiole-3-thione in SH-SY5Y neuroblastoma cells and primary human neurons: Protection against neurocytotoxicity elicited by dopamine, 6-hydroxydopamine, 4-hydroxy-2-nonenal, or hydrogen peroxide. *Brain Res.*, 1197, 159-169.
- Kaaya, A., Najimi, S., Ribera, D., Narbonne, J.F., & Moukrim, A. (1999). Characterization of Glutathione *S*-Transferases (GST) activities in *Perna perna* and *Mytilus galloprovincialis* used as a biomarker of pollution in the Agadir Marine Bay (South of Morocco). *Bull. Environ. Contam. Toxicol.*, 62, 623-629.

- Kazemnejad, S., Rasmi, Y., Sharifi, R., & Allameh, A. (2006). Class-Pi of glutathione S-transferases. *Iran. J. Biotechnol.*, 4, 1-16.
- Knapen, M.F.C.M, Zusterzeel, P.L.M., Peters, W.H.M., & Steegers, E.A.P. (1999). Glutathione and glutathione-related enzymes in reproduction. A review. *Eur. J. Obstet. Gynecol. Reprod. Biol.*, 82, 171-184.
- Laemmli, U.K. (1970). Cleavage of structural proteins during the assembly of the head of bacteriophage T4. *Nature*, 227, 680-685.
- Lee, Y-M., Lee, K-W., Park, H., Park, H.G., Raisuddin, Ahn, I-Y., Lee, J-S. (2007). Sequence, biochemical characteristics and expression of a novel Sigma-class of glutathione S-transferase from the intertidal copepod, *Tigriopus japonicus* with a possible role in antioxidant defense. *Chemosphere*, 69, 893-902.
- Leiers, B., Kampkötter, A., Grevelding, C.G., Link, C., D., Johnson, T.E., & Henkle-Dührsen, K. (2003). A stress-responsive glutathione S-transferase confers resistance to oxidative stress in *Caenorhabditis elegans*. *Free Rad. Biol. Med.*, 34 (11), 1405-1415.
- Liang, X.F., Li, G.G., He, S., & Huang, Y. (2007). Transcriptional responses of alpha- and rho-class glutathione S-transferase genes in the liver of three freshwater fishes intraperitoneally injected with microcystin-LR : relationship of inducible expression and tolerance. *J. Biochem. Mol. Toxicol.*, 21 (5), 289-298.
- Lognonné, J.L. (1994). 2D-PAGE analysis- a practical guide to principle critical parameters. *Cell. Mol. Biol.*, 40, 41-55.
- Looise, B.A.S., Holwerda, D.A., & Foekema, E.M. (1999). Induction of Glutathione S-Transferase in the freshwater bivalve *Sphaerium couneum* as a biomarker for short-term toxicity tests. *Comp. Biochem. Physiol. (C)*, 113 (1), 103-107.
- Mannervik, B., & Danielson, U.H. (1988). Glutathione Transferases – Structure and catalytic activity. *Crit. Rev. Biochem. Mol. Biol.*, 23 (3), 283-337.

- Mannervik, B. & Guthenberg, C. (1981). Glutathione transferase (human placenta). *Methods Enzymol.*, 77, 231-235.
- Mannervik, B., Alin, P., Guthenberg, C., Jensson, H., Tahir, M.K., Warholm, M., & Jornvall, H. (1985). Identification of three classes of cytosolic glutathione transferase common to several mammalian species : correlation between structural data and enzymatic properties. *Proc. Natl. Acad. Sci. USA*, 82, 7202-7206.
- Masella, R., DiBenedetto, R., Vari, R., Filesi, C., Giovannini, C., (2005). Novel mechanisms of natural antioxidant compounds in biological systems: involvement of glutathione and glutathione-related enzymes. *J. Nutr. Biochem.*, 16, 577–586.
- Meister, A. (1988). Glutathione metabolism and its selective modification. *J. Biol. Chem.*, 263, 17205-17208.
- Neuhoff, V., Arold, N., Taube, D., & Ehrhardt, W. (1988). Improved staining of proteins in polyacrylamide gels including isoelectric focusing gels with clear background at nanogram sensitivity using Coomassie Brilliant Blue G-250 and R-250. *Electrophoresis*, 9, 255-262.
- O' Farrell, P.H. (1975). High resolution 2-dimensional electrophoresis of proteins. *J. Biol. Chem.*, 250, 4007-4021.
- Pabst, M.J., Habig, W.H., & Jakoby, W.B. (1973). Mercapturic acid formation: The several glutathione transferases of rat liver. *Biochem. Biophys. Res. Commun.*, 52 (4), 1123-1128.
- Park, H., Ahn, I-Y., Kim, H., Lee, J., & Shin, S.C. (2009). Glutathione S-transferase as a biomarker in the Antarctic bivalve *Laternula elliptica* after exposure to the polychlorinated biphenyl mixture Aroclor 1254. *Comp. Biochem. Physiol.(C)*, 150, 528–536.

- Patterson, S.D. (2000). Proteomics : the industrialization of protein chemistry. *Curr. Opin. Biotechnol.*, 11 (4), 413-418.
- Patterson, S.D. & Aebersold, R.H. (2003). Proteomics : the first decade and beyond. *Nat. Genet.*, 33, 311-323.
- Pérez-López, M., Anglade, P., Bec-Ferté, M.P. (2000). Characterization of hepatic and extrahepatic glutathione S-transferases in rainbow trout (*Oncorhynchus mykiss*) and their induction by 3,3', 4,4'-tetrachlorobiphenyl. *Fish Physiol. Biochem.*, 22, 21-32.
- Prado, S., Romalde, J.L., Barja, J.L. (2010). Review of probiotics for use in bivalve hatcheries. *Vet. Microbiol.*, 145, 187-197.
- Robinson, A., Huttley, G.A., Booth, H.S., & Board, P.G. (2004). Modelling and bioinformatics studies of the human Kappa-class glutathione transferase predict a novel third glutathione transferase family with similarity to prokaryotic 2-hydroxychromene-2-carboxylate isomerases. *Biochem. J.*, 379, 541–552.
- Rodriguez-Ortega, M.J., Grosvik, B.E., Rodriguez-Ariza, A., Goksoyr, A., & Lopez-Barea, J. (2003). Changes in protein expression profiles in bivalve mollusks (*Chamaelea gallina*) exposed to four model environmental pollutants. *Proteomics*, 3, 1535-1543.
- Salinas, A.E, Wong, M. (1999). Glutathione S-Transferases – A review. *Curr. Med. Chem.*, 6, 279-309.
- Sheehan, D., McIntosh, J., Power, A., & Fitzpatrick, P.J. (1995). Drug metabolizing enzymes of mussels as bioindicators of chemical pollution. *Biochem. Soc. Trans.*, 23, 417-420.
- Sheehan, D., Meade, G., Foley, V.M., & Dowd, A. (2001). Structure, function and evolution of glutathione transferases : implications for classification of non-mammalian members of an ancient enzyme superfamily. *Biochem. J.*, 360, 1-16.

- Sheehan, D. & McDonagh, B. (2008). Oxidative stress and bivalves : A proteomic approach. *ISJ.*, 5, 110-123.
- Sheehan, D. & Power, A. (1999). Effects of seasonability on xenobiotic and antioxidant defence mechanisms of bivalve mollusks. *Comp. Biochem. Physiol.(C)*, 123, 193-199.
- Simon, P.C. & van der Jagt, D.L. (1977). Purification of glutathione *S*-transferases from human liver by glutathione-affinity chromatography. *Anal. Biochem.*, 82, 334-341.
- Singh, S.P., Coronella, J.A., Benes, H., Cochrane, B.J., & Zimniak, P. (2001). Catalytic function of *Drosophila melanogaster* glutathione *S*-transferase DmGSTS1-1 (GST-2) in conjugation of lipid peroxidation end products. *Eur. J. Biochem.* 268 : 2912-2923.
- Spector, T. (1978). Refinement of the Coomassie Blue method of protein quantitation. *Anal. Biochem.*, 86, 142-146.
- Tanaka, K., Wahi, H., Ido, Y., Akita, S., Yoshida, Y., & Yoshida, T. (1988). Protein and polymer analyses up to *m/z* 100 000 by laser ionization time-of-flight mass spectrometry. *Rapid Commun. Mass Sp.*, 2, 151-153.
- Tanguy, A., Bierne, N., Saavedra, C., Pina, B., Bachère, E., Kube, M., Bazin, E., Bonhomme, F., Boudry, P., Boulo, V., Boutet, I., Cancela, L., Dossat, C., Favrel, P., Huvet, A., Jarque, S., Jollivet, D., Klages, S., Lapègue, S., Leite, R., Moal, J., Moraga, D., Reinhardt, R., Samain, J-F., Zouros, E., & Canario, A. (2008). Increasing genomic information in bivalves through new EST collections in four species : Development of new genetic markers for environmental studies and genome evolution. *Gene*, 408, 27-36.
- Thiede, B., Höhenwarter, W., Krah, A., Mattow, J., Schmid, M., Schmidt, F., & Jungblut, P.R. (2005). Peptide mass fingerprinting. *Methods*, 35, 237-247.
- Thom, R., Dixon, D.P., Edwards, R., Cole, D.J., & Laphorn, A.J. (2001). The structure of a Zeta class glutathione *S*-transferase from *Arabidopsis thaliana*:

characterisation of a GST with novel active-site architecture and a putative role in tyrosine catabolism. *J. Mol. Biol.*, 308, 949–962.

Townsend, D.M. & Tew, K.D. (2003). The role of glutathione-S-transferase in anti-cancer drug resistance. *Oncogene*, 22, 7369-7375.

Vidal, M.L. & Narbonne, J.F. (2000). Characterization of Glutathione S-Transferase Activity in the Asiatic Clam *Corbicula fluminea*. *Bull. Environ. Contam. Toxicol.*, 64, 455-462.

Vidal M-L., Roumi, P., Debrauwer, L., & Narbonne, J-F. (2002). Purification and characterisation of glutathione S-transferases from the freshwater clam *Corbicula fluminea* (Müller). *Comp. Biochem. Physiol.(C)*, 131, 477–489.

Voet, D. & Voet, J. (2004). *Biochemistry* (Third edition). Hoboken, NJ : John Wiley & Sons, Inc.

Vorum, S.N., & Blum, H. (2000, June). Vorum and Blum Procedures. Paper presented at 48th American Society for Mass Spectrometry Conference on Mass Spectrometry. Long Beach, CA, USA.

Wang, Y., Qiu, L., Ranson, H., Lumjuan, N., Hemingway, J., Setzer, W.N., Meehan, E.J., & Chen, L. (2008). Structure of an insect epsilon class glutathione S-transferase from the malaria vector *Anopheles gambiae* provides an explanation for the high high DDT-detoxifying activity. *J. Struct. Biol.* , 164(2), 228-235.

Wasinger, V.C., Cordwell, S.J., Cerpa-Poljak, A., Yan, J.X., Gooley, A.A., Wilkins, M.R., Duncan, M.W., Harris, R., Williams, K.L., Humphery-Smith, I. (1995). Progress with gene-product mapping of Mollicutes : *Mycoplasma genitalium*. *Electrophoresi.*, 16 (7), 1090-1094.

Wigger, M., Nawrocki, J.P., Watson, C.H., Eyler, J.R., & Benner, S.A. (1997). Assessing enzyme substrate specificity using combinatorial libraries and

electrospray ionization-fourier transform ion cyclotron resonance mass spectrometry. *Rapid Comm. Mass Spectrom.*, 11, 1749-1752.

- Williams, A. (2005). Overview of conventional chromatography. In R.E. Wrostad, E.A. Decker, S.J. Schwartz, & P. Sporns (Eds), *Handbook of food analytical chemistry, water, proteins, enzymes, lipids, and carbohydrates* (pp. 279-281). Hoboken, NJ : John Wiley & Sons, Ins.
- Won, S-J., Novillo, A., Custodia, N., Rie, M.T., Fitzgerald, K., Osada, M., & Callard, I.P. (2005). The freshwater mussel (*Elliptio complanata*) as a sentinel species : vitellogenin and steroid receptors. *Integr. Comp. Biol.*, 45, 72-80.
- Yang, H-L., Nie, L-J., Zhu, S-G., & Zhou, X-W. (2002). Purification and characterization of a novel glutathione S-transferase from *Asaphis dichotoma*. *Biochem. Biophy. Res. Commun.*, 403, 202-208.
- Yang, H-L., Zeng, Q-Y., Nie, L-J., Zhu, S-G., & Zhou, X-W. (2003). Purification and characterization of a novel glutathione S-transferase from *Atactodea striata*. *Biochem. Biophy. Res. Commun.*, 307, 626-631.
- Yang, H-L., Zeng, Q-Y., Li, E-Q., Zhu, S-G., & Zhou, X-W. (2004). Molecular cloning, expression and characterization of glutathione S-transferases from *Mytilus edulis*. *Comp. Biochem. Physiol.(B)*, 139, 175-182.
- Ye, Z., Song, H., Higgins, J.P.T., Pharoah, P., & Danesh, J. (2006). Five glutathione S-Transferase gene variants in 23,452 cases of lung cancer and 30,397 controls: meta-analysis of 130 studies. *PLoS Med.*, 3 (4), 524-534.
- Zablotowicz, R.M., Hoagland, R.E., Locke, M.A, & Hickey, W.J. (1999). Glutathione-S-Transferase Activity and Metabolism of Glutathione Conjugates by Rhizosphere Bacteria. *Appl. Environ. Microbiol.*, 61 (3), 1054-1060

APPENDICES

APPENDIX A : Buffer solution preparation

- i) Homogenizing Buffer (500 μ l protease inhibitor, 1.0 mM EDTA, 0.1 mM DTT, 0.1 mM PTU in Eluting Buffer)

To prepare 50 ml homogenizing buffer, 0.5 ml of protease inhibitor (or 0.5 ml of 10 mM PMSF), 0.019 g of EDTA, 0.0008 g DTT and a half spatula were added in a beaker and dissolved in 50 ml eluting buffer.

- ii) Eluting Buffer – 25 mM Sodium Phosphate Buffer, pH 7.4

3 g of NaH_2PO_4 was dissolved in approximately 900 ml of dH_2O . The pH was adjusted to 7.4 at 20°C and the volume was made up to 1000 ml.

- iii) Buffer A – 0.1 M Sodium Phosphate Buffer, pH 6.5

12 g of NaH_2PO_4 was dissolved in approximately 900 ml of dH_2O . The pH was adjusted to 6.5 at 20°C and the volume was made up to 1000 ml.

- iv) Buffer B – 0.1 M Tris Buffer, pH 9.0

12.114 g Tris base was dissolved in approximately 900 ml of dH_2O . The pH was adjusted to 9.0 at 20°C and the volume was made up to 1000 ml.

- v) Buffer C – 0.1 M Sodium Phosphate Buffer, pH 7.5

12 g of NaH_2PO_4 was dissolved in approximately 900 ml of dH_2O and the pH was adjusted to 7.5 at 20°C. The volume was then made up to 1000 ml.

APPENDIX B – Laemmli Discontinuous SDS Polyacrylamide Gel Electrophoresis

i) SDS sample buffer

The buffer consisted of 62.5 mM Tris-HCl (pH 6.8), 20% glycerol, 2% SDS and 5% β -mercaptoethanol. To prepare a buffer solution of 2 ml, 0.25 ml of 0.5 M Tris-HCl (pH 6.8), 0.4 ml glycerol, 0.4 ml 10% SDS, 0.1 ml β -mercaptoethanol, 0.1 ml of 0.5% (w/v) bromophenol blue and 0.75 ml of mili-Q water were mixed. To prepare sample in sample buffer, the sample was diluted at least 1:4 ratio. Then, the sample was heated at 95⁰C for 4 minutes.

ii) Electrophoresis (Running) Buffer

Running buffer was diluted from Novex® Tris-Glicine SDS Running Buffer (10X). To prepare 1000 ml 1X running buffer, 100 ml of stock was added into 900 ml of distilled water.

iii) Overlay solution (1% SDS)

To prepare 10 ml of overlay solution, 1 ml of 10% (w/v) SDS was mixed with 9 ml water.

iv) Stacking gel (0.125 M Tris-HCl, pH 6.8)

To prepare 10 ml 4% gel, 1.3 ml 30% Acrylamide/Bis, 2.5 ml 0.5 M Tris-HCl, pH 6.8, 0.1 ml 10% (w/v) SDS, 6.1 ml mili-Q water, 0.01 ml TEMED and 0.05 ml 10% (w/v) APS were mixed gently and poured into the electrophoresis plate. All the ingredients except TEMED and APS were mixed up together and degassed for about 5 minutes. The polymerization was initiated by addition of TEMED and APS followed by gentle swirling.

v) Separating gel (0.375 M Tris-HCl, pH 8.8)

To prepare 10 ml 12% gel, 4.0 ml 30% Acrylamide/Bis, 2.5 ml 0.5 M Tris-HCl, pH 6.8, 0.1 ml 10% (w/v) SDS, 3.4 ml mili-Q water, 0.01 ml TEMED and 0.05 ml 10% (w/v) APS were mixed gently and poured into the electrophoresis plate. All the ingredients except TEMED and APS were mixed up together and degassed for about 5 minutes. The polymerization was initiated by addition of TEMED and APS followed by gentle swirling.

APPENDIX C – Electrophoresis in Tris-Glicine Buffer System

i) IEF Cathode Buffer, pH 3-10

The cathode buffer was prepared by addition of 20 ml of 10X Novex® IEF Cathode buffer to 180 ml deionized water.

ii) IEF Anode Buffer, pH 3-10

To prepare 1000 ml of anode buffer 20 ml of 50X Novex® IEF Anode buffer was added to 980 ml deionized water.

iii) IEF sample buffer, pH 3-10

To prepare 10 ml of 2X IEF sample buffer, 2 ml of 10X Novex® IEF cathode buffer, pH 3-10 was added with 3 ml of glycerol. Then, the volume was adjusted to 10 ml with ultrapure water.

APPENDIX D – Coomassie Blue Reagent for Protein Determination

i) According to Spector (1978)

Coomassie Brilliant Blue G-250 (100 mg) was dissolved in 50 ml 95% ethanol. Then, 100 ml of 85% (w/v) phosphoric acid was added to this solution. The resulting solution was diluted to a final volume of 1 liter with distilled water. The solution was left overnight then filtered (Whatman paper) before used. A stock solution of 2mg/ml bovine serum albumin (BSA) was prepared in an appropriate buffer solution.

APPENDIX E – Substrate Preparation and Enzyme Assay conditions

i) 1-chloro-2,4-dinitrobenzene (CDNB)

2.85 ml Buffer A, 0.05 ml sample, 0.05 ml 60 mM GSH (0.0553 g in 3 ml Buffer A), and 0.05 ml 60 mM CDNB (0.2430 g in 20 ml ethanol) were mixed. Changes of absorbance were recorded for 10 minutes at 340 nm. Molar absorption coefficient, ϵ_m is $9600 \text{ M}^{-1}\text{cm}^{-1}$.

ii) 1,2-dichloro-4-nitrobenzene (DCNB)

2.80 ml Buffer B, 0.10 ml sample, 0.05 ml 240 mM GSH (0.2212 g in 3 ml Buffer A), and 0.05 ml 24 mM DCNB (0.2430 g in 20 ml ethanol) were mixed. Changes of absorbance were recorded for 10 minutes at 344 nm. Molar absorption coefficient, ϵ_m is $8400 \text{ M}^{-1}\text{cm}^{-1}$.

iii) *p*-nitrobenzylchloride (NBC)

2.60 ml Buffer A, 0.10 ml sample, 0.25 ml 60 mM GSH (0.0553 g in 3 ml Buffer A), and 0.05 ml 60 mM DCNB (0.2058 g in 20 ml ethanol) were mixed. Changes of absorbance were recorded for 10 minutes at 310 nm. Molar absorption coefficient, ϵ_m is $1900 \text{ M}^{-1}\text{cm}^{-1}$.

iv) Sulfobromophthalein (BSP)

2.60 ml Buffer C, 0.10 ml sample, 0.25 ml 60 mM GSH (0.0553 g in 3 ml Buffer A), and 0.05 ml 2 mM BSP (0.0334g in 20 ml ethanol) were mixed. Changes of absorbance were recorded for 10 minutes at 330 nm. Molar absorption coefficient, ϵ_m is $4500 \text{ M}^{-1}\text{cm}^{-1}$.

v) Ethacrynic acid (EA)

2.80 ml Buffer A, 0.10 ml sample, 0.05 ml 15 mM GSH (0.0138 g in 3 ml Buffer A), and 0.05 ml 12 mM EA (0.0727 g in 20 ml ethanol) were mixed. Changes of absorbance were recorded for 10 minutes at 270 nm. Molar absorption coefficient, ϵ_m is $5000 \text{ M}^{-1}\text{cm}^{-1}$.

vi) Trans-4-phenyl-3-butene-2-one (PBO)

2.80 ml Buffer A, 0.10 ml sample, 0.05 ml 15 mM GSH (0.0138 g in 3 ml Buffer A), and 0.05 ml 3 mM PBO (0.0876 g in 20 ml ethanol) were mixed. Changes of absorbance were recorded for 10 minutes at 290 nm. Molar absorption coefficient, ϵ_m is $-24800 \text{ M}^{-1}\text{cm}^{-1}$.

vii) Nitrocinnamaldehyde (NCA)

2.80 ml Buffer A, 0.10 ml sample, 0.05 ml 60 mM GSH (0.0553 g in 3 ml Buffer A), and 0.05 ml 24 mM NCA (0.0876 g in 20 ml ethanol) were mixed. Changes of absorbance were recorded for 10 minutes at 360 nm. Molar absorption coefficient, ϵ_m is $-3200 \text{ M}^{-1}\text{cm}^{-1}$.

APPENDIX F – Reagent for Proteomic Analysis

i) IPG Strip Rehydration Solution

To prepare 1 ml of rehydration solution, 0.48 g urea was dissolved in approximately 400 μ l milli-Q water followed by addition of 0.02 g CHAPS, 0.0015 g DTT, 0.0017 g thiourea, and 20 μ l ampholyte (pH 3-10). The content was made dissolved completely before the volume made up to 1 ml.

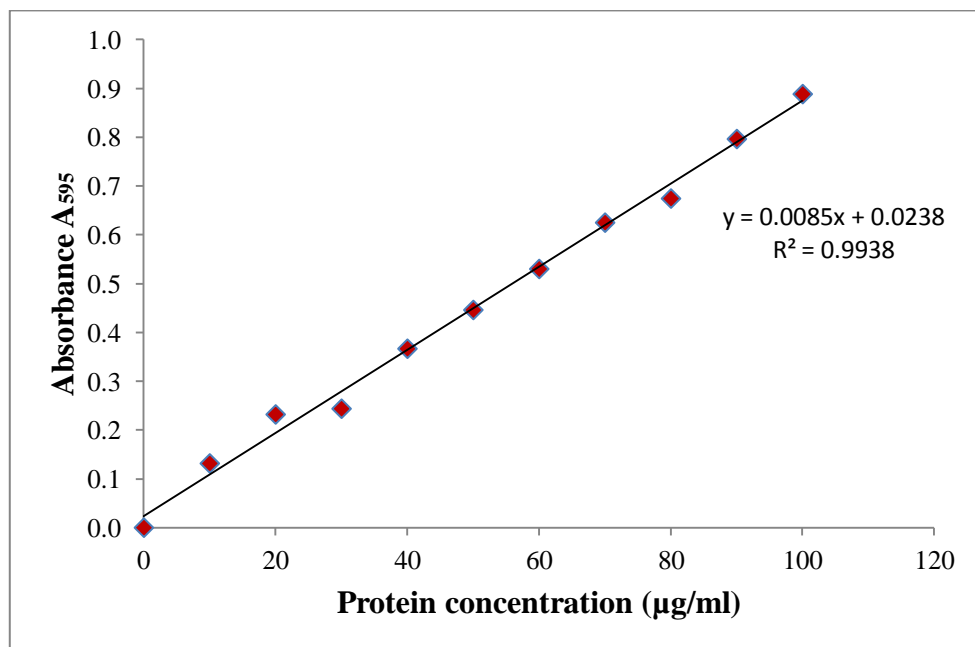
ii) Equilibration solution (ES)

To prepare 20 ml of equilibration solution, 7.2 g urea was first dissolved in approximately 7 ml milli-Q water followed by addition of 0.67 ml 1.5 M Tris-HCl (pH 8.8), 6.9 ml glycerol, and 0.4 g SDS. The solution was then made up to 20 ml. For equilibration solution I, 12.5 mg DTT was added in 5 ml ES. In equilibration solution II, 0.225 g iodoacetamide and traces of bromophenol blue was added in 5 ml of equilibration solution.

iii) Agarose sealing solution

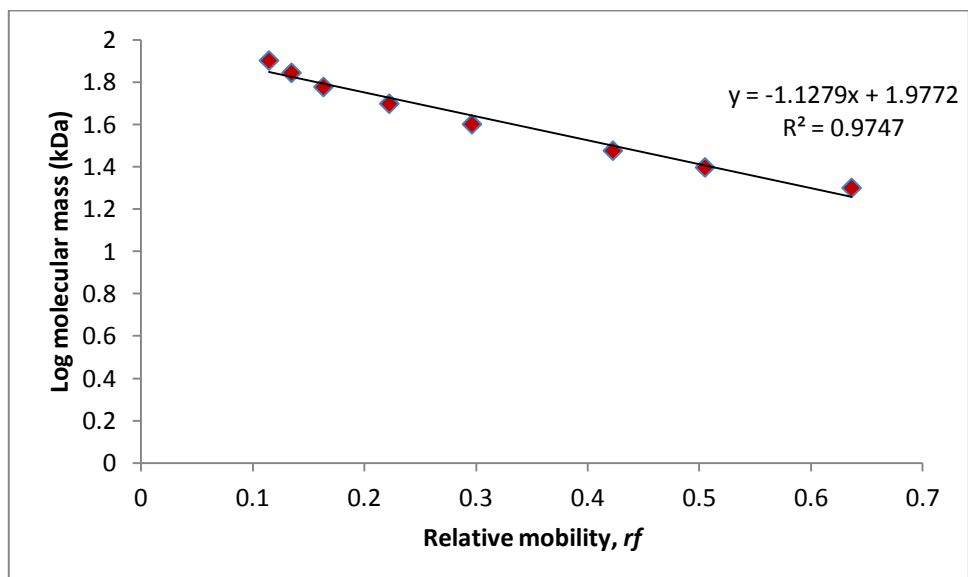
0.5 g agarose and traces of bromophenol blue were added into 100 ml of SDS electrophoresis buffer and swirled to disperse. The microwave was heated in a microwave until agarose was completely melted.

APPENDIX G – Standard Curve of BSA



Standard curve of protein using bovine serum Albumin.

APPENDIX H – Standard Curve of Molecular Weight Protein Marker



Standard curve of log molecular mass (kDa) vs protein marker relative mobility (*rf*)

APPENDIX I – Peptide masses for GSTs purified from GSTrap™HP

i) Spot 1

COM=Project: Proteomics, Spot Set: Proteomics\110117, Label: C7, Spot Id: 37869, Peak List Id: 84812, MS Job Run Id: 11316

805.44434 2393.0605
806.12457 1536.2112
832.3526 1682.6394
856.06854 1355.1366
860.53088 2742.8926
906.53296 2227.7385
935.56281 1454.874
988.6156 2856.8726
1044.0978 1592.2186
1153.6216 1338.2144
1179.6465 1075.1072
1300.1022 1242.1243
1353.7035 4701.4707
1424.7776 1160.3627
1609.8689 1297.0588
1723.967 1070.5883
1882.0631 1047.0588
2163.158 4339.7061
2273.2805 2803.9216
2289.27 2556.9602

BEGIN IONS

PEPMASS=805.44434

CHARGE=1+

TITLE=Label: C7, Spot_Id: 37869, Peak_List_Id: 85441, MSMS Job_Run_Id: 11317, Comment:

112.11942 161.50586
129.14931 106.30453
158.12248 117.44826
172.07455 130.41632
175.1629 719.5589
230.16396 168.6049
245.18246 190.43617
262.20728 524.87402
299.20587 347.71268
315.23712 185.08289
317.21481 553.77612
322.26251 248.24748
342.21622 211.42622
359.24548 735.87701
376.28287 187.78241
386.27615 108.29222
402.29971 178.55859
412.30673 364.40042
472.32724 175.29825
489.36621 204.37746
614.30322 376.74203
617.17438 1292.2406
674.52985 487.28085
756.56195 350.35236
760.59796 377.70764
761.46417 447.23383
775.53491 541.57233

END IONS

BEGIN IONS

PEPMASS=856.06854

CHARGE=1+

TITLE=Label: C7, Spot_Id: 37869, Peak_List_Id: 85438, MSMS Job_Run_Id: 11317, Comment:

172.07457 124.13093
335.16943 121.5791
478.22446 155.34978
622.20343 180.13982
623.12183 209.18585
664.27234 401.522
665.3045 361.27896
666.14978 1455.0112
667.21533 771.11499
668.19098 397.92688
727.5943 290.22226

729.52734 195.37189
809.5401 408.72537
811.22107 1214.0892
812.17877 416.34741
813.26453 362.49289
END IONS
BEGIN IONS
PEPMASS=860.53088
CHARGE=1+
TITLE=Label: C7, Spot_Id: 37869, Peak_List_Id: 85442, MSMS Job_Run_Id: 11317, Comment:
244.2155 641.53528
304.24707 123.61678
335.17441 141.48631
357.3103 142.30511
433.3082 344.17725
480.29855 189.04816
487.33224 537.90991
504.36597 213.808
572.48956 275.56171
589.44147 295.36066
600.42828 338.73969
617.45978 798.02789
666.28992 401.57718
667.33783 503.42569
668.30426 346.79294
669.33813 717.52936
670.33582 420.89688
672.28406 255.31097
674.12177 258.15533
676.07391 359.60529
732.53613 2552.3015
814.34888 729.86505
816.28619 388.8212
END IONS
BEGIN IONS
PEPMASS=873.07318
CHARGE=1+
TITLE=Label: C7, Spot_Id: 37869, Peak_List_Id: 85431, MSMS Job_Run_Id: 11317, Comment:
175.16451 138.69629
682.13147 1565.0696
684.11084 972.66882
827.20532 516.27161
END IONS
BEGIN IONS
PEPMASS=935.56281
CHARGE=1+
TITLE=Label: C7, Spot_Id: 37869, Peak_List_Id: 85439, MSMS Job_Run_Id: 11317, Comment:
129.13455 137.7451
175.15306 612.8974
286.19672 277.24844
303.22183 124.86664
357.27811 191.71901
399.30322 176.44405
416.33575 118.5838
449.26788 199.80447
492.38342 137.29401
520.37457 167.80287
562.37311 230.32191
579.42249 643.69104
605.50134 189.56511
END IONS
BEGIN IONS
PEPMASS=988.6156
CHARGE=1+
TITLE=Label: C7, Spot_Id: 37869, Peak_List_Id: 85443, MSMS Job_Run_Id: 11317, Comment:
86.113708 105.44118
101.09611 119.1199
112.11079 149.00493
175.14795 1933.0784
246.16026 114.79177
271.21567 333.13217
288.25171 356.1041

325.24542 228.13741
343.24826 131.35847
359.26416 227.87845
374.22464 238.18694
384.31863 301.55612
401.35883 203.0831
430.29233 204.87416
455.38272 150.63055
457.29004 158.49028
472.3981 367.05432
475.28918 278.3345
487.32452 159.80385
499.33014 318.90948
542.42487 218.80927
559.46014 191.36612
560.38654 251.06351
570.38184 666.54834
588.39783 879.52368
646.48895 179.09666
701.49023 335.92618
774.56079 256.36917
815.56232 649.39484
833.58112 602.24658
944.68909 1333.4951
946.65295 147.13756
947.66705 440.9288
958.70587 339.49573
END IONS
BEGIN IONS
PEPMASS=1044.0978
CHARGE=1+
TITLE=Label: C7, Spot_Id: 37869, Peak_List_Id: 85440, MSMS Job_Run_Id: 11317, Comment:
175.16402 151.88373
855.16962 562.96124
856.16071 580.53839
857.19543 277.72809
858.16632 225.80754
END IONS
BEGIN IONS
PEPMASS=1179.6465
CHARGE=1+
TITLE=Label: C7, Spot_Id: 37869, Peak_List_Id: 85434, MSMS Job_Run_Id: 11317, Comment:
175.1535 213.73433
303.23907 111.91177
422.22574 196.6682
535.34265 182.91498
758.58051 295.93195
887.61377 197.61443
1135.7339 256.6676
1136.7223 288.77722
END IONS
BEGIN IONS
PEPMASS=1259.725
CHARGE=1+
TITLE=Label: C7, Spot_Id: 37869, Peak_List_Id: 85428, MSMS Job_Run_Id: 11317, Comment:
175.15074 222.04048
338.27057 152.10963
472.40161 143.60559
738.5379 236.90509
788.51447 193.85934
1067.2714 184.81827
1193.7946 1127.6311
1194.77 679.20837
1215.8136 654.06836
END IONS
BEGIN IONS
PEPMASS=1300.1022
CHARGE=1+
TITLE=Label: C7, Spot_Id: 37869, Peak_List_Id: 85436, MSMS Job_Run_Id: 11317, Comment:
175.15138 108.43137
338.22748 148.62193
1233.8075 1290.3977

1254.2378 466.0448
1256.2086 1593.7881
END IONS
BEGIN IONS
PEPMASS=1308.7161
CHARGE=1+
TITLE=Label: C7, Spot_Id: 37869, Peak_List_Id: 85430, MSMS Job_Run_Id: 11317, Comment:
175.15099 401.02942
288.26276 108.67432
303.26425 140.34285
338.25177 154.56978
417.29965 124.70306
530.39319 367.95047
620.44196 142.50497
659.49475 861.3075
774.54791 236.23747
1256.2971 2296.6089
1258.2892 442.85754
1259.2932 245.41379
END IONS
BEGIN IONS
PEPMASS=1353.7035
CHARGE=1+
TITLE=Label: C7, Spot_Id: 37869, Peak_List_Id: 85444, MSMS Job_Run_Id: 11317, Comment:
175.15334 585.93134
288.25391 223.72549
385.28479 201.91936
402.31354 2012.1079
475.27719 190.68469
500.32251 132.85336
517.36682 200.33467
589.33618 251.02515
664.45636 2519.1948
762.47168 161.28192
859.5451 577.29236
876.56433 544.76025
973.61609 260.8577
1311.8333 140.11517
END IONS
BEGIN IONS
PEPMASS=1424.7776
CHARGE=1+
TITLE=Label: C7, Spot_Id: 37869, Peak_List_Id: 85435, MSMS Job_Run_Id: 11317, Comment:
329.21738 139.74588
520.31909 112.50616
591.4198 804.9859
607.35229 517.23315
678.49054 168.12212
706.44354 239.45969
719.52753 580.23828
818.60583 493.06238
933.65576 197.82771
1359.89 264.74677
1381.8248 208.13914
END IONS
BEGIN IONS
PEPMASS=1475.822
CHARGE=1+
TITLE=Label: C7, Spot_Id: 37869, Peak_List_Id: 85429, MSMS Job_Run_Id: 11317, Comment:
175.14581 138.03108
464.31772 594.86255
489.38449 138.97231
588.47369 128.39273
716.54669 163.57602
987.59229 256.52493
END IONS
BEGIN IONS
PEPMASS=1609.8689
CHARGE=1+
TITLE=Label: C7, Spot_Id: 37869, Peak_List_Id: 85437, MSMS Job_Run_Id: 11317, Comment:
175.14409 100.44118
322.22177 908.87256

737.47156 873.91376
1225.7633 322.32767
1475.8939 224.82912
1518.9569 328.3071
1545.0844 442.62714
1545.99 12913.178
1566.9103 240.57861
END IONS
BEGIN IONS
PEPMASS=1638.9551
CHARGE=1+
TITLE=Label: C7, Spot_Id: 37869, Peak_List_Id: 85427, MSMS Job_Run_Id: 11317, Comment:
175.1528 155.04903
288.24695 271.27451
322.22849 107.72575
402.32986 751.48657
737.45306 127.16407
1210.8047 189.89729
1324.9347 138.54491
1575.9915 200.1637
1580.8563 262.81204
1595.0353 368.93317
1610.0421 139.21887
END IONS
BEGIN IONS
PEPMASS=1723.967
CHARGE=1+
TITLE=Label: C7, Spot_Id: 37869, Peak_List_Id: 85433, MSMS Job_Run_Id: 11317, Comment:
503.33044 283.60114
665.43964 128.52585
691.41852 159.4883
865.59729 178.54596
1033.718 1278.1686
1104.7831 297.13544
1191.8202 331.98044
1319.8547 172.68295
END IONS
BEGIN IONS
PEPMASS=1882.0631
CHARGE=1+
TITLE=Label: C7, Spot_Id: 37869, Peak_List_Id: 85432, MSMS Job_Run_Id: 11317, Comment:
646.42206 108.40604
809.52716 205.91454
813.5636 324.98325
1069.6736 1953.2593
1182.7709 323.53409
1393.9125 797.23315
1540.9818 725.91309
END IONS
BEGIN IONS
PEPMASS=2226.0891
CHARGE=1+
TITLE=Label: C7, Spot_Id: 37869, Peak_List_Id: 85426, MSMS Job_Run_Id: 11317, Comment:
1142.6111 504.16068
1144.6243 176.35255
1145.5912 212.42233
1271.6973 247.16327
1316.7662 258.35977
1318.7507 131.32346
1370.8218 256.86133
1445.8138 392.17926
1469.8049 400.12183
1811.1152 365.09631

END IONS

ii) **Spot 2**

COM=Project: Proteomics, Spot Set: Proteomics\110117, Label: C8, Spot Id: 37870, Peak List Id: 84813, MS Job Run Id: 11316

804.46222	20409.043
805.47064	16973.896
860.56152	37803.52
906.56616	27302.457
935.59747	31609.33
988.64954	52797.262
1065.5839	6528.9253
1153.6514	8647.2637
1179.6855	6711.4468
1235.6202	5755.4082
1284.6392	6349.873
1307.7788	5652.626
1308.754	9688.9375
1353.7423	56375.91
1424.8223	7827.8096
1433.8251	5960.3486
1493.8475	7542.7002
1609.9001	6370.1533
1791.8607	6615.686
2163.2288	32600

BEGIN IONS

PEPMASS=804.46222

CHARGE=1+

TITLE=Label: C8, Spot_Id: 37870, Peak_List_Id: 85460, MSMS Job_Run_Id: 11317, Comment:

112.10732	150.59406
175.14917	899.16064
246.16742	129.30183
257.20001	175.15202
262.189	181.26311
274.19397	329.85516
299.20081	206.26802
317.20486	259.63821
359.22992	400.95773
367.26212	119.71044
385.27985	264.22992
402.29886	727.07446
403.25082	264.05368
412.3013	201.81155
472.33743	152.23155
489.35355	110.53223
514.34399	173.52689
531.31873	399.07007
612.36768	246.52164
614.27588	243.77133
617.15479	399.55429
674.48126	412.87646
713.5379	226.93781
759.28741	324.18982
760.49097	266.3811
775.50177	271.54126

END IONS

BEGIN IONS

PEPMASS=860.56152

CHARGE=1+

TITLE=Label: C8, Spot_Id: 37870, Peak_List_Id: 85462, MSMS Job_Run_Id: 11317, Comment:

244.21417	671.52612
335.17352	103.96983
357.31448	143.33492
416.26727	139.47455
433.31662	335.52213
480.2746	138.68388
481.24817	118.02216
482.27341	111.41644
487.31308	616.64545
504.37717	168.32312
524.25232	167.92952
572.4115	211.77733
589.46771	401.1763
600.43146	488.24338
617.44519	793.15009

667.26068	431.96576
668.28351	428.9639
669.36432	612.26886
670.28448	413.8064
671.33643	259.21527
672.20123	530.44086
674.10229	396.95364
676.09296	444.39905
732.53595	2397.3521
814.40857	439.30673
816.25922	530.53552

END IONS
BEGIN IONS
PEPMASS=935.59747
CHARGE=1+
TITLE=Label: C8, Spot_Id: 37870, Peak_List_Id: 85461, MSMS Job_Run_Id: 11317, Comment:

129.13826	144.59308
175.15387	661.9118
286.19257	311.96014
303.23926	179.01961
357.27463	259.069
399.29031	131.60364
416.33228	142.01505
449.27734	167.84929
520.37305	187.03995
562.38593	103.72126
579.42334	549.48645
605.45557	154.03149
819.59784	195.68419

END IONS
BEGIN IONS
PEPMASS=951.53485
CHARGE=1+
TITLE=Label: C8, Spot_Id: 37870, Peak_List_Id: 85445, MSMS Job_Run_Id: 11317, Comment:

112.10693	142.72298
175.16042	409.61337
416.24725	143.72313
617.41901	265.28763
886.61981	693.49042

END IONS
BEGIN IONS
PEPMASS=982.50116
CHARGE=1+
TITLE=Label: C8, Spot_Id: 37870, Peak_List_Id: 85450, MSMS Job_Run_Id: 11317, Comment:

175.15186	322.30569
786.96185	819.86401
935.68591	159.32841
936.50269	432.97421

END IONS
BEGIN IONS
PEPMASS=988.64954
CHARGE=1+
TITLE=Label: C8, Spot_Id: 37870, Peak_List_Id: 85463, MSMS Job_Run_Id: 11317, Comment:

175.14841	985.85767
271.22549	272.64658
288.25092	113.29029
325.2377	141.53139
359.27536	147.92529
384.31613	137.24825
401.34552	114.8522
430.30344	212.97964
457.27866	170.25537
472.36047	214.51962
475.28064	162.37752
487.30975	110.54105
499.32468	157.33916
559.4707	158.49789
570.37585	312.58554
571.35962	104.25291
588.40198	480.28821
646.48578	173.36455
701.4848	245.28102

774.5495 145.19662
 944.68506 716.76239
 958.66681 253.71313
 END IONS
 BEGIN IONS
 PEPMASS=1065.5839
 CHARGE=1+
 TITLE=Label: C8, Spot_Id: 37870, Peak_List_Id: 85454, MSMS Job_Run_Id: 11317, Comment:
 175.16824 384.28687
 346.27686 135.97198
 390.30463 147.82018
 402.3764 427.84653
 574.40613 110.89514
 618.46027 268.7626
 873.18719 327.95633
 END IONS
 BEGIN IONS
 PEPMASS=1179.6855
 CHARGE=1+
 TITLE=Label: C8, Spot_Id: 37870, Peak_List_Id: 85456, MSMS Job_Run_Id: 11317, Comment:
 175.14725 112.15686
 END IONS
 BEGIN IONS
 PEPMASS=1222.7314
 CHARGE=1+
 TITLE=Label: C8, Spot_Id: 37870, Peak_List_Id: 85447, MSMS Job_Run_Id: 11317, Comment:
 175.15424 114.31373
 411.25092 327.77377
 494.32846 106.80286
 568.41083 214.86909
 622.40564 154.59575
 637.37384 187.11797
 732.4469 382.17221
 766.44696 485.27441
 782.46667 244.34055
 812.59784 526.51514
 847.50732 203.19783
 851.52747 435.64795
 879.54333 990.82288
 949.6579 661.53632
 950.63489 349.45984
 960.5777 503.95981
 978.61383 1843.572
 1079.6603 287.38544
 1088.6831 261.74496
 1091.7098 944.60913
 1157.6882 427.1405
 1161.7324 720.44116
 1175.7866 336.37726
 END IONS
 BEGIN IONS
 PEPMASS=1235.6202
 CHARGE=1+
 TITLE=Label: C8, Spot_Id: 37870, Peak_List_Id: 85451, MSMS Job_Run_Id: 11317, Comment:
 175.14215 401.27451
 458.36383 162.98221
 701.51648 220.22708
 END IONS
 BEGIN IONS
 PEPMASS=1284.6392
 CHARGE=1+
 TITLE=Label: C8, Spot_Id: 37870, Peak_List_Id: 85452, MSMS Job_Run_Id: 11317, Comment:
 175.14703 201.76471
 409.26999 153.32298
 468.28259 177.2952
 675.39313 122.64357
 692.43219 2135.5496
 END IONS
 BEGIN IONS
 PEPMASS=1308.754
 CHARGE=1+
 TITLE=Label: C8, Spot_Id: 37870, Peak_List_Id: 85459, MSMS Job_Run_Id: 11317, Comment:

175.15491	314.36276
303.25632	113.03928
338.26196	132.15187
400.30438	109.33163
530.41681	293.32306
659.50317	775.01544
774.5506	247.29179

END IONS
BEGIN IONS
PEPMASS=1353.7423
CHARGE=1+
TITLE=Label: C8, Spot_Id: 37870, Peak_List_Id: 85464, MSMS Job_Run_Id: 11317, Comment:

175.14857	433.13727
288.24362	151.42157
385.2843	177.69656
402.31247	1637.7347
475.2724	141.71541
478.32242	124.68226
500.34802	103.40881
517.36847	169.19553
664.45856	1957.3541
702.41821	103.0509
779.48529	102.41322
859.54865	496.28165
876.56549	464.79016
973.60864	221.28603

END IONS
BEGIN IONS
PEPMASS=1424.8223
CHARGE=1+
TITLE=Label: C8, Spot_Id: 37870, Peak_List_Id: 85458, MSMS Job_Run_Id: 11317, Comment:

591.39862	456.33334
607.32996	308.34717
706.44031	179.59683
719.51776	298.44455
818.57532	199.6012

END IONS
BEGIN IONS
PEPMASS=1445.8105
CHARGE=1+
TITLE=Label: C8, Spot_Id: 37870, Peak_List_Id: 85449, MSMS Job_Run_Id: 11317, Comment:

437.31613	218.78625
591.41534	193.99319
621.41962	205.69411
784.5141	187.22095
898.60321	211.75974
1009.6335	1307.4613
1146.7321	416.0192
1313.8656	505.44281
1381.8826	165.57909
1400.847	299.75934

END IONS
BEGIN IONS
PEPMASS=1475.8751
CHARGE=1+
TITLE=Label: C8, Spot_Id: 37870, Peak_List_Id: 85448, MSMS Job_Run_Id: 11317, Comment:

464.31064	248.80003
830.60681	139.93953
987.62897	107.40086

END IONS
BEGIN IONS
PEPMASS=1493.8475
CHARGE=1+
TITLE=Label: C8, Spot_Id: 37870, Peak_List_Id: 85457, MSMS Job_Run_Id: 11317, Comment:

1365.8475	772.99597
-----------	-----------

END IONS
BEGIN IONS
PEPMASS=1609.9001
CHARGE=1+
TITLE=Label: C8, Spot_Id: 37870, Peak_List_Id: 85453, MSMS Job_Run_Id: 11317, Comment:

175.15118	103.38235
322.21445	439.2406

737.45349	434.96298
1225.7693	143.90398
1475.8983	186.09221
1518.9156	250.45866
1543.9904	160.11156
1545.9894	6619.1211
1560.0626	168.33611
END IONS	

iii) Spot 3

COM=Project: Proteomics, Spot Set: Proteomics\110117, Label: C9, Spot Id: 37871, Peak List Id: 84814, MS Job Run Id: 11316

804.45154	12100.285
860.55396	134108.22
864.51617	18202.994
935.58771	98827.547
969.67786	23113.891
988.63855	177472.17
1044.1158	13421.643
1179.6718	15887.772
1225.6942	12684.486
1300.1083	17508.037
1307.7596	15622.172
1308.7471	19297.338
1353.7332	218871.08
1424.8108	34834.82
1475.8574	11934.844
1609.8964	25298.898
1724.0072	20887.957
1791.8453	11378.916
1852.1019	11634.804
2163.2188	14262.742

BEGIN IONS

PEPMASS=804.45154

CHARGE=1+

TITLE=Label: C9, Spot_Id: 37871, Peak_List_Id: 85471, MSMS Job_Run_Id: 11317, Comment:

112.10414	196.38792
129.1367	102.99443
147.10883	108.96018
158.12622	168.15483
172.08145	479.56
175.15002	1040.647
228.17401	129.00276
244.22264	113.27748
246.1897	176.6357
257.20599	226.96649
258.17395	155.18658
269.17841	237.14087
274.2215	249.00755
286.19824	195.71843
359.26376	239.25601
385.29544	334.89682
402.32596	716.84637
403.24615	233.04741
415.25003	264.72379
610.27582	442.96759
617.14185	1523.9884
628.44086	378.27289
673.50757	494.2225
674.47571	1363.9099
742.43463	552.81897
754.48663	834.76886
756.49237	1108.4432
757.45374	524.10858
780.48932	389.90918
782.45966	426.36084

END IONS

BEGIN IONS

PEPMASS=860.55396

CHARGE=1+

TITLE=Label: C9, Spot_Id: 37871, Peak_List_Id: 85482, MSMS Job_Run_Id: 11317, Comment:

70.086441	185.93138
112.11401	360.23663
129.13928	169.54103
147.13779	158.07384
157.14688	470.73575
175.16182	163.24702
226.19685	470.29413
244.21539	5968.606
259.20526	501.70737
287.19928	297.99612
304.23468	619.43823

348.22461	604.49347
357.32092	1180.1711
374.24023	303.73376
405.30481	501.49655
416.27942	1117.4048
428.37643	473.90353
433.30756	3202.9448
445.29691	855.59656
459.32507	700.67816
476.35574	573.31183
487.32794	5621.9199
504.35449	1910.1249
572.43231	2064.6479
574.85638	492.99829
575.42456	363.56421
589.45697	3125.9219
591.84869	947.099
600.42871	3803.2119
617.45612	5466.2871
635.46765	883.97351
666.19293	956.63812
667.24414	839.1275
668.23315	666.95721
669.27301	733.6781
715.49799	882.43494
731.54993	1235.9187
732.53821	23317.363
811.26801	678.57819
812.24866	1010.6246
816.32495	880.28033
818.59106	883.32166

END IONS

BEGIN IONS

PEPMASS=935.58771

CHARGE=1+

TITLE=Label: C9, Spot_Id: 37871, Peak_List_Id: 85481, MSMS Job_Run_Id: 11317, Comment:

84.103889	399.63113
86.122452	195.84929
101.10224	185.7178
112.11694	309.29938
129.13826	667.40735
158.12587	173.51109
175.15602	3573.4395
228.21613	506.19318
242.19704	220.80959
249.2043	140.34433
286.20148	1657.3655
293.17175	531.841
303.23215	892.30396
357.27737	1176.131
382.26392	317.50983
399.30743	842.33813
402.34378	272.13373
405.2854	272.92883
416.33527	714.08295
421.27884	278.25305
449.28885	1018.3085
492.37073	652.97076
520.37872	952.62292
534.38947	535.29755
562.3913	1227.0983
579.42932	4115.5386
591.43103	382.22253
605.48096	718.51532
633.46558	506.8725
708.48212	580.11835
761.57037	360.84933
819.57489	530.55188
836.60461	337.09402
893.64612	426.54663
900.58746	332.06546

END IONS

BEGIN IONS

PEPMASS=969.67786

CHARGE=1+

TITLE=Label: C9, Spot_Id: 37871, Peak_List_Id: 85478, MSMS Job_Run_Id: 11317, Comment:

129.14224	172.94514
175.16277	1037.3309
200.14218	148.65741
242.20813	184.16905
271.21332	399.65634
288.26608	165.01617
327.26746	164.96959
342.28491	155.01363
359.30978	230.241
370.3154	278.54114
384.33636	302.72156
398.32382	199.39674
441.34561	221.10081
487.3847	178.03136
498.40836	217.87416
558.45532	207.56146
611.47998	305.34918
682.55896	208.06392
726.45514	430.70996
800.5896	358.35413

END IONS

BEGIN IONS

PEPMASS=988.63855

CHARGE=1+

TITLE=Label: C9, Spot_Id: 37871, Peak_List_Id: 85483, MSMS Job_Run_Id: 11317, Comment:

86.115189	461.13922
101.09288	382.9902
112.10873	529.77051
129.13745	274.32959
157.13611	225.77226
158.11617	267.78226
175.14938	6501.8125
215.17787	216.33577
216.13921	231.75406
230.14832	296.69196
246.15556	428.6792
271.21918	1393.4207
288.24643	993.09009
325.23325	792.44519
343.25452	463.09024
359.2485	740.64948
374.22958	659.56946
384.32031	841.86285
401.35092	830.44208
430.30029	827.06628
455.36957	349.49921
457.28186	804.69238
472.39191	1201.804
475.29346	1087.1649
487.33459	570.23096
499.33823	768.45233
517.34369	701.01965
559.44623	1170.0476
560.42139	577.85352
570.38092	2395.5291
571.97168	472.73083
588.40326	2845.3176
646.49194	791.29883
673.47729	452.06235
683.49554	511.85977
701.48669	954.46204
774.57172	761.41949
926.6557	318.04608
929.54968	468.14029
943.64777	315.76355
944.69568	3791.281
947.67133	313.73212
958.69733	930.20996

END IONS
 BEGIN IONS
 PEPMASS=1044.1158
 CHARGE=1+
 TITLE=Label: C9, Spot_Id: 37871, Peak_List_Id: 85473, MSMS Job_Run_Id: 11317, Comment:
 175.15828 479.08771
 646.54242 514.67548
 811.17273 883.14502
 812.15918 245.39952
 853.22223 506.76379
 854.18524 413.0386
 855.17303 1703.0658
 856.1604 4853.0977
 858.15326 529.11993
 996.66077 330.147
 997.70148 267.91092
 999.62335 305.63824
 END IONS
 BEGIN IONS
 PEPMASS=1179.6718
 CHARGE=1+
 TITLE=Label: C9, Spot_Id: 37871, Peak_List_Id: 85474, MSMS Job_Run_Id: 11317, Comment:
 112.11678 189.92216
 129.14081 113.34248
 175.15714 538.03418
 242.19734 197.19432
 293.16522 249.73328
 303.23874 189.89149
 371.23428 152.11101
 404.29279 225.17398
 406.27646 119.63517
 422.22852 523.99554
 500.33749 203.90338
 535.33185 202.59285
 646.41864 210.4749
 663.42267 495.26376
 758.56897 700.17468
 887.62128 405.11591
 934.57294 840.18005
 1051.6698 1203.2523
 1135.7118 672.92554
 END IONS
 BEGIN IONS
 PEPMASS=1225.6942
 CHARGE=1+
 TITLE=Label: C9, Spot_Id: 37871, Peak_List_Id: 85472, MSMS Job_Run_Id: 11317, Comment:
 175.15617 272.59802
 266.203 137.21956
 379.32047 206.97115
 411.24319 253.88858
 494.34711 492.88727
 604.37341 372.60086
 622.42853 662.09521
 637.39276 209.80002
 675.43732 258.42654
 732.46625 2106.3252
 736.49927 586.24048
 737.47668 186.40215
 766.46057 387.27274
 812.63361 346.65677
 847.51678 1124.5031
 851.52618 1484.8914
 879.56091 504.44342
 922.63391 236.43115
 950.62659 1105.1604
 960.6087 1613.2191
 978.63495 969.30652
 1079.6704 1218.2491
 1088.7025 1059.4858
 1091.7527 678.0993
 1097.6903 780.04254
 1161.7878 393.99911

1162.7125 238.95125
1179.8149 342.4617
1190.7367 295.82715

END IONS

BEGIN IONS

PEPMASS=1300.1083

CHARGE=1+

TITLE=Label: C9, Spot_Id: 37871, Peak_List_Id: 85475, MSMS Job_Run_Id: 11317, Comment:

175.1478 355.58826
288.22934 164.65686
338.23721 1101.4216
402.33328 122.44296
421.2222 112.68245
489.26108 188.69386
520.32574 106.24107
591.40967 181.51286
664.47137 214.87727
812.46967 532.633
1111.1602 482.00574
1212.2235 842.42798
1254.2473 3214.1716
1256.1979 17782.232

END IONS

BEGIN IONS

PEPMASS=1308.7471

CHARGE=1+

TITLE=Label: C9, Spot_Id: 37871, Peak_List_Id: 85476, MSMS Job_Run_Id: 11317, Comment:

84.100792 130.24794
112.11981 326.13293
129.13705 257.88712
175.15472 1283.6616
242.2197 141.62387
243.1796 338.8241
288.26129 343.784
303.25854 541.45349
338.24847 767.02954
356.28235 132.80107
358.32785 242.77499
385.28397 341.05725
400.29733 392.63382
402.31512 388.84509
406.28439 188.8098
417.31531 271.97281
433.27579 181.40555
513.40454 196.85718
530.41333 1645.0422
535.36145 160.13187
537.29089 250.42447
591.41418 148.43646
618.43994 211.76927
620.46198 425.59045
659.49432 3131.8574
757.50262 253.84372
774.55072 678.64813
779.47021 411.1366
790.52539 825.50159
1256.2897 5381.3218
1258.2896 2322.5505

END IONS

BEGIN IONS

PEPMASS=1353.7332

CHARGE=1+

TITLE=Label: C9, Spot_Id: 37871, Peak_List_Id: 85484, MSMS Job_Run_Id: 11317, Comment:

70.091423 112.54903
112.11685 293.31689
129.1447 189.86703
136.10573 148.50697
175.15349 2932.1428
201.15942 136.07706
212.15242 136.82253
213.13316 184.60027
228.17519 127.43918

271.22748	167.45146
278.15985	284.97052
288.2493	1086.9608
327.17389	245.05183
346.23312	229.80612
360.21878	254.4317
364.23593	201.38287
365.23703	277.44321
377.23688	239.70021
385.28311	988.34216
402.31335	10347.334
475.25522	1252.7732
478.30237	728.6828
492.28812	180.43546
499.33701	229.97023
500.33163	572.60669
517.35303	1130.6014
544.28961	224.91298
572.31427	219.29057
589.32635	959.15594
622.47058	568.73517
647.42419	300.7384
664.45807	13543.895
674.42285	504.46408
702.43835	733.42499
732.48663	926.86566
750.55853	286.73898
761.49921	274.03723
762.47552	678.15082
779.48785	312.37271
789.5152	314.17813
847.52527	470.02991
859.53333	2521.5769
864.61603	293.46671
876.5705	2910.488
960.62622	705.94269
973.60352	1552.2808
979.65839	903.93646
990.6264	652.23645
1078.7227	505.27164
1088.7384	707.40601
1153.7438	765.85687
1207.8033	745.51117
1225.8024	724.6076
1240.8011	414.86932
1309.8296	416.84189
1311.7958	324.46411
1323.8042	553.10046

END IONS

BEGIN IONS

PEPMASS=1406.8469

CHARGE=1+

TITLE=Label: C9, Spot_Id: 37871, Peak_List_Id: 85465, MSMS Job_Run_Id: 11317, Comment:

129.12764	128.73143
175.155	467.0867
288.2402	120.85375
357.24835	129.20424
385.24283	159.02879
402.30151	455.48666
591.39313	372.94559
629.39984	275.83264
639.39209	317.42978
646.45471	377.25186
757.46429	308.35117
774.50763	291.64862
917.65015	437.73996
1050.7019	952.08954
1161.7461	2595.2473
1277.8492	923.83221
1278.8309	3422.8845
1336.8234	562.4057
1342.8397	611.78363

1353.947 747.94067
1359.8865 547.92242
1361.7961 785.64069
1372.7698 1295.8137
1377.9156 776.48376
1383.7928 548.43793
1385.7784 682.67096

END IONS

BEGIN IONS

PEPMASS=1424.8108

CHARGE=1+

TITLE=Label: C9, Spot_Id: 37871, Peak_List_Id: 85480, MSMS Job_Run_Id: 11317, Comment:

129.12921 197.74533
159.10168 156.76471
228.20213 113.42429
329.20557 381.31296
378.21075 128.45195
464.24023 207.10571
465.24057 441.72397
492.28085 166.53284
520.33087 198.94389
536.29108 142.53101
543.32056 178.01134
564.32629 148.80113
573.39398 294.41754
591.39343 3038.2842
607.33441 1928.9888
635.39984 202.46796
678.43176 482.63934
706.42627 855.55811
719.51233 2237.7993
818.60303 1225.0669
931.59052 262.04813
933.63525.57916
1060.6755 333.80951
1096.7235 377.93668
1207.7576 288.17126
1278.7794 441.03513

END IONS

BEGIN IONS

PEPMASS=1475.8574

CHARGE=1+

TITLE=Label: C9, Spot_Id: 37871, Peak_List_Id: 85470, MSMS Job_Run_Id: 11317, Comment:

175.14499 348.82227
316.15781 110.56023
322.23123 314.76981
402.30124 118.35466
429.26096 124.48022
464.30652 835.32251
489.37665 196.06497
588.47461 259.69281
591.41675 185.44908
737.4588 282.8056
768.47021 241.4948
830.61328 305.4585
883.49768 266.9725
888.54053 312.45844
987.638 429.83899
1319.8644 629.38776
1433.8829 507.25778

END IONS

BEGIN IONS

PEPMASS=1609.8964

CHARGE=1+

TITLE=Label: C9, Spot_Id: 37871, Peak_List_Id: 85479, MSMS Job_Run_Id: 11317, Comment:

175.1459 317.89154
322.22614 3270.2939
437.25815 169.26721
508.30627 136.79279
636.39252 217.49518
645.42133 130.70967
719.45862 207.20929

720.44269	216.06328
737.45953	3225.6838
852.52234	246.86058
906.5274	200.62151
1078.7307	219.54218
1161.7863	627.44214
1225.7592	1135.0323
1475.9238	893.51349
1501.9821	303.92786
1503.9701	326.39328
1518.9691	1427.4333
1544.0994	534.13879
1545.0304	726.17682
1545.9957	41791.566
1550.9185	274.84869
1561.9576	321.37772
1564.0168	122.68846
1564.9052	344.41171

END IONS

BEGIN IONS

PEPMASS=1724.0072

CHARGE=1+

TITLE=Label: C9, Spot_Id: 37871, Peak_List_Id: 85477, MSMS Job_Run_Id: 11317, Comment:

175.13742	135.63725
303.21548	134.72787
498.31601	234.27693
503.33304	546.8067
533.3656	103.77921
536.3728	145.43663
611.43658	244.64156
620.39337	103.78656
665.44507	289.96164
691.44855	432.74118
758.5332	220.21466
778.5473	490.25452
865.59369	755.51447
946.5766	199.2606
1015.703	288.0361
1033.7166	4874.3159
1104.7539	897.46716
1188.7532	358.69424
1191.7909	838.63763
1319.8734	429.20715
1433.0132	191.25578

END IONS

BEGIN IONS

PEPMASS=1791.8453

CHARGE=1+

TITLE=Label: C9, Spot_Id: 37871, Peak_List_Id: 85468, MSMS Job_Run_Id: 11317, Comment:

112.11028	247.05215
175.14218	325.4902
319.24033	114.57606
406.23474	110.13193
520.32422	187.61746
577.36365	194.4352
737.38751	256.61426
753.39233	306.94046
797.47894	118.94456
854.49921	232.62326
894.52203	235.74368
911.53339	268.09232
921.52338	360.54813
927.56543	298.14508
929.54266	119.96706
1095.6638	1351.063
1097.6722	393.04416
1166.7142	951.54108
1168.7048	373.55963
1169.6871	157.57549
1226.7102	338.65524
1253.7537	679.98816
1658.0564	442.54086

1725.1085 414.36237
1743.9843 539.84125
1756.9011 273.76224
1761.9512 530.80951
1766.0652 352.71759
1768.1351 313.09091

END IONS

BEGIN IONS

PEPMASS=1852.1019

CHARGE=1+

TITLE=Label: C9, Spot_Id: 37871, Peak_List_Id: 85469, MSMS Job_Run_Id: 11317, Comment:

498.31564 338.41641
503.31934 218.00356
533.31995 131.18279
551.39197 165.29765
611.39502 305.96823
620.38263 155.69168
664.47192 437.44525
691.41461 266.47379
793.53613 635.77136
887.54901 145.80389
906.651 495.41321
993.71381 522.94043
1161.8043 3411.8787
1232.8375 675.76404
1319.9188 763.56067
1408.9373 738.89636
1724.0953 928.39111
1808.124 427.09448

END IONS

BEGIN IONS

PEPMASS=1995.1289

CHARGE=1+

TITLE=Label: C9, Spot_Id: 37871, Peak_List_Id: 85467, MSMS Job_Run_Id: 11317, Comment:

175.13942 100.93137
274.21725 180.29411
338.23193 110.00609
554.34967 152.56491
626.37164 518.06787
739.48694 271.83551
863.5564 212.6812
886.60138 1157.3768
933.59497 739.69464
950.59381 6088.4565
1045.6821 499.30188
1113.6716 821.03528
1136.7267 383.47925
1200.7208 1910.4186
1256.8287 271.66058
1315.7697 753.22058
1369.8962 466.88779
1428.9164 568.59137
1541.9642 652.5119
1690.1056 523.34253
1754.0682 2479.9375
1913.25 599.47955
1916.2516 485.19107
1925.1935 304.36008
1929.2745 384.4209
1931.2289 11079.924
1948.1814 448.59671
1951.2074 225.53078
1973.0504 434.71011

END IONS

BEGIN IONS

PEPMASS=2384.1172

CHARGE=1+

TITLE=Label: C9, Spot_Id: 37871, Peak_List_Id: 85466, MSMS Job_Run_Id: 11317, Comment:

112.11031 219.17432
129.13692 135.98103
175.15314 268.38235
346.20175 144.6889

403.22931	192.32019
460.271	232.69479
517.30341	287.72342
574.32703	462.99371
661.34515	238.55186
701.38892	200.20717
718.38727	499.91599
881.49268	495.61115
968.52594	230.69127
1025.5652	253.09436
1082.6149	320.86884
1139.62	410.5603
1226.6865	256.98816
1266.6915	225.32597
1283.7252	384.85635
1446.8054	369.10474
1533.8253	386.53915
1734.9374	266.85703
2321.4114	333.4256
2336.2456	700.49182
2341.2827	457.02084
2348.2397	248.84975
2354.1934	1280.0945
END IONS	

iv) Spot 4

COM=Project: Proteomics, Spot Set: Proteomics\110117, Label: C10, Spot Id: 37872, Peak List Id: 84815, MS Job Run Id: 11316

805.45923	4890.4844
806.13171	3009.2764
832.35486	1586.7332
855.07593	2154.905
856.06567	2033.7329
873.07672	1929.347
906.54767	4911.7236
912.6109	9057.8711
1017.5901	4218.0044
1044.1235	3616.272
1097.6594	1872.3473
1153.6381	2673.5498
1173.7074	1943.865
1200.6677	3777.9795
1300.109	3721.0491
1491.8809	2657.4407
1619.9878	2173.0391
2163.2202	6602.9409
2273.3179	1902.4509
2289.3276	2428.4314

BEGIN IONS

PEPMASS=805.45923

CHARGE=1+

TITLE=Label: C10, Spot_Id: 37872, Peak_List_Id: 85499, MSMS Job_Run_Id: 11317, Comment:

112.12329	154.91393
158.13577	109.66594
175.16292	629.77075
230.15817	206.96591
245.17796	209.28882
262.20782	495.29297
299.20084	334.9079
315.23441	148.20016
317.21396	577.43158
342.20901	170.76938
359.23993	834.9093
376.27887	194.40781
402.32874	226.03123
412.29251	313.38727
430.32672	253.82642
455.3187	186.04477
472.3551	312.03134
489.38165	182.57474
542.35651	125.55524
559.38318	179.18663
573.1734	137.55347
614.20898	206.37733
615.26935	212.23891
616.19165	131.52605
617.1803	1332.7405
619.18347	268.33084
763.5238	284.32733
770.47815	147.41925
771.49127	122.17533
775.53668	616.71765

END IONS

BEGIN IONS

PEPMASS=855.07593

CHARGE=1+

TITLE=Label: C10, Spot_Id: 37872, Peak_List_Id: 85492, MSMS Job_Run_Id: 11317, Comment:

581.06201	140.85744
621.10303	187.47444
622.11786	350.17935
623.09656	1168.069
664.15906	365.93683
665.15393	536.08337
666.11554	2831.2998
667.10187	1379.1648
668.07715	544.29895
670.0675	321.25024
809.2309	515.08716

810.18622 242.31035
811.15424 2563.9304
812.14325 1980.026
814.1358 576.42139

END IONS

BEGIN IONS

PEPMASS=873.07672

CHARGE=1+

TITLE=Label: C10, Spot_Id: 37872, Peak_List_Id: 85490, MSMS Job_Run_Id: 11317, Comment:

442.33487 188.73415
571.40125 298.84293
589.41339 201.79654
638.12012 441.5799
640.11597 495.36594
681.1629 432.79846
682.14862 2422.5439
684.11469 1825.0817
686.10663 155.1026
718.48303 239.76495
811.16296 814.19757
827.22748 1294.1176
828.21277 324.76575
829.17407 1174.8942
832.58563 148.43846

END IONS

BEGIN IONS

PEPMASS=912.6109

CHARGE=1+

TITLE=Label: C10, Spot_Id: 37872, Peak_List_Id: 85500, MSMS Job_Run_Id: 11317, Comment:

101.10111 134.95099
112.10908 108.42352
185.15228 131.64581
268.18542 233.30031
313.24622 165.48349
339.24344 179.31372
441.37787 275.27277
444.35699 1719.624
452.31461 309.25681
469.36917 2565.9768
583.43073 515.85547
600.47046 277.07925
664.54504 342.97003
665.60864 190.85509
720.12762 577.48254
723.0531 172.08286
728.54279 217.75636
738.59637 539.16882
766.58069 447.80939
783.6098 232.12808
784.59375 3943.77
849.52869 123.73678
882.66656 230.4213

END IONS

BEGIN IONS

PEPMASS=1017.5901

CHARGE=1+

TITLE=Label: C10, Spot_Id: 37872, Peak_List_Id: 85498, MSMS Job_Run_Id: 11317, Comment:

175.15886 666.37256
212.14394 203.27097
243.1783 130.02126
288.24896 183.92145
325.24585 197.95662
372.2525 468.89368
385.28476 268.44205
457.35028 116.66668
465.33594 223.75775
482.35742 1781.8638
499.39178 737.9881
519.34058 114.27126
629.44836 287.50824
646.48572 1583.6359
775.54291 856.6662

973.57935 208.77089
 975.59448 398.16138
 END IONS
 BEGIN IONS
 PEPMASS=1044.1235
 CHARGE=1+
 TITLE=Label: C10, Spot_Id: 37872, Peak_List_Id: 85495, MSMS Job_Run_Id: 11317, Comment:
 811.16656 554.64722
 812.17615 335.23935
 854.21899 354.28897
 855.16266 1291.1954
 856.17047 4253.4741
 858.14307 594.35889
 1000.2152 387.8602
 END IONS
 BEGIN IONS
 PEPMASS=1097.6594
 CHARGE=1+
 TITLE=Label: C10, Spot_Id: 37872, Peak_List_Id: 85489, MSMS Job_Run_Id: 11317, Comment:
 112.11037 158.23532
 129.1373 111.32405
 175.15257 130.29266
 255.18735 722.9754
 272.21448 973.13733
 316.16943 449.75229
 369.24966 938.06372
 386.27682 420.90982
 401.28012 231.88995
 413.29782 122.37975
 429.27417 675.08459
 485.36493 165.694
 500.33252 216.2047
 514.36353 182.8409
 542.38434 697.16364
 556.41394 210.68315
 613.43091 1032.4194
 669.52032 305.86642
 712.50275 258.41461
 782.61621 2776.3806
 897.66772 637.19965
 907.11981 153.58807
 908.09985 292.09854
 909.13379 885.03961
 911.07867 260.94641
 END IONS
 BEGIN IONS
 PEPMASS=1117.5986
 CHARGE=1+
 TITLE=Label: C10, Spot_Id: 37872, Peak_List_Id: 85486, MSMS Job_Run_Id: 11317, Comment:
 272.21304 183.24245
 437.33945 258.05319
 518.32422 324.61411
 633.37701 356.18555
 681.40625 753.39502
 760.47235 339.03873
 761.48138 284.38104
 818.46735 254.9623
 881.14105 585.159
 882.11578 225.44984
 923.17645 511.26416
 925.1507 1295.4041
 927.11261 404.55893
 1068.2295 777.62482
 1070.1892 1461.0961
 END IONS
 BEGIN IONS
 PEPMASS=1155.6831
 CHARGE=1+
 TITLE=Label: C10, Spot_Id: 37872, Peak_List_Id: 85487, MSMS Job_Run_Id: 11317, Comment:
 312.20514 188.07722
 359.33093 239.92885
 360.2652 170.9046

402.23032 164.95424
425.31412 283.37875
473.31088 219.20924
475.29739 103.2343
547.30017 123.3495
553.42615 174.64545
555.35724 251.6125
565.31268 370.20444
570.42401 318.38522
571.44043 4999.3687
583.32544 389.4635
586.42932 269.8725
683.53351 396.1423
734.54272 789.30994
796.58997 849.45215
821.58051 552.75317
846.61639 346.78403
866.56616 149.93105
876.52893 251.21611
894.52673 576.51337
909.70679 330.25363
979.70691 441.41547
1091.8124 3033.8738

END IONS

BEGIN IONS

PEPMASS=1173.7074

CHARGE=1+

TITLE=Label: C10, Spot_Id: 37872, Peak_List_Id: 85491, MSMS Job_Run_Id: 11317, Comment:

129.12714 111.76523
175.15312 618.65167
416.36853 201.49915
545.42792 322.31601
630.40454 208.44809
655.52716 220.57748
759.4856 210.98163
802.60358 509.67502
809.49268 530.37146
873.63116 383.81375
999.69275 2078.8862
1017.6931 2288.8311
1113.7764 696.40063
1130.754 521.4754
1131.7698 1311.5061

END IONS

BEGIN IONS

PEPMASS=1200.6677

CHARGE=1+

TITLE=Label: C10, Spot_Id: 37872, Peak_List_Id: 85497, MSMS Job_Run_Id: 11317, Comment:

266.14572 130.13329
412.29568 1968.4725
525.40344 417.09302
639.45453 588.12695
676.40216 247.59988
754.51221 278.74261
789.49933 476.65884
825.55426 393.7691
926.57953 943.73828
943.63629 272.30679
954.61212 235.82953
1054.6536 823.48761
1072.6493 213.58304
1165.6805 115.61228

END IONS

BEGIN IONS

PEPMASS=1262.611

CHARGE=1+

TITLE=Label: C10, Spot_Id: 37872, Peak_List_Id: 85488, MSMS Job_Run_Id: 11317, Comment:

474.2468 174.94519
587.34161 310.6788
701.41498 446.50613
816.46527 270.97665
887.50195 328.52808

988.52283	438.07401
1016.5209	169.35638
1067.213	328.39465
1068.2512	276.00455
1134.6305	391.68143

END IONS
BEGIN IONS
PEPMASS=1300.109
CHARGE=1+
TITLE=Label: C10, Spot_Id: 37872, Peak_List_Id: 85496, MSMS Job_Run_Id: 11317, Comment:

1111.1689	250.37331
1212.205	490.05234
1254.2596	2187.8914
1256.1959	14493.154

END IONS
BEGIN IONS
PEPMASS=1491.8809
CHARGE=1+
TITLE=Label: C10, Spot_Id: 37872, Peak_List_Id: 85494, MSMS Job_Run_Id: 11317, Comment:

272.20148	339.06851
369.22501	286.96078
386.27133	159.01897
466.30426	115.07899
485.35016	102.28844
556.37579	174.05632
669.4812	219.82281
710.44452	224.26433
782.60236	1999.652
795.52655	107.2398
822.4585	150.57381
823.53638	224.6456
897.65619	431.69785
936.58685	166.67998
1007.6732	224.85655
1225.8726	200.9677
1300.2661	500.77701
1302.24	266.14154
1362.9574	421.45538

END IONS
BEGIN IONS
PEPMASS=1619.9878
CHARGE=1+
TITLE=Label: C10, Spot_Id: 37872, Peak_List_Id: 85493, MSMS Job_Run_Id: 11317, Comment:

669.49591	100.17683
782.59637	622.59741
897.63116	146.84979
1348.9363	147.00241
1362.9371	177.25558
1430.1189	127.75149
1574.1519	365.87708
1576.1039	178.98468

END IONS
BEGIN IONS
PEPMASS=1733.9934
CHARGE=1+
TITLE=Label: C10, Spot_Id: 37872, Peak_List_Id: 85485, MSMS Job_Run_Id: 11317, Comment:

817.56256	347.24133
932.61163	244.61569
1118.6847	189.63083
1146.6649	245.17879
1259.7424	307.54977
1372.8284	373.91568
1588.0574	302.46484

END IONS

v) **Spot 5**

COM=Project: Proteomics, Spot Set: Proteomics\110117, Label: C11, Spot Id: 37873, Peak List Id: 84816, MS Job Run Id: 11316

805.46021	5603.3047
832.36041	2897.0293
855.06323	3270.2935
906.55157	7268.0313
912.61237	43499.844
974.53485	4329.563
1017.5923	21736.875
1044.1276	4924.6401
1097.6536	8252.8984
1155.7146	6827.7983
1173.7058	7212.729
1174.7106	15001.864
1200.6729	21851.713
1262.5938	6720.1528
1300.1018	5421.373
1433.8079	3373.446
1491.8789	9157.0557
1619.9877	5050
2163.1936	12921.078
2225.1555	3732.1396

BEGIN IONS

PEPMASS=805.46021

CHARGE=1+

TITLE=Label: C11, Spot_Id: 37873, Peak_List_Id: 85512, MSMS Job_Run_Id: 11317, Comment:

175.15703	393.44388
245.18872	113.21539
262.2067	279.16672
299.20667	174.93878
317.21356	347.15488
342.19824	125.07967
359.24146	437.62689
402.30148	188.48848
412.30722	229.29825
430.31699	148.97734
472.34375	152.74342
573.16193	303.2897
614.19617	368.64893
615.24292	355.83246
616.21332	213.89679
617.17175	2336.6504
759.37549	632.96155
775.52887	381.71021

END IONS

BEGIN IONS

PEPMASS=855.06323

CHARGE=1+

TITLE=Label: C11, Spot_Id: 37873, Peak_List_Id: 85506, MSMS Job_Run_Id: 11317, Comment:

172.10023	131.72098
560.2287	323.79785
621.09344	190.86272
622.13446	635.32715
623.08826	713.31244
662.29517	565.12103
663.25244	289.9346
664.1925	627.19983
665.18915	492.77554
666.10284	3056.4377
667.09784	790.81921
668.09381	518.33112
809.32306	1087.3014
810.32294	583.19324
811.15771	2706.2468
812.14099	918.69983

END IONS

BEGIN IONS

PEPMASS=873.07568

CHARGE=1+

TITLE=Label: C11, Spot_Id: 37873, Peak_List_Id: 85503, MSMS Job_Run_Id: 11317, Comment:

172.091	137.65031
400.39233	174.77652

442.33395	254.03261
578.24884	247.07802
638.12433	463.38879
640.12408	777.52332
681.17688	674.0885
682.13129	3126.0986
684.11584	2471.6926
811.17755	1447.8237
812.17639	413.51489
827.21545	1584.2744
829.17841	1493.861

END IONS

BEGIN IONS

PEPMASS=912.61237

CHARGE=1+

TITLE=Label: C11, Spot_Id: 37873, Peak_List_Id: 85520, MSMS Job_Run_Id: 11317, Comment:

101.09186	134.7549
112.11255	148.34692
185.14832	116.12772
268.18668	317.92752
313.24561	195.94186
339.2417	189.85034
441.35834	212.01836
444.35672	1803.0789
452.33044	303.08701
469.36716	3648.3081
583.45715	481.41537
600.47272	261.48059
636.46216	188.29391
653.48584	138.98396
664.57422	393.59735
665.51422	151.25536
711.52789	165.55237
720.19073	487.25647
728.52832	201.33273
738.57007	876.29657
766.58289	564.32483
782.55817	332.91391
783.59076	286.09576
784.59198	5457.1401
865.26935	318.15805
870.67346	230.9062
882.65564	205.38618

END IONS

BEGIN IONS

PEPMASS=974.53485

CHARGE=1+

TITLE=Label: C11, Spot_Id: 37873, Peak_List_Id: 85508, MSMS Job_Run_Id: 11317, Comment:

172.08818	102.24106
438.36902	123.29253
489.28543	184.77016
503.31335	245.01006
531.30505	1065.0125
533.29199	281.92639
662.44696	163.05629
697.40253	302.89087
726.47833	327.48367
728.45117	427.57953
800.52222	217.21945
828.52307	467.25635
846.55365	316.16528

END IONS

BEGIN IONS

PEPMASS=1017.5923

CHARGE=1+

TITLE=Label: C11, Spot_Id: 37873, Peak_List_Id: 85518, MSMS Job_Run_Id: 11317, Comment:

175.15436	690.11823
212.14394	132.29068
243.19002	142.63254
288.24579	240
325.24158	168.0278
372.259	429.46078

385.28149	284.5098
465.33566	172.46713
482.36334	1984.7299
499.39465	518.58496
519.35571	112.84064
629.45441	326.80225
646.48694	1503.041
775.54205	824.88422
958.59149	140.71448
972.27734	120.10564
973.67047	146.66837

END IONS
BEGIN IONS
PEPMASS=1031.6063
CHARGE=1+
TITLE=Label: C11, Spot_Id: 37873, Peak_List_Id: 85505, MSMS Job_Run_Id: 11317, Comment:

175.15044	364.77884
212.136	104.95623
271.22214	106.30878
288.24969	151.53943
385.28265	165.27194
386.2637	279.27469
465.31021	130.58971
482.34552	1041.4884
499.37955	372.3063
629.43414	201.41615
646.47052	626.40936
789.55682	330.70584

END IONS
BEGIN IONS
PEPMASS=1044.1276
CHARGE=1+
TITLE=Label: C11, Spot_Id: 37873, Peak_List_Id: 85509, MSMS Job_Run_Id: 11317, Comment:

811.17273	609.52917
851.25421	154.38896
854.18134	640.60394
855.19287	1513.615
856.16479	3284.5801
1000.2051	270.87167

END IONS
BEGIN IONS
PEPMASS=1097.6536
CHARGE=1+
TITLE=Label: C11, Spot_Id: 37873, Peak_List_Id: 85515, MSMS Job_Run_Id: 11317, Comment:

255.18437	494.25998
272.21237	657.39197
316.17087	231.17639
369.2468	567.44434
386.28119	232.87486
401.26553	161.19438
429.27316	462.03714
485.3689	128.73466
500.33234	164.42113
542.3833	356.16138
556.4082	135.38211
613.41437	596.01721
669.52283	211.87248
712.47583	184.76787
782.61993	1849.8934
897.64185	523.73804
909.12378	566.98505

END IONS
BEGIN IONS
PEPMASS=1155.7146
CHARGE=1+
TITLE=Label: C11, Spot_Id: 37873, Peak_List_Id: 85514, MSMS Job_Run_Id: 11317, Comment:

360.26169	128.03922
473.31955	146.21979
570.40692	225.85437
571.42792	520.8465
586.41846	207.18005
683.51422	362.61185

796.59058 492.64731
846.59686 194.13116
909.72382 215.25775
1091.8065 1688.5398

END IONS

BEGIN IONS

PEPMASS=1174.7106

CHARGE=1+

TITLE=Label: C11, Spot_Id: 37873, Peak_List_Id: 85517, MSMS Job_Run_Id: 11317, Comment:

129.13336 123.67648
175.14651 645.01428
302.18115 142.39877
303.25403 151.32671
416.34598 302.00983
541.40698 112.17601
545.42615 447.30637
630.40625 251.49832
655.50104 156.61513
759.5011 327.6955
785.57965 138.72736
802.58221 323.70969
809.48553 264.86072
873.66132 440.20135
931.66144 259.0224
999.67096 1496.3586
1017.6977 2408.198
1113.7823 667.64435
1130.7887 500.71896
1131.7643 840.0863

END IONS

BEGIN IONS

PEPMASS=1200.6729

CHARGE=1+

TITLE=Label: C11, Spot_Id: 37873, Peak_List_Id: 85519, MSMS Job_Run_Id: 11317, Comment:

266.15698 135.78432
412.28998 2365.0637
525.38666 457.59717
639.45404 641.13989
676.39624 389.49399
754.50677 313.15536
789.49408 469.96027
825.53741 360.90668
898.58826 333.32578
926.58496 1208.4751
943.63031 291.45166
954.59906 265.73535
1054.6564 1069.8604
1072.6604 342.29861
1101.7014 184.09982

END IONS

BEGIN IONS

PEPMASS=1235.6187

CHARGE=1+

TITLE=Label: C11, Spot_Id: 37873, Peak_List_Id: 85504, MSMS Job_Run_Id: 11317, Comment:

175.14076 234.92819
365.17383 102.13953
478.28433 119.40688
607.32672 140.42284
864.53998 215.59937
1044.262 433.31567
1193.6682 398.88794

END IONS

BEGIN IONS

PEPMASS=1262.5938

CHARGE=1+

TITLE=Label: C11, Spot_Id: 37873, Peak_List_Id: 85513, MSMS Job_Run_Id: 11317, Comment:

469.36203 100.69441
474.22067 195.56787
587.33148 210.8994
701.40961 442.67792
703.38446 139.24532
816.47162 278.09732

887.50391	423.72546
988.52124	453.73788
1016.5854	250.15306
1068.2018	268.8569
1134.5985	292.78799
1197.7427	101.72993

END IONS
BEGIN IONS
PEPMASS=1300.1018
CHARGE=1+
TITLE=Label: C11, Spot_Id: 37873, Peak_List_Id: 85511, MSMS Job_Run_Id: 11317, Comment:

1212.2395	248.63916
1215.907	163.36681
1254.2444	1659.2523
1256.2075	8961.9609

END IONS
BEGIN IONS
PEPMASS=1473.8762
CHARGE=1+
TITLE=Label: C11, Spot_Id: 37873, Peak_List_Id: 85501, MSMS Job_Run_Id: 11317, Comment:

272.21765	198.79333
369.2442	191.1638
386.2782	148.62744
692.4364	219.53465
782.62958	1029.6224
805.51459	219.18756
897.67212	305.70419
989.67297	260.9061
1319.8352	231.638
1427.3168	990.41968

END IONS
BEGIN IONS
PEPMASS=1491.8789
CHARGE=1+
TITLE=Label: C11, Spot_Id: 37873, Peak_List_Id: 85516, MSMS Job_Run_Id: 11317, Comment:

272.20328	429.26459
369.23935	283.57614
386.25851	242.92082
395.23315	102.46426
466.32413	118.9043
485.33994	176.73521
556.39673	213.56924
595.35437	115.91996
669.51611	276.992
709.36743	117.01062
710.41595	269.83286
782.59515	2195.7729
823.52271	249.05951
897.63879	520.76208
936.61066	168.44881
1007.6581	242.27238
1106.719	245.48164
1220.7863	199.03258
1300.24	399.64853
1362.9244	515.49036

END IONS
BEGIN IONS
PEPMASS=1619.9877
CHARGE=1+
TITLE=Label: C11, Spot_Id: 37873, Peak_List_Id: 85510, MSMS Job_Run_Id: 11317, Comment:

272.20114	151.2746
369.23169	131.10245
386.24289	125.37368
556.38861	151.28815
669.50507	200.79164
782.58527	1598.8164
838.5238	252.49049
880.60071	104.52577
897.63098	410.68668
951.63019	240.06644
1064.7406	222.31648
1135.8143	308.43597

1234.8574 353.63531
1348.8909 317.76968
1362.9539 644.33899
1430.1046 164.41031
1573.1772 405.72293
1574.0989 140.9817
1575.1078 156.22256
1576.0322 118.76785
1578.0167 168.87544

END IONS

BEGIN IONS

PEPMASS=1733.9744

CHARGE=1+

TITLE=Label: C11, Spot_Id: 37873, Peak_List_Id: 85502, MSMS Job_Run_Id: 11317, Comment:

817.5578 706.9436
917.54816 195.95914
932.6004 458.7533
1118.7037 367.98495
1146.6768 738.6167
1247.7792 240.87396
1259.7589 708.7533
1372.8358 797.32916
1376.8351 303.02481
1459.8619 524.60278
1504.9001 241.8412
1588.0183 388.75281

END IONS

BEGIN IONS

PEPMASS=2225.1555

CHARGE=1+

TITLE=Label: C11, Spot_Id: 37873, Peak_List_Id: 85507, MSMS Job_Run_Id: 11317, Comment:

1142.6158 445.67871
1145.5964 153.00104
1316.7593 231.00677
1370.759 206.34016
1445.822 254.30997
1573.835 281.73465
1811.1331 236.50493

END IONS

vi) Spot 6

COM=Project: Proteomics, Spot Set: Proteomics\110117, Label: C12, Spot Id: 37874, Peak List Id: 84817, MS Job Run Id: 11316

805.45349	4140.1963
832.35248	3703.4312
835.51483	600
860.54401	2491.6382
865.05688	433.02716
887.03656	381.86276
891.5423	567.64709
906.54919	4294.9624
935.57495	1369.1177
1029.6561	3087.1448
1046.6492	724.91504
1069.5839	1334.7555
1153.636	2315.6863
1416.7263	903.80023
1426.8173	3162.6936
1624.8882	860.41193
2163.1968	7109.314

BEGIN IONS

PEPMASS=805.45349

CHARGE=1+

TITLE=Label: C12, Spot_Id: 37874, Peak_List_Id: 85532, MSMS Job_Run_Id: 11317, Comment:

112.11317	155.39217
175.1571	652.58337
230.1627	184.26643
245.18211	116.40026
262.21207	396.056
299.19357	327.28391
315.2359	168.76083
317.2189	615.1532
342.2337	147.86945
359.241	799.2453
376.26505	163.90065
402.32733	262.07721
412.30438	340.50153
430.29947	127.89084
472.34482	250.12047
489.37097	186.79784
544.38098	121.15332
559.40381	225.81824
613.40393	141.70645
617.17859	360.35898
618.17535	110.01474
763.5072	191.82542
775.53613	448.96024

END IONS

BEGIN IONS

PEPMASS=835.51483

CHARGE=1+

TITLE=Label: C12, Spot_Id: 37874, Peak_List_Id: 85523, MSMS Job_Run_Id: 11317, Comment:

325.23972	103.71146
398.28751	777.91443
575.43195	439.62247
608.46063	2202.3787
632.41559	318.02844
644.15308	382.46747
645.13599	124.90913
646.41449	1197.0876
661.47449	349.4429
662.46008	565.99298
663.44318	202.78442
689.48474	366.84113
707.50031	203.44067
721.53735	169.72089
731.52942	137.03169
805.60413	185.24335

END IONS

BEGIN IONS

PEPMASS=860.54401

CHARGE=1+

TITLE=Label: C12, Spot_Id: 37874, Peak_List_Id: 85529, MSMS Job_Run_Id: 11317, Comment:

244.22328	230.49022
433.30292	151.79651
487.31931	190.92821
600.43176	205.05348
617.4458	237.30948
666.22607	183.30559
667.25116	203.48898
668.24121	302.70126
670.21271	266.14346
672.12921	274.72174
674.13843	151.34114
676.06921	368.45181
732.5271	1133.2267
811.29065	237.629
812.23438	160.17934
813.28076	232.87143

END IONS

BEGIN IONS

PEPMASS=865.05688

CHARGE=1+

TITLE=Label: C12, Spot_Id: 37874, Peak_List_Id: 85521, MSMS Job_Run_Id: 11317, Comment:

244.22409	178.70219
433.31702	148.59335
487.37747	125.86494
674.12305	250.04388
675.12451	203.26216
676.11609	1409.0635
678.11279	187.73351
682.09369	160.91106
732.62415	769.67474

END IONS

BEGIN IONS

PEPMASS=891.5423

CHARGE=1+

TITLE=Label: C12, Spot_Id: 37874, Peak_List_Id: 85522, MSMS Job_Run_Id: 11317, Comment:

175.14964	178.30922
491.33151	118.3865
664.47534	235.25755
698.12933	940.79279
700.11444	224.64908
701.06421	221.5813
704.07489	311.58496
843.21667	786.80145
845.17645	218.32382

END IONS

BEGIN IONS

PEPMASS=935.57495

CHARGE=1+

TITLE=Label: C12, Spot_Id: 37874, Peak_List_Id: 85528, MSMS Job_Run_Id: 11317, Comment:

175.14841	219.19685
579.42548	335.76395
890.55457	106.1374

END IONS

BEGIN IONS

PEPMASS=1029.6561

CHARGE=1+

TITLE=Label: C12, Spot_Id: 37874, Peak_List_Id: 85530, MSMS Job_Run_Id: 11317, Comment:

175.14534	648.77454
271.21414	113.76958
287.1817	125.90024
288.25119	103.68723
400.28412	112.04897
415.24527	101.59325
472.39737	294.19376
516.3363	207.36946
569.43481	184.97556
586.48163	202.49673
629.44159	673.29285
985.71991	928.49866

END IONS

BEGIN IONS

PEPMASS=1046.6492

CHARGE=1+
TITLE=Label: C12, Spot_Id: 37874, Peak_List_Id: 85524, MSMS Job_Run_Id: 11317, Comment:
175.15755 115.99469
262.19363 100.88235
855.19019 130.03471
856.20392 617.05377
857.19165 232.28586
859.11292 184.53702
END IONS
BEGIN IONS
PEPMASS=1069.5839
CHARGE=1+
TITLE=Label: C12, Spot_Id: 37874, Peak_List_Id: 85527, MSMS Job_Run_Id: 11317, Comment:
494.34015 103.75776
595.40527 167.51736
723.47894 124.89251
776.48438 149.07903
END IONS
BEGIN IONS
PEPMASS=1416.7263
CHARGE=1+
TITLE=Label: C12, Spot_Id: 37874, Peak_List_Id: 85526, MSMS Job_Run_Id: 11317, Comment:
274.23154 231.51962
768.53864 770.36816
1143.6393 235.13603
1230.8044 229.80859
1296.7849 153.61801
1351.8406 266.08032
1352.8593 5760.876
END IONS
BEGIN IONS
PEPMASS=1426.8173
CHARGE=1+
TITLE=Label: C12, Spot_Id: 37874, Peak_List_Id: 85531, MSMS Job_Run_Id: 11317, Comment:
175.13174 137.13571
368.2814 242.86592
385.32202 144.75491
506.26404 235.24445
515.39301 176.2872
532.41095 106.84846
619.37607.16864
732.46649 282.42581
1212.907 552.13513
END IONS
BEGIN IONS
PEPMASS=1624.8882
CHARGE=1+
TITLE=Label: C12, Spot_Id: 37874, Peak_List_Id: 85525, MSMS Job_Run_Id: 11317, Comment:
175.14609 166.32353
1061.808 133.68561
1337.9033 440.69617
1509.9742 529.2757
1563.0389 195.90578
1581.0154 162.19919
END IONS

vii) Spot 7

COM=Project: Proteomics, Spot Set: Proteomics\110117, Label: C13, Spot Id: 37875, Peak List Id: 84818, MS Job Run Id: 11316
805.45844 7041.7798
806.13416 2526.9561
832.35455 2823.5293
835.5235 2884.804
856.07159 1978.9209
860.54651 9852.9844
864.50757 1471.8901
903.01556 1793.2233
906.55139 8150.4902
921.52899 1369.3379
935.58124 6970.0991
1029.6615 9391.6992
1044.1168 1644.9611

1046.6436	1800.1078
1145.7158	1403.4437
1153.6381	3397.5366
1301.8385	2447.0586
1432.8374	2181.5745
1464.8322	2386.7158
2163.2212	7827.4512

BEGIN IONS
PEPMASS=805.45844
CHARGE=1+
TITLE=Label: C13, Spot_Id: 37875, Peak_List_Id: 85548, MSMS Job_Run_Id: 11317, Comment:

175.15907	424.71573
230.16566	103.3924
245.18669	147.18059
262.21115	296.23108
299.1918	225.19426
317.20978	405.11224
359.24536	533.5553
402.30582	181.68231
412.29465	194.55508
430.32889	133.77049
472.34653	172.08026
489.37479	102.68811
576.44897	101.17966
617.16284	368.14453
775.54749	348.9213

END IONS
BEGIN IONS
PEPMASS=835.5235
CHARGE=1+
TITLE=Label: C13, Spot_Id: 37875, Peak_List_Id: 85546, MSMS Job_Run_Id: 11317, Comment:

398.28049	642.49915
547.42877	183.73027
575.42761	491.44229
608.45667	2500.2354
644.22479	244.68138
645.09497	258.21768
646.30341	187.49069
689.46771	360.94794
707.52576	124.60471
721.54883	253.00117

END IONS
BEGIN IONS
PEPMASS=856.07159
CHARGE=1+
TITLE=Label: C13, Spot_Id: 37875, Peak_List_Id: 85542, MSMS Job_Run_Id: 11317, Comment:

622.16449	188.82933
623.12213	199.25137
665.21246	323.05167
666.13672	735.50519
667.22162	538.77979
668.16681	297.62256
669.2998	258.69339
732.51813	456.53372
811.20679	545.93665
812.16821	395.67215
813.18341	133.05757

END IONS
BEGIN IONS
PEPMASS=860.54651
CHARGE=1+
TITLE=Label: C13, Spot_Id: 37875, Peak_List_Id: 85550, MSMS Job_Run_Id: 11317, Comment:

244.2193	871.94354
304.23416	142.94118
357.3252	187.77811
416.28937	158.68629
433.30286	545.88531
445.29825	158.67044
487.32309	765.19666
504.35397	332.4332
572.44678	293.33322
589.47131	476.12509

600.4328 548.0083
 617.45551 929.35272
 668.23499 422.49289
 669.30353 251.72456
 670.09436 265.3432
 672.14142 359.55652
 676.09869 188.03325
 732.53314 3758.5134
 812.30768 396.95755
 END IONS
 BEGIN IONS
 PEPMASS=873.073
 CHARGE=1+
 TITLE=Label: C13, Spot_Id: 37875, Peak_List_Id: 85537, MSMS Job_Run_Id: 11317, Comment:
 232.1969 137.97601
 638.12787 313.60547
 640.12225 251.87656
 681.17444 432.1105
 682.138 2878.3987
 684.11334 942.03143
 745.49005 437.90961
 827.24731 1383.0847
 829.18274 524.52161
 END IONS
 BEGIN IONS
 PEPMASS=887.04169
 CHARGE=1+
 TITLE=Label: C13, Spot_Id: 37875, Peak_List_Id: 85535, MSMS Job_Run_Id: 11317, Comment:
 654.08826 569.49854
 696.11475 845.10974
 697.08533 647.18671
 698.07227 4248.3472
 843.13281 1783.4316
 END IONS
 BEGIN IONS
 PEPMASS=903.01556
 CHARGE=1+
 TITLE=Label: C13, Spot_Id: 37875, Peak_List_Id: 85540, MSMS Job_Run_Id: 11317, Comment:
 411.31729 183.07129
 479.34164 174.43646
 496.375 602.69867
 659.47192 587.00696
 664.479 6900.3608
 711.35339 422.15936
 712.16736 689.01306
 714.06439 3383.1108
 716.06586 233.05838
 760.53271 361.93341
 778.53748 451.09396
 792.57513 465.64743
 857.18005 275.97162
 859.13495 1436.5692
 END IONS
 BEGIN IONS
 PEPMASS=921.52899
 CHARGE=1+
 TITLE=Label: C13, Spot_Id: 37875, Peak_List_Id: 85538, MSMS Job_Run_Id: 11317, Comment:
 127.11606 111.37255
 333.25308 131.86282
 390.26944 165.80522
 426.31046 395.03391
 503.38315 147.69891
 553.38306 390.27258
 561.41425 165.10287
 589.41644 217.82329
 662.39288 281.15128
 666.47253 364.63593
 730.07471 666.67334
 736.02124 294.2504
 875.14215 460.11017
 END IONS
 BEGIN IONS

PEPMASS=935.58124
 CHARGE=1+
 TITLE=Label: C13, Spot_Id: 37875, Peak_List_Id: 85547, MSMS Job_Run_Id: 11317, Comment:
 175.15724 568.57843
 228.22417 102.46724
 242.20491 108.99285
 286.203 236.42107
 293.19321 116.81372
 303.23776 172.33458
 357.28467 150.27798
 399.30414 109.51945
 416.3324 138.56105
 449.27631 144.95413
 520.36218 142.95668
 562.38556 164.3967
 579.42712 612.0603
 END IONS
 BEGIN IONS
 PEPMASS=1029.6615
 CHARGE=1+
 TITLE=Label: C13, Spot_Id: 37875, Peak_List_Id: 85549, MSMS Job_Run_Id: 11317, Comment:
 112.10699 124.47715
 175.14809 1239.902
 271.22305 186.04343
 287.19312 248.89532
 288.24847 182.08095
 299.23795 103.31369
 325.24106 176.33846
 343.23993 139.90268
 384.33499 159.63582
 400.28033 205.09296
 401.33926 165.13638
 415.2529 198.13908
 444.3201 210.04234
 472.39566 539.21423
 516.32001 334.79623
 541.36243 158.23621
 558.39551 262.94797
 569.43427 318.63156
 584.40277 112.12428
 586.46356 272.79523
 601.44714 146.00621
 611.42529 184.87154
 612.3656 111.87281
 629.42871 1072.9823
 742.52454 284.16714
 815.61462 167.96495
 985.72333 1579.9668
 END IONS
 BEGIN IONS
 PEPMASS=1046.6436
 CHARGE=1+
 TITLE=Label: C13, Spot_Id: 37875, Peak_List_Id: 85541, MSMS Job_Run_Id: 11317, Comment:
 175.16095 155.43398
 262.19052 119.5098
 855.1897 293.20349
 856.18713 771.78979
 857.16779 276.48389
 858.18176 168.22452
 1004.5685 231.18202
 END IONS
 BEGIN IONS
 PEPMASS=1145.7158
 CHARGE=1+
 TITLE=Label: C13, Spot_Id: 37875, Peak_List_Id: 85539, MSMS Job_Run_Id: 11317, Comment:
 536.38885 214.17896
 610.47278 308.36877
 664.46814 175.7274
 723.55237 355.67865
 777.55988 158.41183
 909.65924 229.37929
 957.04242 213.58656

1046.7341 101.7037
 1077.7662 231.53476
 END IONS
 BEGIN IONS
 PEPMASS=1193.6829
 CHARGE=1+
 TITLE=Label: C13, Spot_Id: 37875, Peak_List_Id: 85533, MSMS Job_Run_Id: 11317, Comment:
 659.48199 101.44128
 690.47711 150.00986
 1063.6191 385.92276
 1065.7228 927.1499
 1127.8444 397.40408
 END IONS
 BEGIN IONS
 PEPMASS=1239.6945
 CHARGE=1+
 TITLE=Label: C13, Spot_Id: 37875, Peak_List_Id: 85536, MSMS Job_Run_Id: 11317, Comment:
 491.32468 114.09763
 592.37115 266.17117
 720.45435 484.44266
 835.52991 359.58551
 863.55963 149.27142
 948.62097 284.54303
 END IONS
 BEGIN IONS
 PEPMASS=1301.8385
 CHARGE=1+
 TITLE=Label: C13, Spot_Id: 37875, Peak_List_Id: 85545, MSMS Job_Run_Id: 11317, Comment:
 175.15166 181.76471
 303.26956 232.9902
 1236.8223 384.37189
 1256.2625 1012.027
 END IONS
 BEGIN IONS
 PEPMASS=1367.7999
 CHARGE=1+
 TITLE=Label: C13, Spot_Id: 37875, Peak_List_Id: 85534, MSMS Job_Run_Id: 11317, Comment:
 592.40594 133.07634
 648.45599 131.66994
 720.47437 970.81677
 776.56268 322.1355
 835.52008 446.84573
 877.60461 235.48642
 948.63068 316.5592
 991.69482 289.15649
 1076.7424 460.93585
 1092.7279 268.34967
 1221.7994 506.04257
 1239.7876 445.85037
 1304.7216 376.7496
 1306.8079 243.68401
 END IONS
 BEGIN IONS
 PEPMASS=1432.8374
 CHARGE=1+
 TITLE=Label: C13, Spot_Id: 37875, Peak_List_Id: 85543, MSMS Job_Run_Id: 11317, Comment:
 591.39215 465.63858
 615.36084 293.888
 650.38092 205.17111
 714.44159 192.67563
 719.50751 457.51535
 818.58685 322.6936
 836.45758 118.44497
 923.5177 293.64868
 933.62897 143.30273
 END IONS
 BEGIN IONS
 PEPMASS=1464.8322
 CHARGE=1+
 TITLE=Label: C13, Spot_Id: 37875, Peak_List_Id: 85544, MSMS Job_Run_Id: 11317, Comment:
 591.39807 124.38715
 1349.8398 193.69431
 END IONS

viii) Spot 8

COM=Project: Proteomics, Spot Set: Proteomics\110117, Label: C14, Spot Id: 37876, Peak List Id: 84819, MS Job Run Id: 11316

805.46429	1475.1703
856.07159	1449.2579
873.07965	1395.3204
873.47351	2627.9905
906.54633	2032.9866
1044.1125	2329.8591
1118.616	3113.3347
1179.6707	2483.7781
1194.677	1146.5686
1234.7521	3936.8938
1300.1101	2649.4028
1300.6143	1524.9901
1301.0973	1235.5118
1308.7354	2894.8394
1316.62	1134.3265
1493.8297	2837.3735
1567.8505	1550.9803
1791.8383	1655.8823
2163.1975	2747.5491
2384.0989	1224.1987

BEGIN IONS

PEPMASS=805.46429

CHARGE=1+

TITLE=Label: C14, Spot_Id: 37876, Peak_List_Id: 85560, MSMS Job_Run_Id: 11317, Comment:

112.12309	119.85892
172.08069	112.77946
175.16281	433.34335
245.17088	115.17701
262.20358	274.28815
299.20569	230.4789
317.20938	388.52487
322.25748	456.4519
359.24091	422.56265
376.2796	148.42342
402.31561	179.37054
412.31863	175.2299
437.32745	183.35168
573.17206	383.0242
612.24738	525.31128
614.21552	665.97137
615.18341	187.27522
616.1889	270.15369
617.17957	2844.8716
674.52393	574.76709
759.28149	398.80627
761.21979	509.82788
775.52063	463.01944

END IONS

BEGIN IONS

PEPMASS=856.07159

CHARGE=1+

TITLE=Label: C14, Spot_Id: 37876, Peak_List_Id: 85559, MSMS Job_Run_Id: 11317, Comment:

175.17213	112.79831
581.07422	133.97154
622.14618	293.39151
623.11322	1426.3008
625.10034	121.40439
664.2948	325.68243
665.23431	191.65582
666.13538	2116.7673
667.11407	1586.3093
668.1106	777.70117
669.10449	275.42212
809.23767	269.41083
810.28613	541.2088
811.19293	2736.9785
812.17908	2626.1028
814.15369	640.11591

END IONS

BEGIN IONS

PEPMASS=873.47351
 CHARGE=1+
 TITLE=Label: C14, Spot_Id: 37876, Peak_List_Id: 85565, MSMS Job_Run_Id: 11317, Comment:

169.13031	118.44621
175.14922	340.73529
311.19247	253.83629
332.22607	278.85333
378.24182	263.77521
479.29944	150.56615
546.36322	1148.2539
563.39642	581.1394
638.13995	361.46152
640.11609	258.23697
682.13953	2907.1467
684.10248	1108.9667
685.10034	423.70438
686.14117	152.0015
811.1524	317.97284
827.21222	1643.0375
829.17145	556.41626

END IONS
 BEGIN IONS
 PEPMASS=1044.1125
 CHARGE=1+
 TITLE=Label: C14, Spot_Id: 37876, Peak_List_Id: 85563, MSMS Job_Run_Id: 11317, Comment:

811.17645	487.35941
853.198	288.05206
854.19684	380.03687
855.17725	822.34772
856.16821	2271.0796

END IONS
 BEGIN IONS
 PEPMASS=1118.616
 CHARGE=1+
 TITLE=Label: C14, Spot_Id: 37876, Peak_List_Id: 85569, MSMS Job_Run_Id: 11317, Comment:

272.21295	312.59802
437.31018	134.81187
456.34247	180.99246
585.41583	143.44162
681.3902	235.82124
714.48822	144.11986
734.44611	116.17154
810.50189	179.32909
818.4646	117.2379
847.49219	282.48166
925.09106	138.56348
926.11108	129.76819

END IONS
 BEGIN IONS
 PEPMASS=1165.6554
 CHARGE=1+
 TITLE=Label: C14, Spot_Id: 37876, Peak_List_Id: 85551, MSMS Job_Run_Id: 11317, Comment:

112.11458	105.78203
175.15039	575.7655
303.22513	178.15288
321.211	112.63584
338.23416	236.88733
345.30093	122.86262
357.22989	126.01038
422.26175	110.11971
486.30209	588.35297
503.36795	264.9982
550.3324	188.29323
680.47253	490.94604
923.58075	533.62
976.0282	277.76474
977.00446	146.79716
1121.7181	323.02536

END IONS
 BEGIN IONS
 PEPMASS=1179.6707
 CHARGE=1+

TITLE=Label: C14, Spot_Id: 37876, Peak_List_Id: 85564, MSMS Job_Run_Id: 11317, Comment:
175.15111 196.10112
303.2233 125.48436
404.30197 115.23376
422.24548 265.52069
535.32458 177.37881
663.42444 197.30838
758.56421 380.55612
887.63293 276.75623
1135.7166 384.16089
END IONS
BEGIN IONS
PEPMASS=1194.677
CHARGE=1+
TITLE=Label: C14, Spot_Id: 37876, Peak_List_Id: 85557, MSMS Job_Run_Id: 11317, Comment:
175.14879 223.13937
659.48456 324.83862
774.51495 113.69825
END IONS
BEGIN IONS
PEPMASS=1234.7521
CHARGE=1+
TITLE=Label: C14, Spot_Id: 37876, Peak_List_Id: 85570, MSMS Job_Run_Id: 11317, Comment:
175.14418 293.67645
458.37161 167.40302
486.37259 207.97491
701.49713 151.44156
END IONS
BEGIN IONS
PEPMASS=1246.7477
CHARGE=1+
TITLE=Label: C14, Spot_Id: 37876, Peak_List_Id: 85552, MSMS Job_Run_Id: 11317, Comment:
175.15721 451.06995
272.21417 123.27499
456.36716 170.70551
458.40341 267.55832
466.25656 144.90884
486.37262 243.02798
676.37775 299.46768
END IONS
BEGIN IONS
PEPMASS=1300.1101
CHARGE=1+
TITLE=Label: C14, Spot_Id: 37876, Peak_List_Id: 85566, MSMS Job_Run_Id: 11317, Comment:
175.14145 152.30978
288.23386 100.93138
338.22797 710
421.20432 128.07721
489.25769 155.45032
812.47638 308.96506
1067.1429 393.90231
1212.198 476.47891
1215.8096 788.03522
1254.2198 2860.8145
1256.1937 16411.141
END IONS
BEGIN IONS
PEPMASS=1308.7354
CHARGE=1+
TITLE=Label: C14, Spot_Id: 37876, Peak_List_Id: 85568, MSMS Job_Run_Id: 11317, Comment:
175.15408 245.98039
303.27856 118.02219
338.24054 100.14791
400.29633 120.09835
530.41803 267.47116
659.48468 741.21362
774.5368 176.86153
1256.2709 1153.3851
1257.2957 421.18536
1258.2615 260.7731
1259.2805 349.91553
END IONS

BEGIN IONS
PEPMASS=1316.62
CHARGE=1+
TITLE=Label: C14, Spot_Id: 37876, Peak_List_Id: 85556, MSMS Job_Run_Id: 11317, Comment:
175.1449 321.86276
243.18073 104.40228
288.24216 102.31933
303.25433 184.26459
338.21713 263.36264
400.3201 152.09068
530.46472 278.05066
659.52393 718.31299
1252.714 4152.2036
1256.4664 446.97522
1257.3379 700.49628
END IONS
BEGIN IONS
PEPMASS=1434.8392
CHARGE=1+
TITLE=Label: C14, Spot_Id: 37876, Peak_List_Id: 85553, MSMS Job_Run_Id: 11317, Comment:
593.39685 129.22293
650.41211 573.70227
836.54932 303.32687
923.56146 628.65106
1278.8716 1418.8079
1371.8705 275.56699
1390.9758 462.01886
1392.9363 862.45465
END IONS
BEGIN IONS
PEPMASS=1475.8596
CHARGE=1+
TITLE=Label: C14, Spot_Id: 37876, Peak_List_Id: 85554, MSMS Job_Run_Id: 11317, Comment:
464.31021 228.34525
1427.2773 430.4129
END IONS
BEGIN IONS
PEPMASS=1493.8297
CHARGE=1+
TITLE=Label: C14, Spot_Id: 37876, Peak_List_Id: 85567, MSMS Job_Run_Id: 11317, Comment:
400.2963 110.77946
545.3833 166.83975
728.47723 150.48303
986.73462 264.81674
1365.858 1339.8356
END IONS
BEGIN IONS
PEPMASS=1567.8505
CHARGE=1+
TITLE=Label: C14, Spot_Id: 37876, Peak_List_Id: 85561, MSMS Job_Run_Id: 11317, Comment:
303.26044 196.71568
563.36121 127.19067
1523.8547 129.80376
END IONS
BEGIN IONS
PEPMASS=1707.8625
CHARGE=1+
TITLE=Label: C14, Spot_Id: 37876, Peak_List_Id: 85555, MSMS Job_Run_Id: 11317, Comment:
175.144 187.05882
466.26678 146.8651
503.33292 278.3956
694.41913 122.07867
1661.1172 291.59998
END IONS
BEGIN IONS
PEPMASS=1791.8383
CHARGE=1+
TITLE=Label: C14, Spot_Id: 37876, Peak_List_Id: 85562, MSMS Job_Run_Id: 11317, Comment:
1761.9573 110.96961
END IONS

**ISOLATION AND PURIFICATION OF GLUTATHIONE
S-TRANSFERASES FROM *Donax* sp.**

NORFARHAN MOHD ASSA'AD

**DISSERTATION SUBMITTED IN FULLFILLMENT OF
THE REQUIREMENT FOR THE DEGREE OF
MASTER OF BIOTECHNOLOGY**

**INSTITUTE OF BIOLOGICAL SCIENCES
FACULTY OF SCIENCE
UNIVERSITY OF MALAYA
KUALA LUMPUR**

2011